1-1-2017

Transferrin Receptor Targeted Delivery Of Sirna For Gene Therapy

Yuran Xie
Wayne State University,

TRANSFERRIN RECEPTOR TARGETED DELIVERY OF SIRNA FOR GENE THERAPY

by

YURAN XIE

DISSERTATION

Submitted to the Graduate School

of Wayne State University,

Detroit, Michigan

in partial fulfillment of the requirements

for the degree of

DOCTOR OF PHILOSOPHY

2017

MAJOR: PHARMACEUTICAL SCIENCES

Approved By:

_____

Advisor Date

_____

_____

_____

ACKNOWLEDGEMENTS

I would like to express my most sincere appreciation to my advisor Dr. Olivia Merkel for all her advice, support and patience during my PhD study. She always encourages me to explore in science and overcome failure and depress.

I would like to thank my committee members, Dr. Fei Chen, Dr. Anna Moszczynska and Dr. Guangzhao Mao (Department of Chemical Engineering and Materials Science, WSU) for their support and scientific suggestions. I would also like to thank my previous committee members, Dr. Joshua Reineke (college of pharmacy & allied health professions, South Dakoda State University) and Dr. Sandro R.P. da Rocha (Department of Pharmaceutics, School of Pharmacy, Virginia Commonwealth University) for their professional advices and help. I would like to thank Dr. David JP Bassett for helping us do the animal work and allowing us to use his lab space and equipments. I would like to thank Dr. Lawrence G. Lum and Dr. Archana Thakur for kindly giving the primary T cells to us.

I would like to thank all my the current and previous lab mates, especially Daniel Faldmann and Steven Jones who always kindly offered helps and supports to my research. Special thank goes to my friend Qian Lin who has been always very supportive and helpful when I encountered issue in science, career and life. I

also like to thank Bryan Killinger who gave smart advice in research and life and kept me company in this long journey.

I would like to thank the Department of Pharmaceutical Sciences, Wayne State University to offering this opportunity to join this great graduate program.

In the end, I would like to thank my family and all my friends for their support and love during these years.

TABLE OF CONTENTS

LIST OF TABLES

LIST OF FIGURES

CHAPTER 1 INTRODUCTION

Please note that part of content of this chapter is from a chapter of Nanomedicine for Inflammatory Diseases, "Bridging the Gap between Bench and Clinic; Asthma" is being copyedited and will be published in Nanomedicine for Inflammatory Disease, Taylor & Francis Group, UK, 2016 (in process). The authors of this book chapter include Rima Kandil, Dr. Olivia Merkel and me. Rima Kandil and me are the joint first authors of this book chapter.

1.1 Gene therapy

Gene therapy is the in vivo delivery of therapeutic nucleic acids into cells or tissue to treat or prevent a disease. Nucleic acid mediated therapies include: a) replacing a malfunctioning gene with a functional wildtype gene; b) silencing a mutated gene; c) supplementing a gene encoding a missing protein in cells; d) boosting the immune response toward foreign infectious organisms[1]. Gene therapy is thought to be the solution for hard to cure diseases including genetic diseases, cancer, neurodegenerative disease, immunodeficiency and HIV, and extensive studies in pre-clinic research and clinical trials have been completed and are going-on. Currently, gene therapy can be conducted via two different approaches. One is the ex vivo approach, where nucleic acids are transferred into autologous target cells collected directly from individuals. These gene- corrected cells are returned back to the body and fight the disease. The other is the in vivo

approach, where nucleic acids are directly administrated to patients for nucleic acid delivery to target cells inside the body[2].

By 2012, over 1800 gene therapy clinical trials were performed in 31 countries. Most of these trials (64.4%) focus on treatments of different cancers [3] since the five-year survival rates of certain cancers are still very low, such as liver (17.5%), lung (17.7%) and pancreatic cancer (7.7%) according to a report from the National Cancer Institute (2009-2013). Current pre-clinic research and clinical trials for gene therapies of cancer include several strategies. The first one is the replacement of mutated tumor suppressor genes such as p53. Advexin® is a gene p53 encoding plasmid carried by an adenoviral vector. It showed antitumor activity and improved survival in clinical trials for treatment of head and neck cancer [4]. Another approach is the supplement of a 'suicide gene' encoding a viral/bacterial enzyme which can covert a pro-drug to an active drug in cancer cells [5]. Silencing of gene controlling tumorigenesis (e.g. proliferation and survival), metastasis and drug resistance is also a common approach [6]. In **Chapter 4**, our study reports that silencing of GASC1, an epigenetic factor involved in tumorigenesis, can inhibit the proliferation of basal-like breast cancer cells.

Gene therapy of inflammatory diseases only accounts for small potion in gene therapy clinical trials (0.7%) [3]. However, a large global market of drugs for inflammatory diseases [7] encourage research groups and pharmaceutical companies

to develop new therapies consequently increasing the number of pre-clinical research approaches and clinical trials of gene therapy for inflammatory diseases. For example, gene therapy approaches for asthma include DNA vaccines to induce immune tolerance [8], delivery of antisense oligonucleotides [9], small interfering RNA (siRNA) [10] and deoxyribozymes (DNAzyme) [11] for the selective silencing of asthma related genes. Currently, there is one gene therapy approach for asthma in clinical trial using SB010. SB010 is a DNAzyme which can cleave GATA-3, a key factor in asthma pathogenesis. It can achieve anti-inflammatory effects and improved lung function in asthmatic patient [11]. In **Chapter 2 & Chapter 3**, the application of siRNA as novel therapies of asthma will be discussed.

1.2 Delivery of nucleic acids

1.2.1 Viral delivery system

Many viruses naturally have the ability to effectively transfer their genetic material and express proteins in host cells as part of their replicate cycle. Therefore, they offer the potential to deliver nucleic acids to mammalian cells for gene therapy. In a viral delivery system, the gene which is essential for viral duplication is deleted and replaced by a therapeutic gene. Viral delivery systems show advantages, including high in vivo transduction efficiency and constant expression of the target gene [12]. Viral vectors, including adenovirus, retrovirus, adeno-associated virus, herpes simplex virus and lentivirus, are the most common

delivery system of nucleic acid in clinical trials of gene therapy [3]. The number of gene therapy clinical trials increased dramatically since the first gene therapy was approved in 1990. The first trial aimed to treat a kind of severe combined immune deficiency (SCID) which lacks a gene encoding adenosine deaminase (ADA). Patients were administrated autologous T cells transduced by retroviral vectors carrying genetic material encoding ADA. Even though this trial only showed modest results, it demonstrated the feasibility and potential of gene therapy in clinical use [13]. However, concerns regarding safety of viral vector from the public and from researchers arose while increasing numbers of clinical trials of gene therapy have been approved. One of the major setbacks of gene therapy was the case of Jesse Gelsinger. In 1999, 18-year-old Jesse Gelsinger, who suffered from a metabolic disorder due to partially defect ornithine transcarbamylase (OTC), entered a clinical trial of gene therapy aiming to supplement OTC using an adenoviral vector containing genetic material encoding OTC. Tragically, Gelsinger died from a severe and unexpected immune reaction to the viral vector. In 2000, the United States Food and Drug Administration (USFDA) stopped this trial and some other trials employing gene therapy. The FDA announced new programs and restrictions, including the Gene Therapy Clinical Trial Monitoring Plan and the Gene Transfer Safety Symposia, to protect patients better [14]. Another common viral vector, retrovirus vector, was used in a clinical trial to treat 11

children who had severe combined immunodeficiency (SCID)-XI disease which was the first success in gene therapy [15]. However, 5 children developed leukemia-like illness which was believed to be due to insertion of the retrovirus vector which triggered the expression of proto-oncogenes [16]. Extensive efforts have been devoted to improve the safety of viral vectors and promising progress has been made. Several new drugs for gene therapy were approved. Genedicine, an adenoviral vector carrying wildtype p53 gene, is the first gene therapy drug in the clinic for treatment of head and neck squamous cell carcinoma approved by the China Food and Drug Administration (CFDA). Another drug for gene therapy is Glybera, an adeno-associated virus carrying gene encoding human lipoprotein lipase (LPL), approved by the European Medicines Agency (EMA) and USFDA for treatment of lipoprotein lipase deficiency. Despite the improved safety of viral vectors and the success in the clinic, concerns of potential severe side effects, such as immunogenicity and carcinogenesis, caused by viral vectors never vanished and additional care is taken regarding the approval of gene therapy using viral vectors. On the other hand, the complexity of viral vectors manufacture and limited DNA packaging capacity also limit the large scale clinical use [17].

1.2.2 Non-viral delivery system

1.2.2.1 Challenges of delivery of nucleic acids

Because of the limitations and concerns mentioned above, the application and development of non-viral delivery became more popular. Non-viral vectors demonstrate many advantages compared to viral vector. First of all, non-viral vectors have better and tunable safety profiles than viral vectors. Biocompatible materials can be selected to achieve less immunogenicity and toxicity. Non-viral vectors can be also synthesized by biodegradable materials to reduce the toxicity and accumulation in the body. Moreover, applications of non-viral vectors for gene therapy can avoid insertional mutagenesis. Non-viral vectors have larger capacity for delivery of nucleic acid and are less complicated in their manufacture process which makes it easier for scaling up the production. More importantly, because the relatively simple chemical structure of non-viral vectors, such as polymer-based materials, various modifications have been done to achieve efficient and selective gene delivery, better safety and optimal pharmacokinetic profiles [18]. For example, non-viral vectors are commonly modified with targeted ligands such as folic acid [19] and transferrin [20] to achieve cell/tissue specific delivery. PEGylating non-viral vectors has been utilized to increase the biocompatibility and circulation time [21] and to achieve tissue specific accumulation [22]. Despite the numerous studies which have been performed to

develop and optimize non-viral vectors, their gene delivery efficiency is still relatively poor especially compared to their viral counterparts. Consequently, only a few non-viral vectors are mature enough to enter clinical trials [18].

Non-viral vectors will encounter various challenges when they are applied to deliver nucleic acids systemically. Nucleic acids are easily degraded by endogenous nucleases in the circulation. The half-life of nucleic acids in the blood stream is short, for instance, the half-life of naked plasmid DNA injected intravenously (i.v.) has been reported to be 10 minutes in mice. Nucleic acids carried by non-viral vectors are not readily degraded by nucleases and have longer circulation half-lives. Chemical modification in nucleic acid can also facilitate to protect them against the cleavage by nuclease and increase their in vivo stability. Common modification include incorporation of 2'-O- methyl to replace the 2'-OH group in the ribose in siRNA and combination of 2-thiouridine and 5-methylcytidine in mRNA [18].

Non-viral vectors need to overcome several biological barriers to deliver nucleic acids to target cells/tissues. Most non-viral vectors contain polycations or cationic lipids to condense nucleic acids which have negatively charged backbones. Nucleic acids can electrostatically interact with non-viral vectors and form polyplexes or lipoplexes which commonly have a net positive surface charge. This positive charge can induce non-specific association with non-target cells and

interaction with serum proteins in circulation. Vectors covered with a corona of serum proteins are easily recognized and trapped by the reticuloendothelial system (RES), such as liver, spleen and bone marrow. Consequently, only a small dose of i.v. administrated cationic nanoparticles can be delivered and accumulate at the target site. One of the strategies to reduce the positive charge and non-specific delivery is to decorate the vectors with polyethylene glycol (PEG), a hydrophilic and charge-neutral polymer. PEG shields the polyplexes/lipoplexes in the blood stream and avoids non-specific delivery. Most importantly, it prevents interaction with serum proteins and reduces accumulation in the RES which significantly increases the circulation time of polyplexes/lipoplexes [23].

Another challenge is selective accumulation in the tissue of interest. The behavior of non-viral vectors of nucleic acids in the body is highly dependent on their size, shape and surface properties. Typical non-viral vectors carrying nucleic acids, such as lipoplexes and polyplexes, are of spherical shape and in the nanometer range. Large lipoplexes/polyplexes (> 200 nm) tend to accumulate in liver and spleen and micrometer size particle (2-5 um) rapidly accumulate in the capillaries of the lung. Therefore, particle sizes around 100 nm are preferred [24]. Normal blood vessels have tight interendothelial junctions and prevent extravasation of lipoplexes/ polyplexes from the blood stream. In certain cases, such as inflammation and injury, leakage and dysfunction occur in the blood

vessel and lead to accumulation of lipoplexes/polyplexes at these sites. This strategy is commonly utilized to target tumors. The blood vessels supporting tumor growth are fenestrated, and tumors often lack efficient lymphatic drainage. This phenomenon is termed the "enhanced permeability and retention (EPR) effect". Modifications in vectors to prolong circulation time, such as PEGylation, can increase the accumulation at the tumor site. Another consideration is fluid dynamics of lipoplexes/ polyplexes. Particles with spherical shape demonstrate less lateral drift in the blood stream compared to non-spherically shaped particles which result in lower association with endothelial cells and extravasation from the blood stream [24].

Once the lipoplexes/polyplexes reach their selective site, even if some hydrophobic vectors can diffuse directly through the cellular membrane, most vectors require active internalization. Ligand modification in vectors can enhance cellular uptake via receptor mediated internalization. Moreover, vectors equipped with cell penetration peptides, such as trans-activating transcriptional activator (TAT) from the human immunodeficiency virus 1 (HIV-1), can also mediate efficient cellular uptake. Endocytosis of lipoplexes/polyplexes involves formation of intracellular vesicles termed endosomes. Endosomes eventually merge with lysosomes, which are vesicles that contain a highly acidic and enzyme rich environment and are capable of degrading the vectors and therapeutic nucleic

acids. Therefore, escape from the endosome is required for vectors to avoid degradation and to release nucleic acids into cytoplasm. To facilitate endosomal escape, the vectors can be modified with endosomolytic peptides, such as melittin, to disrupt the endosomal membrane [25]. Cationic polymers which have a high buffer capacity, such as poly ethyleneimine (PEI), can absorb protons and lead to an increased influx of counter ions (chloride) and water. Eventually, the increased osmotic pressure leads to bursting of the endosome and the release of materials inside the vesicles. This theory is called "proton sponge effect". Another reason why cationic polymers and lipids can achieve efficient endosomal escape is called "flip-flop" mechanism. The polymer/lipid with positive charge can electrostatically interact with vesicle membranes with negative charge and lead to membrane flipping and destabilization [23].

Different kinds of therapeutic nucleic acids face different challenges in the cytosol. Plasmid DNA (pDNA) needs to be delivered into the nucleus and requires access to the transcriptional machinery to express protein. Direct microinjection of pDNA carrying the thymidine kinase genetic information into nuclei of cells lacking thymidine kinase induces thymidine kinase expression in 50-100% of the cells. However, little activity of thymidine kinase was observed in the cells microinjected with pDNA into the cytoplasm. Furthermore, pDNA can express proteins efficiently in fast proliferating and dividing cells, since during mitosis the

nuclear envelope breaks down and the nucleus becomes more accessible to pDNA in the cytoplasm. In contrast, pDNA transfection results in poor protein expression in slow dividing cells due to their nucleic envelope being intact. These studies indicate that the nuclear envelope is the major barrier for delivery of pDNA to the nucleus. To overcome this barrier, modification with nuclear localiztion signal (NLS) sequences in non-viral vectors have been prepared and result in enhanced nuclear delivery efficiency and protein expression [26]. Small interfering RNA (siRNA) requires to be successfully incorporated into the RNA-induced silencing complex (RISC) to achieve gene silencing. The least stably hybridized 5' terminal of siRNA tends to load into the RISC, therefore, modification of the 5' end of siRNA is not recommended [18]. Application of longer double stranded RNA (dsRNA) to trigger gene silencing results in higher gene silencing efficiency. Synthetic long dsRNA (25-30 base pair) demonstrated 100-fold higher gene silencing efficiency compared to corresponding shorter siRNA (21 bp). It is believed that long dsRNA is a substrate of Dicer, a RNase-III class endoribonuclease, involved in RNA interference. Dicer can facilitate siRNA loading into the RISC and plays a role in RISC assembly. Therefore, more efficient gene silencing can be achieved when its substrate, long dsRNA, is provided to Dicer compared with delivery of conventional synthetic siRNA (21 bp) to RISC [27].

1.2.2.2 Synthetic non-viral vector

Non-viral vectors include polymers, cationic lipids, synthetic peptides, RNA/DNA chimera and inorganic nanoparticles (e.g. gold, magnesium) [28]. This section will focus on introducing the application of polymeric vectors for gene delivery.

There are three strategies of how polymeric vectors can carry nucleic acids: encapsulation, adsorption and electrostatic interaction. Nucleic acids can be encapsulated into biodegradable polymers, such as poly lactide-co-glycolide (PLGA), poly lactic acid (PLA) and poly beta-amino esters, to prevent enzymatic degradation in vivo and to achieve controlled release. The backbone of biodegradable polymers usually contains ester linkages which can be hydrolyzed and cleared easily in the body. The kinetics of nucleic acid release is tunable via adjustment of the hydrolysable parts in the polymer [29]. PLGA is a popular biodegradable polymer for gene delivery since it is approved for human use worldwide. PLGA can successfully encapsulate plasmid DNA, a relatively large nucleic acid, and achieve efficient transfection [30]. Small nucleic acid such as siRNA can be also encapsulated into PLGA. However, there are several challenges in this process including leakage of siRNA from PLGA particles, low loading efficiency and encapsulation efficiency [31]. Moreover, degradation of nucleic acids may happen during the encapsulation process since they are exposed

to organic solvents and sonication or long term solvent evaporation may be required. Degradation may also happen inside the particle due to the low pH environment caused by hydrolyzation of esters in the polymer [29]. To overcome these limitations, an adsorption loading strategy has been developed. Adsorption is a technique that combines both encapsulation and electrostatic interaction strategies. A cationic polymer can be incorporated into a biodegradable polymer [32] or adsorbed onto the surface of formed particles [33]. Therefore, nucleic acids can efficiently be loaded by the cationic moiety to avoid the harsh encapsulation process and hydrolyzation environment [29]. The most common strategy to pack nucleic acids using polymers is electrostatic interaction. This technique takes advantage of the anionic nature of nucleic acids, contributed by the phosphate group connecting the ribose molecules. Nucleic acids can electrostatically interact with cationic polymers and form particles suitable for efficient gene delivery [29].

Many cationic polymers are exploited for gene delivery including poly- L-lysine (PLL), acrylate based polymers, poly(amino-ester) based polymers, polyamidoamine (PAMAM) dendrimers and PEI based polymers. For example, PLL is a biodegradable polymer which is one of the first cationic polymers to be utilized in gene transfer. Despite the favorite biocompatibility of PLL, the short half-life in circulation and low transfection efficiency limit its use. PAMAM dendrimer is a symmetric macromolecule which has repetitive units of amido-

amines and primary amines located at the terminal surface. The controlled synthesis process of PAMAM dendrimers results in its narrow molecular weight range and defined spheroidal shape. Surface primary amine can efficiently condense nucleic acids and can easily be chemically modified with functional groups (e.g. targeting ligands, PEG, cyclodextrin). More importantly, large amount of internal tertiary amino group can serve as "proton sponge" to buffer pH change in endosome resulting better endosomal escape [34].

Among the cationic polymers, PEI is one of the most extensive studied polymers for gene delivery and is considered as the gold standard transfection reagent. PEI can be synthesized in different molecular weight and structure such as linear and branched. PEI usually contains primary amines and secondary amines as well as tertiary amines if its structure is branched. This amine rich structure renders PEI the ability to efficiently compact nucleic acids and protect them from degradation. Similar to PAMAM dendrimers, PEI has a large buffer capacity leading to high transfection efficiency. Researchers have developed various PEI based polymers to achieve better transfection efficiency and better biocompatibility. S. Kim et al. reported that low molecular weight PEI (2000 Da) conjugated with hydrophobic lipids such as cholesterol and myristate demonstrated enhanced transfection efficiency of plasmid DNA encoding β-galactosidase in 293 cell lines. The exact mechanism of how lipid modification of

PEI increases transfection efficiency is still unclear. It is hypothesized that the hydrophobic lipid increases the association with the lipophilic cell membrane [35]. Other hydrophobic modifications have been used for PEI, including phospholipids [36], alkanes [37], fatty acids [38] and hydrophobic poly (amino acids) [39]. M. Zheng and her co-workers described that grafting PEI with poly-caprolactone-b-PEG (PCL-b-PEG) increased the buffer capacity of copolymers compared to non-modified PEI and resulted in corresponding enhanced transfection efficiency. Biodegradable PCL served as a linker between PEI and PEG. Moreover, the hydrophobicity of PCL is believed to facilitate the association between the PEI-PCL-PEG copolymers and the cellular and endosomal membrane [40]. To increase the endosomal escape, endosomolytic peptides modifications (e.g. mellitin [41] and truncated HGP [42]) and cell penetration peptide modifications (e.g. TAT [43]) in PEI have been developed and demonstrated enhanced transfection efficiency. One of the limitations of endosomolytic peptides is their lytic activity under physiological conditions which can lead to destabilizations of plasma membrane and cell lysis. S. Boeckle et al. developed a PEI based polymer equipped with mellitin analogs. The neutral glutamines in mellitin (Mel) were replaced by glutamic acid residues resulting in high lytic activity at endosomal pH (pH 5) rather than physiological pH (pH 7). Different mellitin analogs (MA) were conjugated to PEI at cysteine modified C-termini (CMA-PEI). At endosomal pH 5, strong erythrocyte lysis was

observed after the treatment with CMA-2-PEI and CMA-3-PEI but not with CMA-4–PEI, CMA-1-PEI and Mel-PEI. Accordingly, CMA-2–PEI and CMA-3–PEI mediated more efficient transfection of plasmid DNA encoding a reporter protein Luciferase in 4 different cell lines (CT 26, HeLa, Neuro2A and A-10 cells) compared to Mel-PEI, unmodified PEI, CMA-1-PEI and CMA-4-PEI. However, increased corresponding toxicity was observed at high DNA doses (4 and 8 μg/ml) [41]. Another attempt to attenuate the toxicity of Mel under physiological condition has been approached by the same group. M. Meyer et al. utilized dimethyl maleic anhydride (DMMAn) to reversibly react with the lysines in Mel which could reduce the lytic activity. Since the DMMAn can be cleaved from Mel in acidic environment, this modified Mel (Mel-DMMAn) is believed to only demonstrate lytic activity in the endosomal environment. The author conjugated Mel-DMMAn to PLL and evaluated the transfection efficiency of plasmid DNA encoding luciferase in Neuro2A cells. As expected, Mel-DMMAn-PLL induced less erythrocyte lysis and cytotoxicity compared to Mel-PLL. Moreover, it mediated higher luciferase expression compared to Mel-PLL and unmodified PLL at different polymer and nucleic acid ratios (N/P ratios) [25]. We were able to modify 25k Da PEI with Mel-DMMAn following the same strategy. This Mel-DMMAn-PEI can deliver siRNA against green fluorescent protein (GFP) and mediate

significantly more GFP knockdown compared to unmodified PEI in H1299 cells, a lung cancer cell line, expressing GFP (Figure 1).

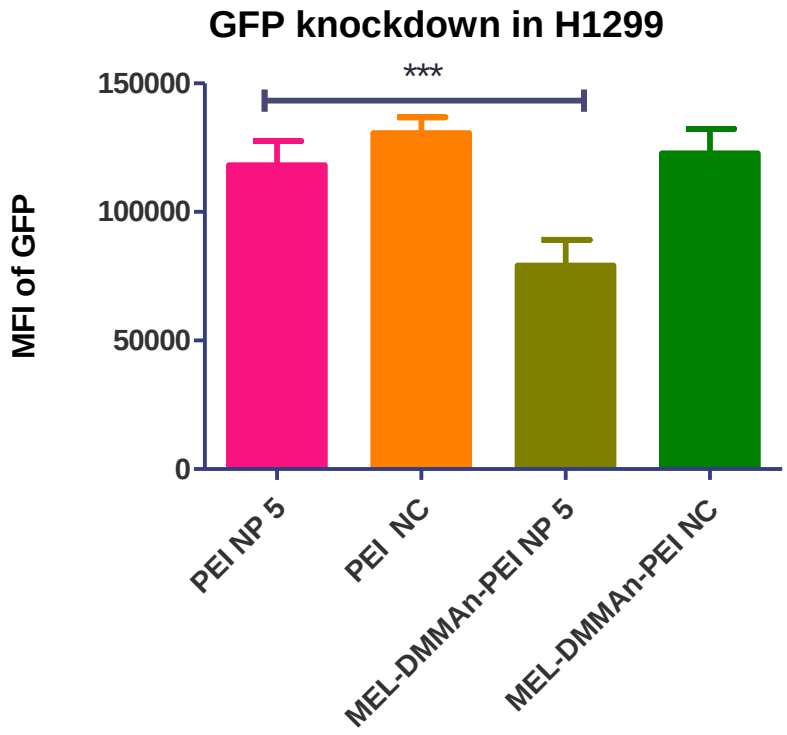

Figure 1 GFP knockdown in H1299 using Mel-DMMAn-PEI. The GFP knockdown mediated by PEI and Mel-DMMAn-PEI polyplexes containing siRNA against GFP or scramble siRNA (NC) in H1299/GFP cells. Polyplexes were prepared with 50 pmol of siRNA at N/P= 5 and transfected for 48 h. The MFIs were quantified by flow cytometry. (Data points indicate mean +/- SD, n= 3. One-way ANOVA, Newman-Keuls post-test, *** p <0.001).

To increase the selectivity to certain tissue/cells. PEI has been modified with different targeting moieties. For example, to target cancer cells, transferrin [44], folic acid [19a], tripeptide motif Arg-Gly-Asp (RGD) in vitronectin, fibronectin and fibrinogen [45] and epidermal growth factor (EGF) [46] were conjugated to PEI or PEI

based polymers. In 2009, our group demonstrated two different approaches to conjugate RGD mimics to PEI. In the first one, RGD mimics with maleimide modification were reacted directly with the primary amines in PEI-PEG. In the other approach, a PEG linker containing two functional groups, orthopyridyl-disulfide and succinimidyl propionic acid (NHS-PEG-OPSS) were used for coupling the RGD mimetic. NHS functional groups can react with the primary amines in PEI and the OPSS group can couple to the thiol group in the sulfhydryl derivative of the RGD mimics. Different RGD-PEIs were evaluated MeWo cells, a human malignant skin melanoma cell line, overexpressing integrin receptors and A549 cells, a lung epithelial cell line, expressing low levels of integrin receptors. Results suggested that RGD-PEI can preferentially bind to MeWo cells and efficiently deliver radio labeled plasmid DNA into MeWo cells rather than A549 cells. RGD-PEI polyplexes containing plasmid DNA encoding luciferase also mediated significantly higher luciferase expression in MeWo cells compared to unmodified PEI[47].

Despite the high transfection efficiency of PEI-based polymers, potential toxicity induced by high density of cationic charges arose concern regarding applying PEI in vivo. To avoid the toxicity caused by positive surface charge, several ways were developed to shield the particle, including PEGylation, coating with serum protein transferrin [44] or hydroxyl rich “skin”, termed “hydroxylation

camouflage" [48]. X. Luo et al. modified 25k Da PEI with 5-ethyl-5-(hydroxymethyl)-1,3-dioxan-2-oxo (EHDO) via an aminolysis reaction. The properties of PEI-EHDO directly depended on the hydroxylation degree on the surface. A high percentage of hydroxyl substitution on polymer PEI-EHDO$_{34.5\%}$ yielded polyplexes with plasmid DNA and demonstrated reduced surface charge compared to unmodified PEI and PEI-EHDO$_{19.9\%}$ polymer with lower percentage of hydroxyl substitution. Accordingly, reduced cytotoxicity in 293T and Hela cells and minimal hemolytic effects were observed after PEI-EHDO$_{34.5\%}$ treatment. Furthermore, less BSA protein was absorbed on the surface of PEI-EHDO$_{34.5\%}$ polyplexes compared to PEI and PEI-EHDO$_{19.9\ \%}$ complexes, indicating a good serum tolerance ability. This property lead to high efficiency of PEI-EHDO$_{34.5\%}$ to deliver plasmid DNA carrying luciferase gene in 293T and Hela cells in the presence of serum [48].

On the one hand, the transfection efficiency and potential toxicity are both related to the molecular weight of PEI. High molecular weight PEI (> 25k Da) can mediate efficient transfection but demonstrates cytotoxicity. On the other hand, low molecular weight PEI (600 – 25k Da) is less efficient and less toxic. To reduce the potential toxicity, high molecular weight PEI synthesized from low molecular weight PEI and crosslinked via reducible disulfide bonds or inert/biodegradable polymers has been developed. These PEI based polymers are

sensitive to redox stimuli. Glutathione (GSH) is a main reducing factor inside and outside the cellular environment. The concentration of GSH in the extracellular (2.8 μM) and intracellular (10 μM) environment differs strongly. Therefore, these biodegradable polymers can breakdown once they enter cells, especially in the low pH endosomal environment, and release their gene cargo [49]. Disulfide bond-crosslinked low molecular weight PEI was first reported by M. Gosselin. The author crosslinked 800 Da PEI using two crosslinkers, dithiobis-(succinimidylpropionate) (DSP) and dimethyl-3,3′-dithiobispropionimidate 2HCl (DTBP). The transfection efficiency of PEI-DSP and PEI-DTBP polyplexes containing plasmid DNA encoding luciferase gene was evaluated in CHO cells. The results suggested that transfection efficiency depended on the linker, crosslink degree and N/P ratio. Crosslinked PEI at low N/P ratios (5 and 9) mediated less luciferase expression compared to 25k PEI, while at high N/P ratios (13 and 18), crosslinked PEI with crosslinking degree of 1 mediated comparable luciferase expression to 25k PEI [50]. Q. Peng et al. synthesized thiolated PEI (800 Da) which can be oxidized by DMSO and yields disulfide crosslinked PEI (PEI-SS). Less cytotoxicity of PEI-SS-PEI in Hela cells compared to 25k PEI was observed as well [51].

Because of the promising properties of PEI, PEI is commonly used in proof of concept studies or pilot studies for optimizing experimental conditions. **In**

Chapter 3, 4 & 5, the application of branched PEI modified with targeteing moieties to deliver siRNA for potential treatment of asthma and cancer will be discussed.

1.3 RNAi for gene therapy

1.3.1 RNAi

RNA interference (RNAi) is endogenous sequence- specific mRNA degradation process and first discovered in plant but later RNAi was reported as a universal process in most eukaryotic organisms. On 1998, Andrew Fire and Craig C. Mello discovered that double strand RNA (dsRNA) can efficiently suppress expression of gene in the nematode worm Caenorhabditis elegans and later were awarded the 2006 Nobel Prize in Physiology or Medicine for this contribution.

Many cellular components are involved in RNAi. Dicer is an enzyme belonging to RNase III family and specifically cleaves dsRNA. Cleavage of Dicer generate small interference RNA (siRNA) in a range of 21- 25 nucleotides. siRNA is loaded in a protein complex termed RNA- induced silencing complex (RISC). The sense strand (passenger strand) in siRNA is degraded in RISC while antisense strand is integrated into RISC and serves as a guide strand. mRNA containing complementary sequence of antisense strand can be recognized by siRNA/RISC complex and cleaved by Argonaute 2 (Ago2), the component that has cleavage activity in RISC. Another kind of small RNA (21-28 nucleotides) called micro-

RNA (miRNA) can also induce gene silencing. A long miRNA precursor called primary miRNA (pri-miRNA) is cleaved by an enzyme Drosha in the nucleus to generate precursor-miRNA (pre-miRNA). The pre-miRNA is exported from nucleus and incorporated into microribonucleoprotein complex (miRISC) or RISC in some cases to cleave the mRNA containing complementary sequence (Figure 2). miRNA and siRNA are in similar size range and both processed by Dicer followed by gene silence. However, there are clear differences between siRNA and miRNA. miRNA is single stranded but siRNA is found in double strands which is relative more stable. The pair with mRNA of miRNA don't require perfect complementary match but do in siRNA induced gene silencing. Furthermore, many targets of discovered miRNA haven't been identified. Therefore, siRNA attracted extensive attention to exploit its therapeutic application [52].

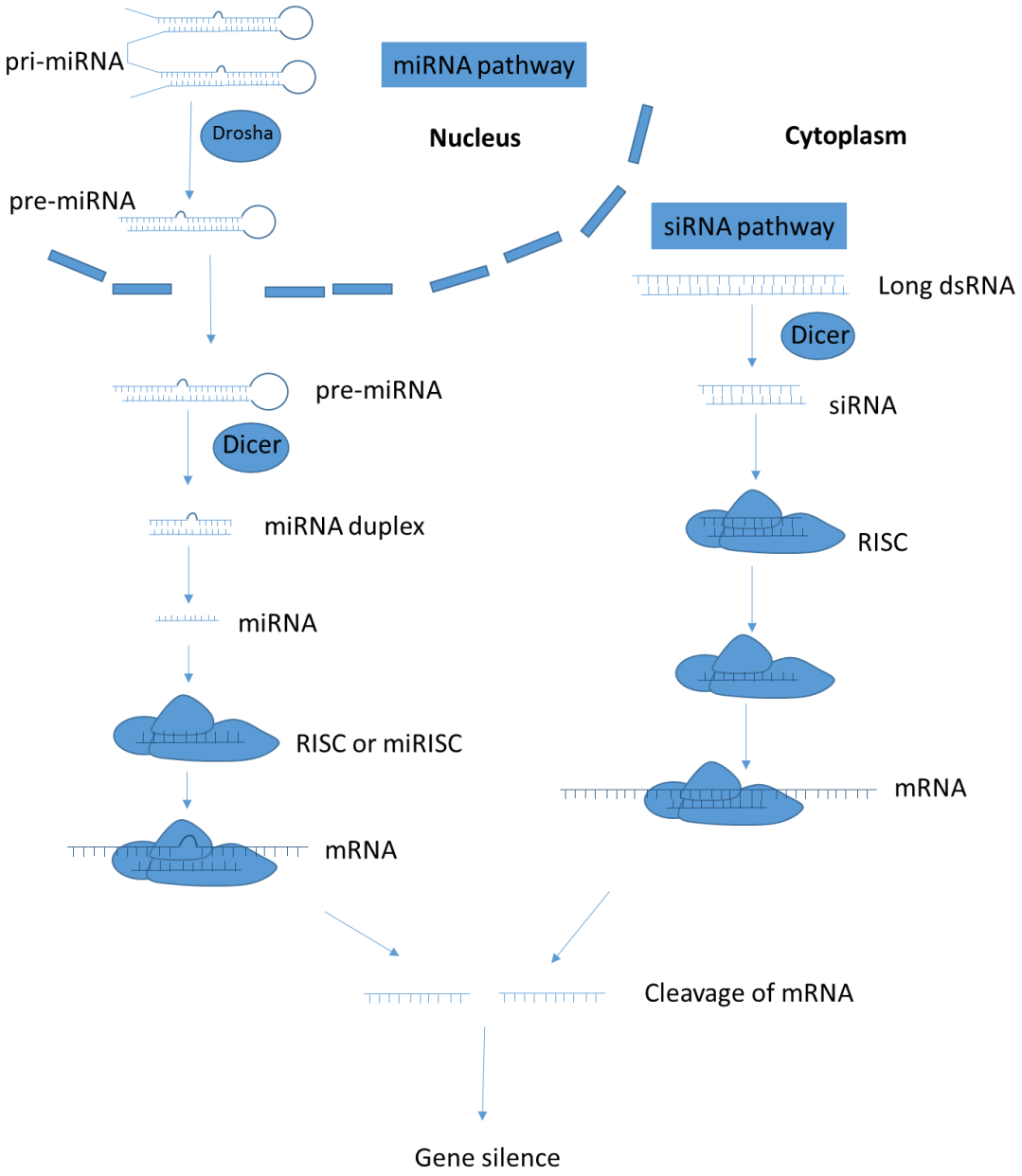

Figure 2 Gene silence pathway.

1.3.2 siRNA for gene therapy

In 2001, S. Elbashir et al. first described that delivery of synthetic siRNA against luciferase was sufficient to suppress the expression of luciferase in

different mammalian cell lines including HeLa (human), NIH/3T3 (mouse) and CHO (Chinese hamster) [53]. Ever since, numerous siRNA sequences targeting traditional non-drugable biological molecules have been in preclinical development as potential therapies of difficult to treated diseases, and some have entered clinical trials. Diseases which have been targeted by siRNA therapy in clinical trials include cancer, ocular diseases, asthma, infectious diseases and skin disorders. Local delivery of siRNA was the major administration approach in initial clinical trials. Extensive effort has been put into the development of non-viral delivery systems of siRNA, increasing the number of clinical trials utilizing systemic administration of siRNA and its vectors.

The first clinical trial of siRNA therapy was for the treatment of ocular disease initiated by Opko Health Inc. In this trial, siRNA against vascular endothelial growth factor (VEGF), named Bevasiranib, was administrated intravitreally (IVT) to inhibit retinal neovascularization for the treatment of age-related macular degeneration (AMD), a leading cause of blindness among people age 60 and older, and diabetic macular edema (DME). However, its Phase III results suggested that Bevasiranib can’t efficiently prevent vision loss in AMD. Afterward, two other siRNA formulations, administrated IVT, for therapy of AMD and DME which target VEGF receptor-1 (VEGFR1) entered clinical trials. Neither formulation could achieve sufficient therapeutic effects to prevent vision

loss. However, Macugen, a RNA aptamer against VEGF for AMD therapy, as the only RNA therapy approved by the USFDA encouraged pharmaceutical companies to keep exploiting this field. PF-655 is a siRNA formulation targeting an upstream regulator, apoptosis stress-response gene RTP801/REDD1, controlling VEGF production. Phase II results suggested that IVT administration of PF-655 can improve the mean visual acuity. Another formulation of siRNA for ocular disease is based on eye drops. SYL040012, a siRNA formulation against β2-adrenergic-receptor (ADRB2), was developed by Sylentis, S.A. for treatment of open angle glaucoma. It demonstrated well tolerability in patients with ocular hypertension or glaucoma in a Phase I study. A completed Phase II study suggested that SYL040012 (300 µg/ eye/ day) can significantly reduce intraocular pressure compared to placebo. The same company initiated another clinical trial of an siRNA eye drop formulation, SYL1001, targeting transient receptor potential cation channel subfamily V member 1 (TRPV1) for alleviation of ocular pain related to dry eye syndrome. Its recent Phase II results reported that one dose (1.25 %) among four different doses (0.375%, 0.75%, 1.125% and 2.25%) can alleviate ocular pain and hyperaemia compared to placebo [54].

An intranasal delivery formulation of siRNA against nucleocapsid protein of respiratory syncytial virus (RSV), ALN-RSV01, was developed by Alnylam Pharmaceuticals. ALN-RSV01 was proposed to be used in lung transplant patients

with RSV infection. Phase II results indicated that ALN-RSV01 treatment achieves a promising clinical outcome including reduction of incidence of new/progressive bronchiolitis obliterans syndrome on day 90 and day 180 post-treatment. However, there hasn't been a Phase III trial initiated since 2012 [54b].

Another approach to locally deliver siRNA to the lung is inhalation. Excellair™ is an inhaled siRNA formulation targeting spleen tyrosine kinase (Syk), an important factor involved in the inflammation process, for treatment of asthma. As reported by ZaBeCor Pharmaceuticals, the Phase I study suggested that Excellair™ was well tolerated and safe. Furthermore, Excellair™ treatment can improve the lung function of patients with asthma and reduced frequency of using immediate relief medication. The Phase II trial of Excellair™ has been announced in 2009, however, there have not been any results reported yet[54b].

In 2007, Quark Pharmaceutical initiated the first clinical trial in which a siRNA formulation was proposed to be systemically administrated in humans. This siRNA therapy, QPI-1002, targets stress-response gene p53 for prevention of Delayed Graft Function (DGF) in patients undergoing deceased donor kidney transplantation. QPI-1002 treatment can reduce the incidence of DGF and reduced the frequency of dialysis for 30 days post-transplant. A Phase III trial to evaluate the safety and therapeutic efficacy of QPI-1002 in large groups of patients (estimated 634 people) is currently recruiting participants[54b].

Currently, systemic siRNA therapies in clinical trials are mostly carried by lipid nanoparticles (LNP). LNP preferentially accumulate in liver and kidneys. Therefore, many clinical developments of siRNA aim to target hepatic genes. TKM-ApoB is a siRNA therapy targeting apolipoprotein B (ApoB), the major apolipoproteins in low-density lipoprotein particles (LDL) which are generated primarily in the liver, for the treatment of hypercholesterolemia. This formulation is administrated i.v. and therapeutic siRNA is carried by the first generation of stable nucleic acid lipid particles (SNALP). Reduced ApoB/LDL was observed after TKM-ApoB treatment, however, some patients experienced flu-like symptom indicating potential immunostimulation by TKM-ApoB. Later, Alnylam Pharmaceuticals initiated a clinical trial using the same carrier SNALP to pack two sequences of siRNA against VEGF and kinesin spindle protein (KSP), important factors involved in cell survival and proliferation, as therapy for primary and secondary liver cancer. Successful suppression of VEGF has been achieved in some patients who received siRNA treatment. A liver targeted strategy has been developed to more selectively deliver siRNA to the liver with lower doses and reduced toxicity. siRNA conjugated with triantennary N-acetylgalactosamine (GalNAc) can trigger internalization of hepatocyte-restricted asialoglycoprotein receptor (ASGPR). A GalNAc conjugated siRNA (ALN–PCS02) targeting proprotein convertase subtilisin/kexin type 9 (PCSK9), an enzyme specifically

degrading LDL receptor, was developed by Alnylam Pharmaceuticals for treatment of hypercholesterolemia. In a Phase I trial, a single dose of i.v. administration of ALN–PCS02 can reduce PCSK9 by 70% and LDL in circulation by 40%. A subcutaneous administrated formulation of the drug, ALN–PCSsc, entered a Phase I study to evaluate its efficacy in terms of reducing blood LDL. Treatment of ALN–PCSsc was well tolerated and can achieve up to 83% reduction of LDL. More importantly, Phase I results suggested a potential for a bi-annual dosing [54b].

Application of siRNA therapies in cancers attracts large attention since there is no effective treatment for some cancers which lead to high mortality rates. A siRNA carried by anionic liposomes and targeting breakpoint cluster region–Abelson murine leukemia oncogene (bcr-abl) tyrosine kinase was proposed as therapy of Chronic Myeolid Leukemia (CML). A patient with imatinib-resistant CML received siRNA formulation i.v. (10 μg/kg body weight) on day 426 post-transplantion of blood stem cells. Additionally, 300 μg siRNA was injected into one subcutaneous CML node. Later, 2 additional doses were given to the patient within 32 days after the first dose. The siRNA treatment transiently slightly reduced the bcr-abl mRNA in CML cells and ex vivo results suggested that the treatment can inhibit proliferation and induce apoptosis in CML cells. However, ex vivo transfection results also suggest that CML cells may develop resistance to

siRNA application [55]. Ligand coated nanoparticles have been applied to increase the delivery efficiency of siRNA targeting tumors in the clinic. Calando Pharmaceuticals developed a delivery system containing three components in the carrier including 1) a cationic cyclodextrin based polymer to carry siRNA, 2) an adamantane polyethylene glycol could enhance the stability in the blood stream and 3) a human transferrin to target the tumor. This formulation CALAA-01 targeting the M2 subunit of ribonucleotide reductase, an important factor involved in cancer cells proliferation, was evaluated in the clinic for treatment of relapsed or refractory cancers/solid tumors. The siRNA induced mRNA cleavage was confirmed by a rapid amplification of complementary DNA ends (RACE) PCR. However, two patients experienced dose-limiting toxic events. Moreover, no objective anti-tumor effect was observed, and 29% patients showed increased tumor sizes which lead to termination of this trial. Despite more optimization still being required to achieve efficient in vivo gene knockdown using nanoparticle, this trial demonstrated the feasibility to systemically administrate ligand guided polymeric nanoparticles [56].

1.4 Transferrin receptor

Transferrin (80k Da) (Tf) is a glycoprotein present in serum and contains two subunits linked by a spacer. Tf can deliver iron into cells mediated by interaction with its receptor, the transferrin receptor (TfR). Iron is a factor

involved in essential cellular procesess including DNA synthesis and metabolism. Therefore it is essential for cell proliferation and differentiation. Dietary iron is taken up through the intestine and becomes the oxidized form Fe^{3+}. However, cellular processes require Fe^{2+} and Fe^{3+} can be toxic to the cells. Tf can bind Fe^{3+} and transport it as a non-toxic complex in circulation. Each subunit of Tf can bind to one iron ion, therefore, there are two forms of Tf/iron complexes, monoferric Tf and diferric Tf (holo-Tf). Additionally, apo-Tf represents Tf that is not bound with iron or other metals. Tf/ iron complexes demonstrat higher binding affinity with TfR compared to apo-Tf. For example, the association constant of holo-Tf with TfR is 500 fold higher than apo-Tf with TfR.

TfR is a transmembrane receptor that can mediate endocytosis of Tf/iron complexes. Holo-Tf can bind to TfR and be endocytosed in clathrin-coated pits. The pH is reduced inside the endosome leading to a conformation change of holo-Tf. Consequently, Fe^{3+} is released from holo-Tf and reduced to Fe^{2+} in the endosomal environment before it enters the cytoplasm. Apo-Tf/ TfR complexes are recycled back to the cell surface and apo-Tf is readily dissociated from TfR due to its low affinity. The expression of TfR is regulated by the intracellular iron level. Cellular events, such as DNA synthesis that consume iron lead to reduced intracellular iron levels eventually resulting in an upregulation of TfR. TfR is universally expressed at low level in most cells/ tissues and upregulated in certain

cells such as actively proliferating cells, vascular endothelium of brain capillaries, and activated peripheral blood mononuclear cells. Additionally, upregulation of TfR is also observed in various cancer cells including glioma, breast cancer, lung adenocarcinoma and lymphoma.

1.4.1 TfR and diseases

Tf has been utilized as a targeted ligand for selective delivery of therapeutic cargos in various diseases. Conventional therapies of cancer can eliminate cancer cells but also commonly cause toxic effects in normal cells/ tissue. Since TfR is often upregulated in cancer cells, Tf or TfR targeted moieties have been conjugated to chemotherapies, toxic proteins and large molecules including liposomes and nanoparticles. For example, Cisplatin, an anti-cancer drug interrupting DNA synthesis, is a common chemotherapy used in various cancers including breast cancer, brain tumors and lung cancer. To reduce the side effect and increase tumor selectivity, Cisplatin conjugated with Tf (MPTC-63) was developed and evaluated in pre-clinical research and clinical trials. MPTC-63 demonstrated higher cytotoxicity in Hela cells compared to non-modified cisplatin. In a murine tumor model, suppressed growth of the tumor and reduced metastasis of the tumor in the lung were observed in the MPTC-63 treated group. Later, in a Phase I clinical trial, MPTC-63 treatment achieved positive response in 36% of patients with advanced breast cancer[57]. Polymers and liposomes are common non-

viral carriers for therapeutic cargos such as chemotherapies, macromolecules (e.g. DNA, RNA and proteins). A Tf modified liposome encapsulating oxaliplatin (L-OHP), MBP-426, was developed to increase the circulation time and tumor cell selectivity by targeting TfR eventually to achieve enhanced anti-tumor efficacy. Safety and pharmacokinetics of MBP-426 were evaluated in a Phase I clinical trial and a favorable safety profile was achieve [57b, 58]. Currently, an ongoing Phase Ib/II trial is evaluating the therapeutic efficacy of MBP-426 combined with leucovorin and 5-fluorouracil in patients with advanced or metastatic solid tumors. SGT-53 is another TfR targeted liposome under clinical evaluation. SGT-53 is a liposome formulation decorated with antibody fragments that target TfR and carrying DNA encoding p53. A phase I clinical trial suggested that SGT-53 is well tolerated in patients bearing advanced solid tumors. SGT-53 demonstrated targeted delivery to tumor cells and achieved anti-tumor activity. There are 4 active clinical trials of SGT-53 ongoing to evaluate its efficacy in refractory or recurrent solid tumors[57b].

The blood–brain barrier (BBB) is a barrier that separates the circulation system from the brain and prevents most macromolecules from entering the brain. Certain receptors, such as TfR, are expressed on the endothelium of brain capillaries for the introduction of essential nutrients and proteins (e.g. Tf). Therefore, TfR has been exploited extensively in preclinical studies as a potential entry for therapeutic reagent, particularly for macromolecules, to the brain. For

proof of concept studies, a mouse monoclonal antibody against rat TfR, OX26, has been conjugated to various molecules including neuroprotective agents, neurotrophic factor and liposomes for brain delivery. For example, brain-derived neurotrophic factor (BDNF), a neuroprotective agent, was coupled to OX26 and evaluated in a rat stroke model. Animals administrated i.v. with OX26-BDNF demonstrated 243% improvement in their ability of motor function compared to unmodified BDNF. This result suggested more efficient brain delivery was achieved by OX26-BDNF. OX26 has also been utilized to decorate liposomes for gene delivery to the brain. Intravenous delivery of OX26-liposomes carrying DNA encoding β-galactosidase resulted in β-galactosidase expressed in the brain of rats [59].

Activated T cells (ATCs) overexpress TfR and play an important role in inflammatory diseases. Our group is the first to exploit the possibility to deliver nucleic acids in a targeted manner to ATCs as potential treatment of inflammatory diseases, for instance, asthma. We demonstrated that Tf modified PEI can selectively deliver siRNA to human primary ATCs *ex vivo* [60] and ATCs in the lung of asthmatic mice *in vivo* [61].

1.5 Conclusion & significance

In the following chapters of this dissertation, I will discuss the most important findings in my development and optimization of TfR targeted polymers

for delivery of siRNA in various diseases. In **Chapter 2**, the progress and current status of application of siRNA therapies in asthma is summarized. In **Chapter 3**, the development and characterization of Tf conjugated PEI (Tf-PEI) as a potential therapy of asthma is described. Also, the selective delivery of siRNA to ATCs is confirmed *ex vivo* and *in vivo*. In this chapter, we proved the feasibility of efficiently delivering siRNA to ATCs via TfR targeted strategy which would benefit the development of a novel therapy for inflammatory diseases involving ATCs. This approach could also be utilized to transfect ATCs in fundamental studies since ATCs are difficult-to-transfect cells. Besides targeting ATCs in asthma, the TfR selectivity of Tf-PEI is evaluated in breast cancer cells in **Chapter 4**. Tf-PEI can achieve more efficient delivery of therapeutic siRNA against GASC1, to basal-like breast cancer cells, an aggressive phenotype of breast cancer, compared to unmodified PEI. In this chapter, we investigated a potential siRNA therapy of basal-like breast cancer via suppressing a novel epigenetic target, the histone demethylase GASC1. This potential treatment may demonstrate a better safety profile in vivo due to its TfR selectivity and may be combined with current anti-cancer therapy to achieve a better therapeutic outcome. In **Chapter 5**, two peptides against TfR, alternative TfR targeting moieties, are conjugated to PEI and both peptide-PEI conjugates are evaluated in lung cancer cell lines. One of the targeted conjugate, HAI-PEI, demonstrated higher

transfection efficiency in lung cancer cells overexpressing TfR compared to unmodified PEI. In this chapter, the feasibility of selectively delivering siRNA to lung cancer cells overexpressing TfR using peptide-PEI was confirmed. This peptide could be an alternative for holo-Tf to modify particles. Because of the high stability of peptides and their ability to non-competitively bind to TfR, peptide modified nanoparticles could be a better approach to achieve *in vivo* TfR targeted delivery.

CHAPTER 2 PULMONARY DELIVERY OF SIRNA VIA POLYMERIC VECTORS AS THERAPIES OF ASTHMA

Please note that part of the content of this chapter is from a review article, "Pulmonary Delivery of siRNA via Polymeric Vectors as Therapies of Asthma", was published in Archiv der Pharmazie (**Y. Xie**, O.M. Merkel, 2015). The authors of this article include Dr. Olivia Merkel and me. I am the first author of this review article, searched the literature, and wrote the review.

2.1 Introduction

Asthma is one of the major worldwide public health problems affecting 334 million people [62] and accounting for 250,000 annual deaths [63]. It is estimated that there would be additional 70 million asthmatic patients in 2025[62] and that the global market for asthma and chronic obstructive pulmonary disease (COPD) drugs would increase to $47.1 billion in 2017[64]. Asthma can be effectively controlled in most of the patients by current therapies including inhaled β_2-adrenergic receptor agonists, inhaled corticosteroids and injected immunoglobulin E (IgE) antibody [65]. Nevertheless, compliance of inhaled corticosteroids is poor due to the requirement of frequent inhalation and concerns of long-term side effect [66]. In contrast, common overuse of β_2- adrenergic receptor agonists (CDC,2007) increases the risk of systemic side effects [67]. Moreover, there are 5-10% asthmatic patients who lack adequate response to current therapies of asthma. The patients within that group who also have common asthmatic comorbid conditions, such as

rhinosinusitis and chronic infections, will experience worse symptoms of asthma and a higher risk of morbidity [68]. Thus, it is necessary to develop safer and more efficient additional treatments for asthma.

Asthma is a chronic inflammatory disorder and airway disease characterized by limitation of airflow, airway hyperresponsiveness (AHR), mucus hypersecretion and infiltration of inflammatory cells. In the pathogenesis of asthma, common environmental stimuli (e.g. dust, pollen) are recognized inappropriately by the immune system as antigen and consequently induce IgE-dependent inflammatory response. The asthmatic symptoms are majorly driven by inflammatory cells, for example, mast cells, eosinophils, dendritic cells, lymphocytes, macrophage and their cytokines [69,70]. Dendritic cells, the most efficiently antigen presenting cells (APCs), can present allergens to naïve T helper cells (Th0) and promote the differentiation of T helper 2 cells (Th2). Th2 cells can orchestrate the allergic response of asthma via secretion of Th2 interleukins (IL-4, IL-5 and IL-13) [69]. For instance, IL- 4 can promote differentiation and proliferation of Th2 cells and together with IL-13 stimulates B cells to proliferate and produce IgE. IL-5 can recruit and activate eosinophils as well as maintain their proliferation and survival. IL-13 is associated not only with IgE synthesis but also with chemoattraction of eosinophils, AHR, airway remodeling and mucus cell hyperplasia [69,70-71,72]. Other than Th2 cells, mast cells also contribute to asthmatic

inflammation by secreting histamine, tryptase and prostaglandin D_2 (PGD_2) which can induce potent bronchoconstriction, airway edema and lung fibroblast proliferation as the result of IgE-dependent stimulation by allergens [69]. Another essential type of inflammatory cells are eosinophils which can produce lipid mediators and pro-inflammatory cytokines to directly damage epithelial cells, induce bronchoconstriction and amplify inflammatory responses [73].

New drugs for asthma in pre-clinic research or clinic trails include new bronchodilators and corticosteroids as well as inhibitors of novel therapeutic targets, for example, kinase inhibitor and cytokine/chemokine blockage. siRNA induced gene silence is thought to be an efficient approach to block the functions of molecular targets. siRNA mediated therapies are post-transcriptional, transient and based on sequence-specific gene silencing, hence they are believed to offer a more potent and specific treatment with less side effects for different diseases [74]. Pulmonary delivery of siRNA as a non-invasive and local administration can reduce systemic side effects and prolong the lung retention period for the treatment of lung diseases like asthma. Furthermore, rapid therapeutic effects and lower dose requirement can be achieved due to the physiological properties of the lung such as the large alveolar surface, absence of serum proteins and the presence of a thin epithelium [75]. Despite of the advantages of pulmonary delivery of siRNA,

the biggest obstacle of clinical application of siRNA in asthma is the lack of biocompatible vectors to efficiently deliver siRNA into target cells.

In this chapter, we will discuss the molecular targets for siRNA mediated therapies and the formulation of siRNA applied in experimental asthma and will summarize available siRNA delivery systems that are targeted to immune cells.

2.2 Therapeutic Molecular Targets of siRNA in Asthma

As described in the introduction, asthma is a very complex inflammatory disease implicating numerous cells and cellular factors. The common therapeutic molecular targets for RNAi therapy include cytokines/chemokines, transcription factor, tyrosine kinase/ tyrosine kinase receptor, costimulatory molecules. Additionally, new biological targets have been discovered, such as the transient receptor potential cation channel (TRPV1) [76], nerve growth factor [74b], soluble membrane N-ethylmaleimide-sensitive factor attachment protein receptor protein (syntaxin4)[77].

2.2.1 Cytokines and chemokines

It is known that cytokines/chemokines, particularly Th2 cytokines, play prominent roles in airway inflammatory response and remodeling, thus, blockage of cytokines/chemokines and their corresponding receptors by using siRNA has been reported. Examples are the downregulation of suppressor of cytokine signaling 3 (SOCS3) [78], IL-4[79] and IL-5. Given that presence of eosinophils is

implicated in airway hyperresponsiveness and remodeling and IL-5 is the most important cytokine involved in eosinophils growth, activation as well as recruitment, siRNA against IL-5 was applied to reduce inflammatory response in ovalbumin (OVA)-induced murine asthma model. Huang et al. showed that intratracheal (i.t.) administration of lentivirus containing a siRNA against IL-5 expressing cassette (SEC4) to asthmatic mice for three consecutive days reduced the expression of IL-5 in the lung by 50% quantified by real time PCR (RT-PCR). Reduced eosinophilia was observed in SEC4 treated animals confirmed by less eosinophils in the bronchoalveolar lavage fluid (BALF) cells and H&E staining slides as well as less eosinophils chemoattractive cytokine (eotaxin) in the BALF. Consequently, The AHR was significantly relieved according to non-invasive whole body plethysmography (PenH) and invasive techniques [80].

2.2.2 Transcription factors

Blockage of a single mediator or receptor cannot achieve great therapeutic effects due to the complexity of asthma. Therefore, the upstream molecules of the inflammatory process have become more attractive therapeutic targets. Transcription factors that control the production of cytokines/chemokines and are involved in the growth and differentiation of major inflammatory cells were reported as targets for siRNA mediated treatment, such as GATA-3, transducer and activator of transcription 6 (STAT6), and receptor interacting protein 2

(Rip2)[81]. GATA-3, a transcription factor highly expressed in Th2 cells, can determine the differentiation of Th2 cells and promote the production of Th2 interleukins [82]. Antisense therapeutic intervention of GATA-3 in experimental asthma has been achieved not only with siRNA. Finotto et al. reported that 200 μg intranasally (i.n.) administrated GATA-3 anti-sense oligonucleotides for four continuous days to mice with OVA-induced inflammation can achieve local anti-inflammatory effects which were comparable to the positive control group treated with the first-line drug dexamethasone [83]. This report of therapeutic effect of blockage of GATA-3 in asthma is in line with the observation by Lee et al. who i.n. delivered GATA-3 small hairpin RNA with a lentiviral vector (2.2×10^6 IFU) to OVA-induced asthmatic mice [84]. The only asthma therapy study involving GATA-3 siRNA was published by Sel et al. To assess the efficacy of GATA-3 specific DNAzyme (Gd21) to prevent and treat experimental allergic asthma, they i.n. applied 200 μg Gd21 to mice with acute experimental asthma and compared to animals that were i.n. treated with 200 μg siRNA against GATA-3 or GATA-3 anti-sense oligonucleotides. These treatments were alternative antisense strategies in contrast to the DNAzyme. They concluded that Gd21 can more effectively reduce the inflammation than GATA-3 specific oligonucleotide and siRNA because these alternative antisense therapies showed a less efficient reduction of the number of eosinophils in the BAL cells and decreased the IL-5/IFN-γ ratio less

successfully [85]. However, their results also showed that GATA-3 specific siRNA treatment can reduce the number of mucus-producing goblet cells and AHR comparably to the Gd21 treatment. In addition, the authors did not use any delivery system for siRNA, anti-sense nucleotides or DNAzyme administration, and "naked" nucleic acids were applied directly. The approach of delivering free nucleic acids has been reported to lead to less efficiency in silencing genes in vivo and in vitro compared with the delivery via any kind of vector. Therefore, the therapeutic effect of GATA-3 siRNA or even anti-sense oligonucleotides is worth to be further evaluated in vivo. STAT-6, another promising target, is the transcription factor that controls the onset and maintenance of GATA-3 expression and is involved in T cells differentiation and IgE production [86]. The anti-inflammatory effect of i.n. administration of 100 µg siRNA against STAT-6 to asthmatic mice was described by Darcan-Nicolasien et al. They showed a decreased amount of infiltrated leukocyte in the BALF and reduced AHR in the STAT-6 siRNA treatment group compared with animals treated with siRNA against green fluorescent protein (GFP) which served as a negative control. Additionally, decreased levels of IL-4, IL-5, IL-13 and less histological alterations as well as less T cells infiltration were observed in lung tissue from the STAT-6 siRNA treatment group. However, the biodistribution of nanoparticles in the central and peripheral area of the lung was majorly in airway epithelial cells

instead of lymphocytes, where the expression of STAT-6 is most important in asthma. This observation may lead to higher required doses to obtain efficient therapeutic effects [87].

2.2.3 Tyrosine kinase / tyrosine kinase receptor

Other upstream targets are kinases involved in the inflammatory process such as spleen tyrosine kinase (Syk) and the nuclear factor kappa-light-chain-enhancer of activated B cells (NF-κB)[88]. Spleen tyrosine kinase (Syk) is widely expresses in immune cells and can initiate or mediate various cellular signaling pathways, including the development and maturation of B cells, proliferation of T cells, and production of inflammatory mediators from macrophages and mast cells [89]. It was described by Stenton et al. that three i.n. aerosolized doses of Syk antisense oligodexoynucleotides (ASO)/ liposome to OVA-induced asthmatic rats can reduce the infiltration of leukocytes found in the BALF and inhibit the antigen induced up-regulation of adhesion molecules in eosinophils, neutrophils and macrophages. However, there was no statistical difference of pulmonary inflammation between the Syk-ASO treatment and the saline treatment group according to the histological analysis of lung sections, and two doses of Syk-ASO treatments were not sufficient to inhibit the airway inflammation like three treatments did. Therefore, Syk-ASO is not a very efficient anti-inflammatory therapy but Syk was provento be a valuable target [90]. Inspired by this study, Huang

et al. i.n. instilled 10 μg siRNA against Syk on three consecutive days before the induction of acute lung inflammation and correlated less infiltration of inflammatory cells with the treatemnt[91]. Moreover, Excellair™ (ZaBeCor, Bala Cynwyd, PA, USA), a therapeutic siRNA against Syk, moved to Phase II clinical trials as a new drug for asthma in 2009 and confirmed the potential of Syk as a therapeutic target in asthma. A different potential target is the tyrosine kinase receptor C-kit of which the ligand is stem cell factor (SCF). Wu et al. reported that i.n. administration of methylation modified siRNA against C-kit (35 μg/day) for three days to mice with experimental allergic asthma can significantly reduce the levels of IL-4, IL-5 and SCF in the BALF and inhibit the infiltration of eosinophils as well as histology alteration due to pulmonary inflammatory [92].

2.2.4 Costimulatory molecules

APCs can initiate and maintain the airway inflammatory response, particularly a Th2-mediated response. The interaction between APCs and T cells requires the facilitation of costimulatory molecules such as CD86 and CD40[93]. Asai-Tajiri et al. reported that bone marrow derived dendritic cells (DCs) in vitro transfected with siRNA against CD86 can lose their ability to activate Th2 cells. In an OVA-induced murine asthma model, after i.n. administration of Texas Red labeled CD86 siRNA (12.5 μg), it was observed that Texas Red-siRNA was able to pass through the epithelial barrier and co-localized with DCs. With this

biodistribution result in mind, they i.n. applied siRNA against CD86 (12.5 µg/ day) for three days and achieved reduction of Th2 interleukins levels, less eosinophils infiltration and reduced AHR. However, treatment of CD86 specific siRNA did not reduce the goblet cell-mediated hyperplasia, indicating that higher dose of CD86 specific siRNA may be required to alleviate sufficiently the symptoms of asthma [94].

2.3 Targeted Polymeric Delivery of siRNA for asthma therapy

As summarized in Table 1, pulmonary delivery of siRNA is the most common administration approach for the treatment of experimental asthma and the majority of the formulations is either naked/modified siRNA or use lentiviral vectors.

Table 1 Summary of biological molecular targets for siRNA therapies of asthma

Administration	Formulation/vector	Target Molecule	Ref
Intratracheal	Naked/Modified siRNA	CD86	94
		Rip2	81
	Lentivirus	IL-5	80
		Nerve growth factor	74b
	Atelocollagen	Syntaxin4	77
Intranasal	Lentivirus	GATA-3	84

	Naked/Modified siRNA	GATA-3	85
		STAT-6	87
		Syk	91
		c-kit	92
		SOCS-3	78
		IL-4	79
Intravenously	Plasmid	CD40	93

Considering the large size, instability and negative surface charge, siRNA is easily enzymatically degraded, phagocytically cleared, aggregates with serum proteins, and does not readily cross physiological membranes[22,95]. Hence, viral or non-viral carriers are needed, even though there are many reports in the literature of pulmonary delivery of naked/modified siRNA[96]. Due to the safety issues of viral vectors such as immunogenesis and insertional mutagenesis, non-viral delivery vectors, particularly polymeric carriers, are more attractive and favorable approaches to deliver siRNA. With the flexible and modifiable chemical structure, polymeric carriers have the potential to overcome extracellular barriers including instability in the blood stream, cell/tissue targeted delivery and biological membranes as well as intracellular barriers like endosomal escape and cytoplasmic siRNA release. Additionally, polymeric vectors can maintain a high capacity of

siRNA loading, biocompatibility and the ability to co-deliver small molecular drugs [97].

There are many polymeric delivery carriers that have been prepared and optimized for pulmonary delivery of siRNA, such as polyethylenimine (PEI) and chitosan [96]. However, administration of polymeric nanoparticles encapsulating siRNA is limited in asthma therapy, due to the potential side effects induced by non-specific cellular uptake and the difficulty to transfect differentiated immune cells like lymphocytes in vivo. Receptor-ligand mediated targeted delivery of siRNA could be a solution.

2.3.1 T cell targeted delivery systems

It is believed that Th2 cells can initiate and aggravate symptoms of asthma via the production of Th2 interleukins. For this reason, there are many studies that aim to block the effects of Th2 responses via RNAi. Currently, the most popular lymphocytes transfection method is electroporation/nucleofection which, however, is not suitable for in vivo application[98]. Moreover, T cells generally resist the transfection of conventional polymeric or lipid-based (e.g.lipofectamine) vectors. Therefore, the difficulty to efficiently transfect T lymphocytes hinders the clinical application of RNAi in asthma. Recently, a few polymeric siRNA delivery systems specific for T lymphocytes have been discovered. CD7 is a surface antigen of human T cells which rapidly internalizes upon binding of an antibody.

To target and deliver nanoparticles encapsulating siRNA to T cells for the therapy of HIV infection, Kumar et al. conjugated a CD7 specific single-chain variable fragment with oligo-9-arginine peptide (scFvCD7-9R). Oligo-arginine is a positively charged cell-penetrating short peptide which has been reported to efficiently encapsulate siRNA and enhance the membrane permeability of nanoparticles [99]. scFvCD7-9R was accordingly able to transduce FITC-labeled siRNA selectively to primary human CD3+ T cells but not macrophages or B cells in vitro. The in vivo specificity of nanoparticles was tested in two kinds of humanized mice models implanted with human peripheral mononuclear cells (Hu-PBL and Hu-HSC). The i.v. injection of 50 µg siRNA against CD4 with scFvCD7-9R on two consecutive days significantly reduced the expression of CD4 on activated CD3+ T cells in Hu-PBL mice as well as on the rest/naïve CD3+ T cells in Hu-HSC mice. Additionally, to test the therapeutic effect, the authors systemically administrated scFvCD7-9R encapsulating a mixture of anti-viral siRNA including CCR5, Vif and Tat to Hu-PBL mice. Nanoparticles were shown to protect Hu-PBL mice implanted mit HIV-seronegative donor's PBMCs from HIV-1 challenge and significantly inhibited the viral replication. Furthermore, treatment of antiviral-nanoparticles of the Hu-PBL mice implanted with HIV-seropositive donor's PBMCs can protect the CD4+ cell loss compared with the animals treated with nanoparticles encapsulating siRNA against luciferase, which

served as a negative control. When PBMCs were exposed to nanoparticles in vitro, negligible toxicity was confirmed by percentage of Annexin V positive cells and production of IFN-γ. However, this scFvCD7-9R conjugate was optimized for i.v. administration for the therapy and prevention of HIV infection so it remains to be answered whether this conjugate can also efficiently and selectively deliver siRNA to T lymphocytes through pulmonary administration. This study should be highlighted because it demonstrates the feasibility to selectively deliver siRNA to T lymphocytes in vitro and in vivo which could be potentially applied in different inflammatory diseases like asthma and arthritis[100]. Another scFvCD7 conjugate was described by Lee et al. who conjugated scFvCD7 with chitosan and measured the in vitro transfection efficiency in T cell lines (Jurkat and A3.01 cells). Chitosan is a biocompatible and biodegradable polymeric vector, and chitosan/modified chitosan have been widely studied for pulmonary delivery of siRNA. It is thus a promising candidate to deliver siRNA in asthma therapy. The scFvCD7-chitosan/siRNA nanoparticles were around 300 nm in size and had a slightly positive zeta-potential of +17 mV. There was significantly higher uptake of scFvCD7-chitosan encapsulating FITC-siRNA compared with that of chitosan in T cell lines and increased uptake was observed as the molar ratio of scFvCD7 per total chitosan increased. scFvCD7-chitosan nanoparticles prepared with siRNA against CD4 were tested for in vitro gene silencing, and the CD4 gene

knockdown efficiency was similar to that of Lipofectamine 2000 but significantly higher than that of chitosan measured by flow cytometry and RT-PCR. However, scFvCD7-chitosan condensed CD4 siRNA at a weight ratio of chitosan to CD4 at 40:1 indicating that the siRNA encapsulation efficiency of the conjugate was fairly low. Additionally, scFvCD7-chitosan did not show better transfection efficiency in T cells lines than Lipofectamine 2000, thus high doses of nanoparticles may be required to achieve efficient gen silencing. Furthermore, the authors have not performed any in vivo study, and the pulmonary delivery efficiency of siRNA via scFvCD7-chitosan remains to be tested[101].

In asthma pathogenesis, activated T cells, particularly Th2 cells, play an essential role but not naïve T cells. However, CD7 is expressed on the majority of mature T cells resulting in the fact that a CD7 targeted siRNA delivery system will non-selectively deliver siRNA to both naïve and activated T cells. Therefore, a pulmonary siRNA delivery system that can selectively transport siRNA to activated T cells but not naïve T cells could achieve more efficient anti-inflammatory effect and reduce potential side effects. In 2013, our group described a selectively pulmonary delivery system of siRNA for activated T cells in which the transferrin receptor (TfR) was targeted instead of CD7. TfR is an iron uptake membrane receptor universally express at low level on most cells/tissues, in contrast, it is overexpressed on highly proliferating and differentiating cells. It was

reported that activated T lymphocytes highly express TfR to meet the iron requirement for further differentiation and growth while naïve T lymphocytes do not. For this reason, we linked transferrin (Tf), the native ligand which can trigger TfR internalization, with low molecular weight PEI (LMW-PEI). PEI is the most popular polycation for pulmonary delivery of siRNA, and applying low molecular weight PEI can dramatically reduce the toxicity induced by the high density of cations, which is the biggest obstacle limiting the clinical application of PEI. To determine the selective delivery efficiency of Tf-LMW-PEI in vitro, primary human activated T cells (ATC) or naïve T cells were transfected by Tf-LMW-PEI encapsulating Alexa Fluor488-labeled siRNA. Flow cytometry quantified cellular uptake of Tf-LMW-PEI/siRNA in ATCs was significantly higher than that of non-modified LMW-PEI as well as Lipofectamine 2000. Additionally, the uptake of Tf-LMW-PEI and LMW-PEI was minimal on naïve T cells compared with that on ATCs indicating that the conjugate can distinguish ATCs from naïve T cells[60]. Our group also determined the biodistribution of Tf-LMW-PEI formulated with Alexa Fluor 647 labeled siRNA in OVA-induced asthmatic mice. Significantly higher cellular uptake of Tf-LMW-PEI nanoparticles in CD4+ T cells in asthmatic mice compared with that of LMW-PEI was observed. In addition, there was no difference in terms of cellular uptake of Tf-LMW-PEI/siRNA, LMW-PEI/siRNA and free siRNA-AF647 on CD4+ T cells in healthy control animals. In vitro and in

vivo studies proved that Tf-LMW-PEI is another promising candidate for pulmonary delivery of siRNA for asthma treatment.

2.3.2 Macrophage targeted delivery systems

Macrophages are the most abundant inflammatory cells in the lung and are potentially involved in airway remodeling and eosinophilic inflammation in asthma. However, macrophages can perform anti-inflammatory as well as pro-inflammatory effects, so the role of macrophage in asthma is not yet clear [102]. A delivery system of siRNA that targets macrophages can be not only a therapeutic delivery vector but also a tool to facilitate the understanding of the role of macrophage in asthma. Kim et al. described a siRNA delivery system targeting macrophages through a macrophage expressing nicotinic acetycholine receptor (AchR) that binds the peptide rabies virus glycoprotein (RVG). To target and deliver siRNA to the macrophages in the nerve system for the treatment of neuroinflammatory diseases, RVG was linked with nona-D-arginine residues (RVG-9R). The authors first confirmed that RVG-9R can selectively deliver FITC-labeled siRNA to primary splenic murine macrophage (CD11b+) in vitro. Then the in vivo targeted delivery to peripheral and nerve system macrophages mediated by AchR were shown by comparing the median fluorescent intensity of CD11b+ macrophages from wild type or AchR knock out mice that had been i.v. administrated with RVG-9R/FITC-siRNA. The therapeutic effect of RVG-9R

prepared with siRNA against TNF-α was test in a lipopolysaccharide (LPS)-induced murine inflammatory model. I.v. administration of RVG-9R/ siTNF-α was reported to significantly inhibit the increased secretion of TNF-α in blood and brain compared with RVG-9R/luciferase siRNA and was shown to protect the neurons from LPS-induced apoptosis [103]. Another macrophage targeting system is mediated by folic acid as it has been discovered recently that folate receptors are upregulated on activated macrophage during the inflammatory process [104]. Inspired by this property, Yang et al. linked folic acid with chitosan (FA-chitosan) to target macrophages for anti-inflammatory effects. Up to 62% in vitro gene silencing was achieved with FA-chitosan nanoparticles prepared with siRNA against GAPDH on LPS activated RAW 264.7 cells. The biodistribution of i.v. injection of FA-chitosan encapsulating Cy5 labeled siRNA was monitored in a murine subcutaneous inflammation model using an IVIS® 200 imagine system. Accumulation of Cy5-siRNA/FA-chitosan nanoparticles was observed in the LPS induced lesion site while no clear fluorescent signal was detected in the Cy-5siRNA/chitosan group [105].

2.3.3 Targeted delivery systems for other cell types

Dendritic cells (DCs), the most efficient antigen presenting cells (APCs), can initiate and maintain the inflammatory response; hence they are another popular target cell type in asthma. A strategy to target DCs was described by

Zheng et al who encapsulated siRNA in liposomes decorated with DC-specific antibody DEC-205 which are so-called immunoliposomes (siILs). The siILs prepared with siRNA against CD40 were shown to more efficiently silence the expression of CD40 in DCs derived from bone marrow (BMDCs) compared with GenePORTER® in vitro. The biodistribution of siILs encapsulating Cy3-labeled siRNA after i.v. injection was observed on the tissue sections of liver, spleen and kidney. was Accumulation of siILs/Cy3-siRNA in the spleen at 4 hours and even stronger accumulation at 8 hours after injection was observed, but no detectable siILs were found in the kidney at any time point. In contrast, naked Cy3-siRNA was cleared through kidney soon after injection, suggesting siILs nanoparticles may selectively accumulate in the DCs-rich tissues like the spleen and have a long circulation time with slower clearance via kidney. The in vivo gene silencing of siILs prepared with CD40 siRNA was determined in mice with inflammation induced by keyhole limpet hemocyanin/complete Freund adjuvant. Significant CD40 knockdown in DCs was achieved in animals treated with siILs/CD40 siRNA or naked CD40 siRNA compared to mice administered with siILs/ negative control siRNA, IgG coupled non-targeted liposome and PBS. However, silencing of CD40 expression induced by siILs/CD40 siRNA can last at least 12 days while that induced by naked CD40 siRNA did not last this long. Meanwhile, the authors also measured the expression of CD40 in B cells and concluded that the CD40

silencing of siILs nanoparticles selectively happened in DCs[106]. In contrast, another APC-targeted delivery system can transport siRNA to more than just DCs. TLR9 is an endosomal location toll like receptor (TLRs) which can bind with CpG oligonucleotides and facilitate the uptake of siRNA to the cytosol. This receptor is as well expressed on various APCs including DCs, B cells and macrophages. Uncontrollable growth of immune cells can result in blood cancer, for example, B cells lymphoma. Immunosuppression is a common obstacle in cancer therapy, and therefore, immune cells are important therapeutic targets in anti-cancer treatment. To target and deliver siRNA to human hematopoietic cells for anti-tumor therapy, siRNA against STAT3 was covalently linked to CpG oligonucleotides by Zhang et al. The selective cellular uptake of CpG-Cy3-siRNA in primary human DCs, monocytes and B cells was observed via flow cytometry but not in T cells and natural killer cells. After intratumoral injection of the CpG-siSTAT3 in murine subcutaneous tumor models (established by KMS-11, MonoMac6, MV4-11 or A20 tumor cells), the in vivo gene silencing in tumor cells and the inhibition of tumor growth were significantly higher than with the control CpG- luciferase specific siRNA [107].

Except inflammatory cells, lung structure cells are thought to be therapeutic targets for asthma. Beta2-adrenergic receptor (β_2-AR) is abundant on bronchial smooth muscle cells and is the target for β_2-AR agonist bronchodilators. Therefore,

Luo et al. conjugated β_2-AR agonist salbutamol to guanidinylated chitosan (SGCS) as a pulmonary delivery carrier of siRNA to improve the efficacy of gene silence. SGCS formulated with siRNA against EGFP yielded nanoparticles with sizes of around 100 nm and zeta-potentials of 2-4 mV. Nanoparticles were nebulized and the aerosol was collected and was i.t. sprayed into the lung of EGFP transgenic mice on three consecutive days. The in vivo GFP gene silencing of SGCS was significantly better than that of non-targeted GCS determined by confocal microscope and western blot [108].

2.4 Conclusion

In the last decades, many groups have tried to translate siRNA mediated RNAi into a biocompatible, efficient and long term therapy to treat the airway inflammation in asthma. Lots of novel therapeutic targets have been discovered and numerous studies have been performed with the results of significant anti-inflammatory effects. However, asthma is such a complex inflammatory disorder which involves various factors, thus blockage of a single mediator or receptor cannot efficiently relieve the symptoms. Accordingly, the delivery of siRNA mixtures against multiple genes or against the upstream factors in the inflammatory process such as transcription factors, kinases or costimulatory molecules may be more effective. Furthermore, the lack of efficient and specific siRNA delivery systems results in low therapeutic efficiency and high potential of

side effects. Although, there are several ligand-receptor mediated targeted delivery systems of siRNA that could potentially be applied in asthma, none of the current immune cell targeted delivery systems has been optimized for asthma disease except the Tf-LMW-PEI conjugate reported by our group. Therefore, further studies and tests are required to develop an efficient siRNA delivery system for asthma therapy.

CHAPTER 3 TARGETED DELIVERY OF SIRNA TO ACTIVATED T CELLS VIA TRANSFERRIN-POLYETHYLENIMINE (TF-PEI) AS A POTENTIAL THERAPY OF ASTHMA

Please note that part of the content of this chapter is from a research article, "Targeted Delivery of siRNA to Activated T Cells via Transferrin-Polyethylenimine (Tf-PEI) as a Potential Therapy of Asthma", was published in Journal of Controlled Release (**Y. Xie,** et al., 2016). The authors of this article include Na Hyung Kim, Venkatareddy Nadithe, Dana Schalk, Archana Thakur, Ayşe Kılıç, Lawrence G. Lum, David JP Bassett, Olivia M Merkel and me. I am the first author of this research paper. I performed the experiments and wrote the paper.

3.1 Introduction

siRNA mediated gene therapy could potentially be an alternative and safer therapy for asthma. However, as discussed in **Chapter 2**, lack of an efficient in vivo delivery system of siRNA and an effective molecular biological target limits the clinic application of siRNA in asthma. Inflammation in asthma is driven by an infiltration of inflammatory cells such as activated T cells (ATCs), eosinophils and mast cells. Among infiltrated inflammatory cells, ATCs, specifically, T helper 2 cells (Th_2) play a critical role in orchestrating pathological processes of asthma via the production of Th_2 cytokines [69-70, 109]. Therefore, blockage of the functions of

Th_2 interleukins (e.g. IL-5 [110]) or silencing of upstream transcription factors which promote the production of Th_2 interleukins (e.g. GATA-3 [11]) have been investigated as potential therapies of difficult-to-treat asthma.

Substantial investigations have been undertaken for applying siRNA to silence asthma related genes in Th_2 cells (e.g. IL-5 [80] and GATA-3 [111]). Nevertheless, safe and effective delivery of siRNA is facing several challenges. The hurdles are to overcome various physiological barriers including enzymatic degradation, non-specific binding to non-target tissues or cells, negatively charged cellular membranes, endosomal escape after endocytosis, and many more [112]. Moreover, delivery of siRNA to Th_2 cells is particularly difficult because T cells are in general resistant to non-viral vector-based transfection methods [98a]. T cells do not actively endocytose nanoparticles because they do not express caveolin and are devoid of caveolae [113]. Conventional transfection approaches of T cells are viral delivery systems [114] or electroporation [98b]. However, the fabrication of viral vectors is time and cost consuming, and their potential safety issues limit their clinical application [97a]. On the other hand, electroporation is not a suitable method for in vivo administration of siRNA [115]. Various delivery systems have been discovered to target T cells, including CD3 targeted polyethylenimine (PEI) [116], CD40L targeted liposomes [117], CD7 targeted chitosan [101] or oligo-arginine [100]. However, their efficiency and potential systemic side effects for asthma therapy

remain to be tested. Since CD7 and CD3 are pan T cell surface antigens and since nanomedicines targeting these receptors were all applied through systemic administration in their respective in vivo studies, it would be expected to observe side effects with these strategies.

In order to avoid potential systemic side effects and to increase the selectivity for activated T cells, the key mediators in asthma pathogenesis and development, our group has developed a pulmonary siRNA delivery system based on transferrin-polyethylenimine (Tf-PEI). This ligand-polymer conjugate takes advantage of the increased expression of transferrin receptors (TfR) on T cells after activation [118]. TfR is a membrane protein expressed at low level on most cells and can bind to the iron transport glycoprotein Tf, which consequently triggers fast internalization [57b]

. Previously, we showed that only activated primary T cells take up siRNA delivered by Tf-PEI, while naïve T cells with a basal level of TfR expression cannot be reached efficiently with the Tf-PEI conjugate for siRNA delivery [91]. Low molecular weight PEI (5k Da) is used as a carrier of siRNA to facilitate cellular internalization and endosomal escape [119] with minimal toxicity [51, 120]. N-succinimidyl 3-(2-pyridyldithio) propionate (SPDP) as a crosslinker can introduce a disulfide bond between Tf and PEI. Disulfide bonds are stable extracellularly but

can be reduced in the endosome compartment [101] and allow PEI/siRNA polyplexes to be released from the Tf/TfR complex prior to rapid recycling of TfR.

In this chapter, a pulmonary delivery system that can selectively and efficiently deliver siRNA to activated T cells in the lung was developed and could be potentially applied for asthma therapy. In the following present work, Tf-PEI exhibited optimal physicochemical properties in terms of siRNA condensation efficiency, size, zeta-potential and stability in the presence of lung surfactant and mucin. In vitro studies revealed that Tf-PEI can efficiently deliver siRNA to primary human ATCs or Jurkat cells and mediated significant gene knock down. Biodistribution of Tf-PEI polyplexes formulated with fluorescently labeled siRNA in a murine asthmatic model after intratracheal administration confirmed that Tf-PEI can selectively deliver siRNA to ATCs in vivo.

3.2 Material and Method

3.2.1 Materials

N- succinimidyl 3-(2-pyridyldithio) propionate (SPDP) was purchased from Pierce (Rockford, IL), SYBR Gold dye and Lipofectamine 2000 were obtained from Life Technologies (Grand island, NY), branched low molecular weight (LMW) 5k Da PEI (Lupasol® G100) was from BASF (Ludwigshafen, Germany), murine transferrin, picrylsulfonic acid solution (TNBS, 5% w/v), Dulbecco's phosphate buffered saline (PBS), dimethyl sulfoxide (DMSO),

ethylenediaminetetraacetic acid disodium salt dehydrate (EDTA), type II mucin from porcine stomach, and albumin from chicken egg white (OVA) were bought from Sigma-Aldrich (St. Louis, MO). Chloroquine diphosphate was from MP biomedicals (Santa Ana, California), human holo-transferrin was purchased from EMD Millipore (Billerica, MA), 1,4-Dithio-DL-threitol (DTT, 99%) was obtained from Alfa Aesar (Ward Hill, MA). Amine modified siRNA (5´-pACCCUGAAGUUCAUCUGCACCACcg, 3´-ACUGGGACUUCAAGUAGACGUGGUGGC), human glyceraldehyde- 3-phosphate- dehydrogenase (GAPDH) siRNA (5´-pGGUCGGAGUCAACGGAUUUGGUCgt, 3´-UUCCAGCCUCAGUUGCCUAAA- CCAGCA), and scrambled siRNA (5´-pCGUUAAUCGCGUAUAAUACGCGUat, 3´-CAGCAAUUAGCGCAUAUUAUGCGCAUAp) were purchased from Integrated DNA Technologies (Coralville, IA) (indication of modified nucleotides: “p” denotes a phosphate residue, lower case bold letters are 2´-deoxyribonucleotides, capital letters are ribonucleotides, and underlined capital letters are 2´-O-methylribonucleotides). A 0.4% trypan blue solution in phosphate buffered saline was purchased from HyClone GE healthcare (Buckinghamshire, UK).

3.2.2 Synthesis of transferrin-polyethylenimine (Tf-PEI) conjugate

For the first reaction, 5k PEI (1 mg/ml) dissolved in HEPES buffered saline (HBS) (20 mM HEPES, 150 mM NaCl, pH=7.5) was mixed with a 10-fold molar excess SPDP (20 mM) in dry DMSO and stirred for overnight. A Tf solution (10 mg/ml, human or murine) was dissolved in HBS and stirred with a 5-fold molar excess SPDP for 2 h. Purification of PEI-SPDP and Tf-SPDP were performed via 3,000 or 10,000 MWCO centrifugal filters (Millipore, Billerica, MA) with HBS/1 mM EDTA (pH=7.1), respectively. To estimate the concentration of SPDP in the PEI-SPDP solution, 100 µl of 50-fold diluted PEI-SPDP solution was reacted with 1 µl of a 150 mM DTT solution for 30 min, and the pyridon-2-thion release was measured spectrophotometrically at 343 nm in a 96-well UV plate (Corning). Subsequently, a 10-fold molar excess DTT was mixed and reacted with the remaining PEI-SPDP under nitrogen protection for 2 h. Reduced PEI-SPDP was purified by 3,000 MWCO centrifugal filters with HBS/20 mM EDTA (pH=7.1). For the coupling reaction, Tf-SPDP was added stepwise to PEI-SPDP and stirred overnight at 4 C°. Purification of Tf-PEI was achieved on an ÄKTA FPLC system (GE healthcare) equipped with 2 connected 1 ml HiTrap SP HP cation exchange column (GE healthcare) as described before [121]. Free Tf was washed out with 0.5 M NaCl/20mM HEPES and Tf-PEI was eluted after initial binding to the column after switching to 3 M NaCl/20 mM HEPES. Further purification and desalination

was performed by 30,000 MWCO centrifugal filters (Millipore) with HBS. The concentration of Tf in the Tf-PEI conjugate was determined spectrophotometrically at 280 nm. To determine the concentration of PEI in Tf-PEI, a standard curve was generated by diluting PEI in a solution containing a constant concentration of Tf. According to the standard curve, the concentration of PEI in Tf-PEI conjugate was assessed at wavelength 405 nm using a TNBS assay[122].

3.2.3 Preparation of polyplexes

Polyplexes were prepared in either HBS or 5% glucose. An equal volume of Tf-PEI or PEI was added to a defined amount of siRNA solution to yield different amine to phosphate ratios (N/P ratios) and incubated for 20 min before further measurement or transfection. Lipofecatmine 2000 (LF) lipoplexes preparation was performed according to the manufacturer's protocol. Briefly, every 10 pmol siRNA were formulated with 0.5 µl LF. The amount of PEI or Tf-PEI needed at different N/P ratio for 50 pmol siRNA were calculated according to the following equation: m (PEI in pg) = 50 pmol × 43.1 g/mol × N/P × 52 (protonable unit of PEI = 43.1 g/mol, number of nucleotides of 25/27mer siRNA = 52).

3.2.4 Hydrodynamic size and zeta-potential measurement

For the measurement of size, PEI or Tf-PEI polyplexes were prepared with 50 pmol siRNA in HBS at different N/P ratios. The total volume of 100 µl polyplexes was added into a disposal micro cuvette (Brand GMBH, Wertheim, Germany) and the size was measured using a Zetasizer Nano ZS (Malvern Instruments Inc., Westborough, MA). The measurement was set up at 173° backscatter angle and 15 runs were performed three times for each sample. For data analysis, 0.88 mPa*s for viscosity and 1.33 for refractive index were used with the Zetasizer Software (Malvern). Subsequently, polyplexes were diluted with Nanopure water (Thermo scientific) to 1 ml and transferred to a folded capillary cell (Malvern) and zeta-potential measurements were performed three times for each sample using the Zetasizer Nano ZS (Malvern).

3.2.5 SYBR gold dye binding assay

To measure siRNA condensation efficiency of the conjugates in comparison to the unmodified polymer, siRNA in 5% glucose was distributed in a FluoroNunc 96-wells white plate (Thermo Fisher Scientific, Waltham, MA) at a concentration of 50 pmol/50 µl per well followed by adding 50 µl of different concentration of either PEI or Tf-PEI to form polyplexes at different N/P ratios. After 20 min incubation, 30 µl of 4 × SYBR gold solution was added to each well and incubated for 10 min in the dark. SYBR gold fluoresces when it intercalates

with free siRNA but not if siRNA is not accessible due to condensation and protection by polymers. The fluorescence was quantified using a Synergy 2 multi-mode microplate reader (BioTek Instrument, Winooski, VT) at excitation wavelength of 485/20 nm and emission wavelength of 520/20 nm. Fluorescence of free siRNA (N/P=0) represents 100% of free siRNA.

To evaluate the stability of polyplexes, release of siRNA from polyplexes in presence of lung surfactant Alveofact® (Boehringer-Ingelheim, Germany) or mucin was determined by a modified SYBR gold assay [22]. While the surfactant assay measures siRNA release from polyplexes by surface-active phospholipids, the mucus assay determines polyplexes instability in presence of mucus glycoproteins. Tf-PEI and PEI polyplexes were prepared with siRNA at N/P 7.5 and distributed in a 96-well white plate at a concentration of 50 pmol siRNA/100 µl per well. After 15 min incubation, 50 µl of 4 x SYBR gold solution was added to each well and incubated for 10 min in the dark. Subsequently, 50 µl of a serial dilution of Alveofact® or mucin was added (final concentrations: 0, 0.0005, 0.005, 0.05, 0.25, 0.5 mg/ml) and incubated for additional 20 min in the dark before measurement of the fluorescence. To account for the autofluorescence of mucin, free siRNA samples were prepared in the presence of according concentration of mucin. The experiment was performed in replicates of three and fluorescence of free siRNA represents 100% siRNA release.

3.2.6 Cell culture

Peripheral blood mononuclear cells (PBMCs) were obtained from healthy donors (KCI protocol 2007-012). This protocol was approved by the Wayne State University Human Investigation Committee. PBMCs were cultured at a concentration of 10^6 cells/ml in RPMI-1640 with HEPES & L-Glutamine cell culture medium (Lonza, Walkersville, MD) supplemented with 10 % heat inactivated fetal bovine serum (FBS) (v/v) (Sigma), 1 x penicillin/streptomycin (pen/strep) (Corning, Corning, NY) and 2 mM L- Glutamine (Gibco® Thermo Fisher Scientific). Peripheral resting T cells in PBMCs were stimulated with anti-CD3 monoclonal antibody (OKT3, Ortho Biotech, Horsham, PA) at a final concentration of 20 ng/ml and expanded with 100 IU/ml human recombinant interleukin-2 (IL-2), Novartis). Jurkat cells, a human T lymphocytes cell line, were a kind gift from Dr. Larry H. Matherly (Karmanos Cancer Institute). Jurkat cells were cultured in the same media as primary T cells. A549 cells, a human epithelial cell line derived from lung carcinoma, were obtained from ATCC (Manassas, VA, USA) and cultured in DMEM media (Corning) supplemented with 10% FBS and 1× pen/strep. All cells were grown at a humidified atmosphere with 5% CO_2 at 37 C°. Primary ATCs were frozen at -130 C° in 50% FBS, 40% growth media and 10% DMSO on different post-activation days for later experiment.

3.2.7 Immunofluorescent staining

Human ATCs, harvested on different post-activation days, or Jurkat cells were washed with PBS and 400,000 cells per sample were resuspended with 10 µl 50-fold diluted human FcR binding inhibitor (ebioscience, San Diego, CA) for 5 min on ice, followed by staining with 2 µl of PE labeled human CD71 antibody (OKT9, ebioscience) or PE labeled mouse IgG1 isotype control antibody (P3.6.2.8.1, ebioscience) for 30 min at 4 °C protected from light. Afterward, cells were washed twice and resuspended with 400 µl ice cold PBS/2 mM EDTA before they were analyzed with an Attune® Cytometer (Life Technologies). The cellular suspensions were measured with 488 nm excitation and the emission filter set of 574/26 nm. On day 6 post-activation, ATCs were counterstained with a CD71 antibody and a PE-Cy7 labeled human CD3 antibody (UCHT1, Molecular probes). The samples were measured with 488 nm excitation and emission filter of 574/26 nm and 640 LP in an Attune® Cytometer (Life Technologies). A viable lymphocyte population was gated according to morphology based on forward and sideward light scattering within which 10,000 events were evaluated. All results are given as median fluorescent intensity (MFI). Data analysis was performed using Attune® cytometer software (Life Technologies).

3.2.8 Quantification of cellular uptake

Amine modified siRNA was labeled with succinimidyl ester (NHS) modified Alexa Fluor 488 (AF488) (Life technologies) following the manufacturer's protocol and purified by ethanol precipitation and spin column binding as described previously [123]. For uptake experiments, 50 pmol siRNA-AF488 was prepared with Tf-PEI or PEI in 5% glucose at different N/P ratios (N/P ratio: 5, 7.5, 10, 15, 20) or with LF. The day before the experiment, 400,000 ATCs or Jurkat cells were seeded in 96 well plates (Thermo scientific) at a concentration of 2×10^6 cells/ml and transfected with the polyplexes/lipoplexes for 24 h. Samples were washed three times and resuspended in 400 µl PBS/2 mM EDTA. For initial experiments, ATCs were transfected with low N/P ratio treatment groups were analyzed using a BD LSR II flow cytometer (BD bioscience, San Jose, CA). For later experiments, ATCs or Jurkat cells were transfected with high N/P ratios (10, 15, 20, or 5, 10, 20), and samples were analyzed using an Attune® Cytometer (Life Technology) with 488 nm excitation and emission filter of 530/30. The cells were gated according to morphology within which 10,000 events were evaluated.

For trypan blue quenching assays, ATCs were treated by Tf-PEI or PEI polyplexes at N/P 20 or LF lipoplexes for 24 h. Each sample was divided into two halves; one half was washed once with 0.4% trypan blue to quench the extracellular fluorescent signal then washed with cold PBS/2 mM EDTA three

times, the other half was only washed three times. Samples were resuspended in 400 µl PBS/2 mM EDTA and analyzed with an Attune® Cytometer (Life Technology) as described above.

For the competition cellular uptake study, 400,000 Jurkat cells were seeded in 96 well plates at a concentration of 4×10^6 cells/ml. Subsequently, Tf was dissolved in growth media as a Tf stock solution (20 mg/ml), and predetermined amounts of Tf stock solution and growth media were added into the cell suspension to achieve desired Tf concentrations (0, 0.1, 2 mg/ml) at a fixed cell concentration (2×10^6 cells/ml). The cells were then incubated with free Tf for 30 min and transfected afterwards with Tf-PEI or PEI at N/P ratio 15 for 4 h. Cellular uptake was quantified using flow cytometry as described above. The experiment was conducted in duplicate.

3.2.9 Confocal Laser Scanning Microscopy

Jurkat cells were seeded in 96 well plates as described above and transfected with Tf-PEI and PEI polyplexes formulated with 50 pmol siRNA-AF488 at N/P ratio of 15. LF was included as control. After 24 h incubation, cells were transferred to 1.5 ml tubes and washed once with PBS followed by fixation with 4% paraformaldehyde (PFA) solution in PBS (Affymetrix, Thermo Fisher) for 20 min. After fixation, the cells were washed with PBS and the nuclei were stained with 5 µM of DRAQ5 (Invitrogen, Thermo Fisher) for 5 min followed by

washing the cells with PBS. The cell pellet was resuspended in 20 µl Fluoromount mounting medium (Southern Biotech, Birmingham, AL, USA), and the cell suspension was dropped on slide and covered with a coverslip (Fisherbrand, 12CIR. -1). Slides were imaged by a Leica TCS SPE-II laser scanning confocal microscope (Leica, Wetzlar, Germany), and the images were exported from the Leica Image Analysis Suite (Leica).

3.2.10 In vitro GAPDH gene knockdown

For gene silencing experiments, 400,000 ATCs or Jurkat cells were seeded in a 96 well plate and triplicates of samples were treated with Tf-PEI, PEI or LF polyplexes/lipoplexes prepared with 50 pmol for ATCs or 100 pmol for Jurkat cells for 24 h using either hGAPDH siRNA or scrambled siRNA at N/P 15. Cells were harvested and processed to isolate total RNA using the PureLink^{TM} RNA mini kit (Life techonologies) according the manufacturer's protocol with DNase I digestion (Thermo scientific). Synthesis of cDNA from total RNA and PCR amplification were performed with Brilliant III ultra-fast SYBR® green QRT-PCR master mix kit (Agilent Technologies, Santa Clara, CA) using a Stratagene Mx 3005P (Agilent Technologies). Cycle threshold (Ct) values were determined by MxPro software (Agilent Technologies). A standard curve including 5 points was made from a 1:5 serial dilutions of an untreated sample and assigned concentrations of each point (1, 0.2, 0.004, 0.0008, 0.00016) were plotted vs. their

corresponding Ct values. The gene expression of GAPDH was normalized by the expression of β-actin. Hs_GAPDH_2_SG primers for GAPDH and Hs_ACTB_2-SG primers for β-actin (Qiagen, Valencia, CA) were used in experiment.

3.2.11 Cytotoxicity assay

For measuring the biocompatibility of polyplexes, 8,000 A549 cells were seeded in a sterile, white 96 well plate (Corning) at a concentration of 40,000 cells/ml for 24 h. Polyplexes were prepared with Tf-PEI, 5k PEI and 25k PEI with 50 pmol scrambled siRNA at different N/P ratios (1, 3, 5, 7.5, 10, 15, 25, 30, 40) and diluted with 5 % glucose to a final volume 40 µl. The polyplexes were then mixed with 60 µl of growth media, old media in the well plate was removed, and 100 µl media containing polyplexes was added and incubated for 24 h. The release of lactate dehydrogenase (LDH) from the cells was determined using a CytoTox-ONE™ kit purchased from Promega (Madison, WI) following the manufacturer's protocol. The "no cell" control served as 0% LDH release and cells treated with lysis buffer represent 100% LDH release. Experiments were conducted in triplicate.

3.2.12 Cellular distribution of polyplexes in a murine asthma model

All animal experiments were approved by a Wayne State University Institutional Animal Care and Use Committee. Balb/c mice were purchased from Charles River Laboratories (Boston, MA) and used at 5 weeks' age. The murine

asthma model was established as described before [75a]. Briefly, animals were sensitized by intraperitoneal (i.p.) injection of 0.2 ml suspension of ovalbumin (OVA) and $Al(OH)_3$ (10 µg OVA and 2 mg $Al(OH)_3$) on day 0 and day 14 (Figure 13 A). On days 24, 25, and 26, mice were challenged by inhalation of aerosolized 1% OVA for 1 h to establish experimental asthma while mice that inhaled saline were used as healthy control group. On days 35, 36, 37 and 38, mice were intratracheally (i.t) instilled (under ketamine/xylazine anesthesia) with 50 µl Tf-PEI or PEI polyplexes, prepared with 750 pmol Alexa Fluor 647 (Life technologies) labeled siRNA at N/P 7.5, or free siRNA-AF647 as control. On days 36, 37 and 38, before the i.t. administration, a second series of daily OVA or saline challenges was performed. On day 39, noninvasive lung function of animals was determined by whole-body plethysmography. Changes in the delayed pause in breathing as an indicator of altered bronchial responsiveness to increasing aerosol challenge concentrations of β-methacholine was monitored (Buxco Electronics Inc., Wilmington, DE) [124]. On day 40, all animals were sacrificed under i.p. ketamine/xylazine anesthesia, exsanguinated and perfused with PBS. Bronchoalveolar lavage fluid (BALF) and BALF cells were collected [125] and lung cell suspensions were prepared as reported before [60]. BALF cells and lung suspension cells were counterstained with PerCP-Cy 5.5 labeled anti-CD45 (30-F11, ebioscience), PE-Cy7 labeled anti-CD4 (GK1.5, eBioscience), a primary anti-

prosurfactant protein C antibody (proSPC) (1:100, abcam), pacific blue labeled goat anti-mouse IgG secondary antibody (1:100, Life Technologies), pacific orange labeled anti-F4/80 (invitrogen), APC-Cy7 labeled anti-CD19 (MB19-1, molecular probes), and PE labeled anti-CD49d (R1-2, Molecular Probes) antibodies following the manufacturer's protocols. Cell differentiation was performed on a BD LSR II flow cytometer (BD bioscience). The staining strategy was shown in Table 2. The different cell populations of macrophage/monocytes (F4/80+), T cells (CD4+, F4/80-), eosinophils (CD4-, CD49d+), and epithelial Type II pneumocytes (proSPC+) were gated, and the MFI of siRNA-AF647 in all different cell populations was quantified. To quantify cellular uptake of polyplexes in T cells only, lung suspension cells were stained with a PE-Cy7 labeled anti-CD4 antibody. T cells were gated based on morphology, and the MFI of siRNA-AF647 was quantified within CD4+ cells by an Attune® Cytometer (Life Technology). The concentration of interleukin-5 (IL-5) and interleukin-13 (IL-13) in BALF was determined by the mouse cytokine 20-plex panel (Invitrogen) using a Bio-Plex® System (Bio-Rad Lab., Hercules, CA) following the manufacturer's protocol. Interleukin concentrations below the detection limitation were reported as 0 pg/ml.

Table 2 Strategy to differentiate cellular populations of BALF cells

	CD45(PerCP-Cy5.5)	CD4(PE-Cy7)	Pro-SPC(Pacific Blue)	F4/80 (Pacific Orange)	CD19 (APC-Cy7)	CD49d(PE)
Macophage/ Monocytes	+	+		+		+
B cells	+				+	+
Dendritic cells				+		+
T cells		+				+
Eosinophils						+
Type II pneumocytes			+			

3.2.13 Statistics

All results are given as mean value ± standard deviation (SD). One-way ANOVA with Bonferroni posthoc post-test and calculation of area under the curve (AUC) were performed in GraphPad Prism software (Graph Pad Software, La Jolla, CA).

3.3 Result and Discussion

3.3.1 Synthesis Outcome

Transfection efficiency and toxicity of PEI are often correlated to its molecular weight [126]. Here, low molecular weight PEI (5k Da) was chosen to decrease potential toxicity and non-specific transfection efficacy. Holo-Tf preferentially binds to TfR [57b] and has been reported as a targeting ligand for various diseases involving TfR overexpression using lipid-based [127] or polymer-based delivery systems carrying pDNA [44, 128], siRNA [129] or oligonucleotides [93] for anti-sense therapy. To target ATCs, holo-Tf was conjugated to PEI to increase the intracellular internalization efficiency. As shown in Figure 3, holo-Tf and 5k PEI

were reacted with the bifunctional crosslinker SPDP, respectively, and PEI-SPDP was activated by the reducing reagent DTT. Activated PEI-SPDP* (see Figure 3) was conjugated to Tf-SPDP to yield Tf-PEI. The final concentration of Tf was determined by UV absorbance at 280 nm, and the concentration of PEI was assessed by TNBS assay. The resulting molar ratio of Tf to PEI was approximately 1.5: 1. Due to the difference of molecular weights between Tf (80 kDa) and LMW PEI (5 kDa), higher coupling degrees were not expected and could in fact be disadvantageous for the interaction between PEI amines and siRNA phosphate groups.

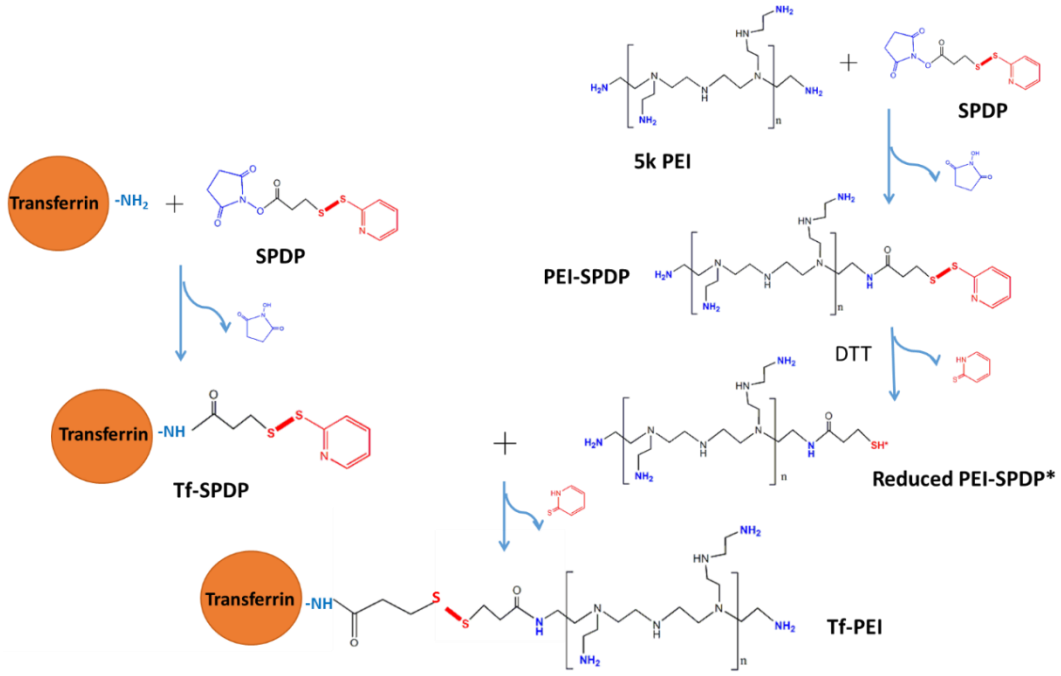

Figure 3 Synthesis scheme of transferrin-coupled polyethylenimine (Tf-PEI). Transferrin (Tf, left side) and PEI (right side) are reacted with N-succinimidyl 3-(2-pyridyldithio)-propionate (SPDP) in separate reactions. PEI-SPDP is activated by dithiothreitol (DTT) and coupled with Tf-SPDP to form a disulfide bond and the resulting Tf-PEI.

3.3.2 siRNA condensation of Tf-PEI

The siRNA condensation efficiency of a polymer is an important property to evaluate the suitability of a carrier for siRNA. To determine whether the presence of Tf would affect the ability of PEI to condense siRNA, the condensation efficiency of Tf-PEI was determined by SYBR® Gold assays, and unmodified 5k PEI was used as a control. SYBR gold is a nucleic acid-intercalating fluorescent dye. When siRNA is condensed by polymer and becomes inaccessible to SYBR gold, consequently a decrease of fluorescence is observed. As shown in Figure 4, PEI can completely condense and protect the siRNA at N/P 5 which was consistent with previous reports [75b]. On the other hand, both human and mouse Tf-PEI condensed siRNA to 80% at N/P 5, and complete condensation of siRNA was observed at N/P 7.5. The difference may be due to steric hindrance of Tf which impacts the interaction between siRNA and the primary amines in PEI. It also needs to be taken into consideration that by coupling Tf to PEI, a few primary amines would be expected to no longer be available for interaction with siRNA. However, the influence of the Tf modification on condensation efficacy of the conjugate is limited, with full condensation still achievable at a comparably low N/P ratio of 7.5.

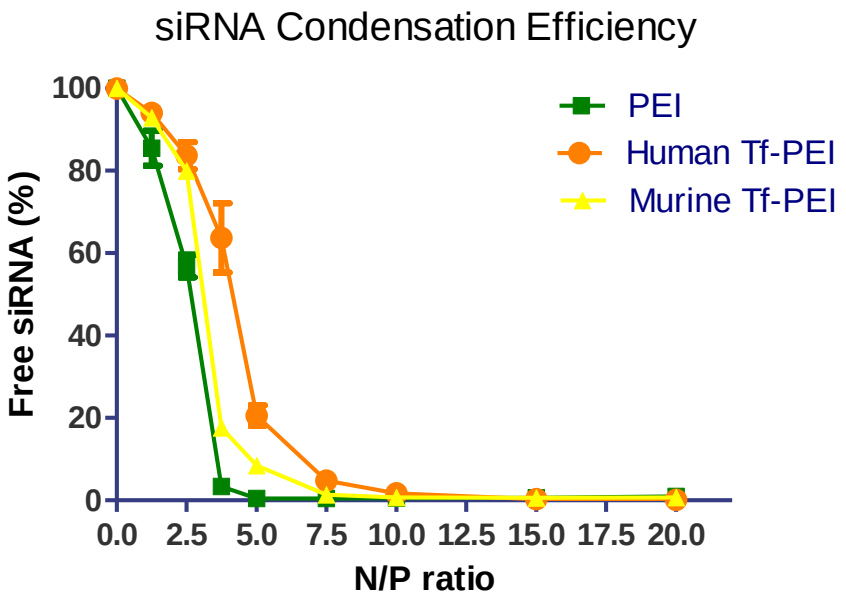

Figure 4 SYBR gold assay of PEI and Tf-PEI. The siRNA condensation efficiency of PEI and Tf-PEI was measured by SYBR gold assay at different N/P ratios: 0, 1.25, 2.5, 3.75, 5, 7.5, 10, 15, 20. Fluorescence of free siRNA (N/P= 0) represents 100% free siRNA. (Data points indicate mean +/- SD, n= 2-3; Green square: PEI polyplexes, orange circle: human Tf-PEI, yellow triangle: murine Tf-PEI)

3.3.3 Hydrodynamic diameter and zeta potential

Optimal physicochemical properties of polyplexes such as size and surface charge can facilitate efficient siRNA delivery in vitro and in vivo. Therefore, Tf-PEI or PEI polyplexes, prepared with the same amount siRNA in HBS buffer at different N/P ratios, were fully characterized for size, polydispersity index (PDI) and zeta potential by dynamic light scattering and laser Doppler anemometry. As shown in Figure 3.3 A, Tf-PEI formulations demonstrated small sizes ranging from 72 to 197 nm and PDIs ranging from 0.24 to 0.39. In comparison, PEI formed larger particles of 1133 nm to 1595 nm in size with PDI of approximately

0.3. Both formulations demonstrated acceptable size distributions with PDIs mostly below 0.3 indicating homogeneous morphology and little aggregation which is an important factor for successful transfection. Size of polyplexes is another key factor for efficient transfection, and small sizes (<200 nm) of the Tf-PEI polyplexes could ensure higher stability and better intracellular uptake efficiency especially into ATCs compared with large PEI polyplexes (>1000 nm) [130]. Considering that Tf is a very soluble glycoprotein, it is possible that Tf decorates the surface of Tf-PEI polyplexes and a resulting steric stabilization of Tf contributes to the much smaller size of the particles [128]. Consistent with this hypothesis, it has been reported that low molecular weight PEI tends to form large particles with siRNA [131] and a tendency of aggregation of PEI has been observed when preparing polyplexes in high ionic strength buffers such as HEPES buffered saline [128].

Zeta potentials of both Tf-PEI and PEI polyplexes increased with increasing N/P ratio (Figure 5 B). Tf-PEI polyplexes displayed negative charges in the range of -20 to -7 mV which is in agreement with the assumption that the negatively charged Tf may shield the positive charges of PEI and is located on the surface of the polyplexes, resulting in an overall negative zeta potential [132]. On the other hand, except at N/P 2 where the zeta potential was -28.6 ± 3.9 mV, all PEI formulations showed slightly positive charges in the range from 8.5 mV to 26 mV.

Due to the relatively “rigid” structure of short duplex siRNA and the fact that not all positively charged groups in PEI are sterically available to interact with siRNA, most of the siRNA may be on the surface of the polyplexes at a low excess of polymer, i.e. N/P 2. This could explain why a negative charge was observed at N/P 2. At higher N/P ratios, excess amount of PEI more efficiently interacts with the negative charges of siRNA resulting in positive zeta potentials of the polyplexes. Positive zeta potentials of polyplexes may hamper their penetration through lung mucus and surfactant which have negative charge [75a] and also increase their chance of non-specific delivery via adsorptive endocytosis. Additionally, multiple pulmonary administrations of positively charged nanoparticles can increase local and systemic toxicity, while in comparison, anionic nanoparticles are well tolerated [133]. Therefore, we hypothesize that Tf-PEI polyplexes would be a more efficient and safe pulmonary administrated system than PEI.

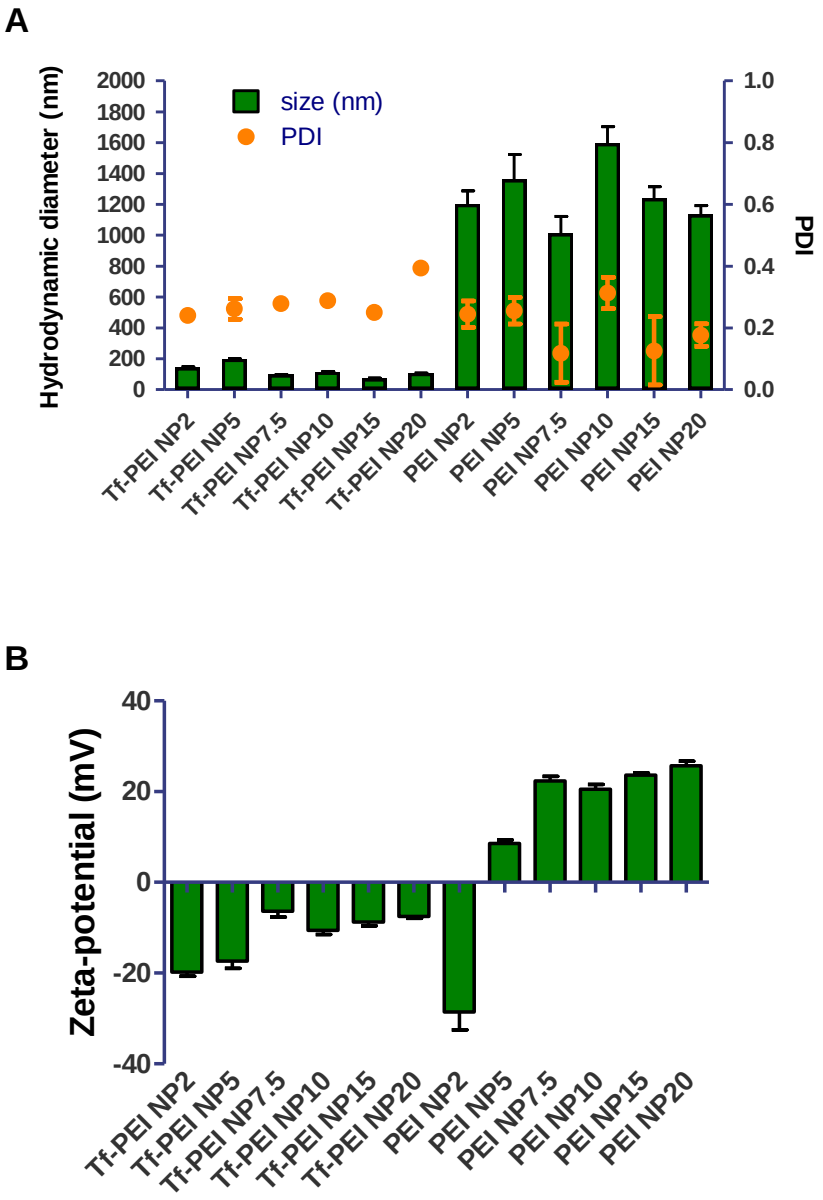

Figure 5 Size and zeta-potential of Tf-PEI and PEI. (A) Hydrodynamic diameters (left x-axis) and polydispersity indices (PDI, right x-axis) and (B) zeta-potentials of Tf-PEI and PEI polyplexes formulated with 50 pmol siRNA in HEPES buffered saline at different N/P ratios :2, 5, 7.5, 10, 15, 20. (Data points indicate mean + / - SD, n=3)

3.3.4 Stability of polyplexes in the presence of lung surfactant

The instability of polyplexes in the blood stream limit their suitability for systemic administration. To overcome this challenge, pulmonary delivery is favorable for the treatment of lung diseases due to the large application area, the absence of serum proteins, and the reduced nuclease activity [75b]. However, there are other biological barriers associated with using the airway route that need to be overcome to deliver siRNA to the lung. If epithelial cells in the upper airway are to be targeted, polyplexes need to penetrate a mucus layer before they reach the epithelium. In asthma therapy, polyplexes are mostly expected to be delivered to the deep lung, where the alveolar surface is covered by lung surfactant which presents another barrier [75a]. To investigate the stability of polyplexes in the lung, a modified SYBR® Gold assay was performed in the presence of lung surfactant Alveofact® or mucin and released siRNA was quantified. Tf-PEI polyplexes demonstrated higher stability compared with PEI polyplexes at increasing concentrations of mucin (0.0005 - 0.5 mg/ml) (Figure 6 A). Similarly, at low concentrations of surfactant (0.0005 - 0.05 mg/ml), the ability of Tf-PEI to retain siRNA was also better than that of PEI. Only 1% siRNA release from Tf-PEI polyplexes but 4.3% from PEI polyplexes was observed at 0.05 mg/ml. At a concentration of 0.25 mg/ml, PEI and Tf-PEI polyplexes released 10.9% and 10.2% siRNA, respectively. As described above, there are indications that Tf is located

on the surface of the polyplexes and consequently shields PEI/siRNA from interaction with surfactant or mucin. In contrast, at the highest concentration of surfactant (0.5 mg/ml), PEI more efficiently retained siRNA than Tf-PEI (Figure 6 B). While 13.5% of siRNA were released from PEI, 16.2% of siRNA were released from Tf-PEI polyplexes. High concentration of surfactant may induce structural changes in Tf, as a result, the ability to retain siRNA in the polyplex simply depends on electrostatic interaction between siRNA and PEI. It is expected that Tf-PEI polyplexes would release more siRNA since unmodified PEI demonstrated slightly better ability to condense siRNA compared with Tf-PEI. In 2009, we reported also that PEGylated PEIs release siRNA more efficiently than unmodified PEI [22]. It should be noted that in 2009, 25 kDa PEI was described, whereas here we used 5 kDa PEI which showed slightly lower stability in presence of surfactant and mucin compared to 25 kDa PEI complexes. However, the studied concentrations of surfactant, of which predominant composition is phospholipids (up to 70% being dipalmitoyl phosphatidylcholine (DPPC)) [134], are much higher than that in a reported simulated lung fluid (0.02% (w/v) DPPC), used for dissociation tests of inhaled pharmaceutical formulations [135]. At physiological surfactant concentrations, Tf-PEI polyplexes therefore seem to exhibit enhanced stability compared to PEI polyplexes. This observation could lead to beneficial stability after aerosol deposition in the peripheral airways. On the other hand, 91%

and 97% of siRNA, respectively, were released from Tf-PEI and PEI polyplexes at a very high concentration of 0.5 mg/ml mucin. In comparison, complexes of PEGylated 25 kDa PEI which mediated highly efficient gene knockdown in the lung showed about 30% siRNA release at mucin concentrations as low as 0.33 mg/ml [22]. Instability of siRNA polyplexes at exaggerated mucin concentrations therefore seem not to hamper efficient gene knockdown at physiological conditions. While surfactant is only present in the alveolar region, mucus lines in the upper and bronchial airways where the polyplexes are expected to mediate their therapeutic effects. Based on our experiments, mucus stability of future nanocarriers should be optimized. However, it is possible that stability in presence of surfactant plays a more important role in vivo where Tf-modification of the polyplexes was advantageous. Therefore, we hypothesize that Tf could protect the polyplexes for sufficient stability during pulmonary administration.

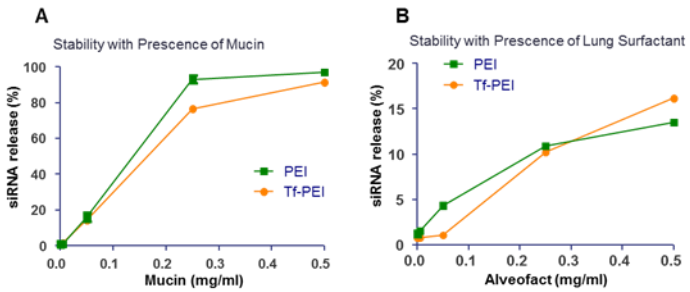

Figure 6 Stability of Tf-PEI and PEI polyplexes. Stability of Tf-PEI and PEI polyplexes at N/P 7.5 was determined by modified SYBR gold assay after 20 min incubation with increasing concentration of (A) mucin and (B) lung surfactant (0.005-0.5 mg/ml). Free siRNA represents 100% siRNA release. (Data points indicate mean + / - SD, n=3; Green square: siRNA release from PEI polyplexes, orange circle: siRNA release from Tf-PEI polyplexes)

3.3.5 Determination of expression of TfR

To confirm the expression of TfR on human ATC [136], human PBMCs were activated by anti-CD3 antibody (OKT3), and the expression of TfR was quantified by flow cytometry over time. On day 0 (Figure 7 A), the TfR expression was at a basal level in PBMCs whereas the TfR expression increased dramatically from day 1 to day 5 after activation. T lymphocytes undergo rapid differentiation, proliferation, and up-regulate TfR (CD71) to meet their high consumption of iron [118]. The TfR expression level slowly decreased after day 5 post-activation, but a clearly increased level of TfR expression compared to day 0 was maintained up to day 14 post-activation. This observation may be due to the fact that T cells are activated very early and that activation also leads to proliferation[137] [118, 137]. It is possible that a) the rate of proliferation and differentiation of T cells slows down after 5 days post-activation and that b) a percentage of activated T cells becomes apoptotic resulting in lower TfR levels compared to earlier time points. However, the activated status of T cells maintains a relatively high consumption of iron compared to the resting status [118].To characterize the lymphocyte population in PBMCs after activation and to confirm the high expression of TfR on T cells, on day 6 post-activation, activated PBMCs were immunologically counter-stained with antibodies against CD3 and CD71 (TfR). Of the total cell population, approximately 90% of the cells were CD3 positive, and within this population,

more than 60% cells were TfR and CD3 dual positive cells confirming activation stimulates T cells to overexpress TfR (Figure 7 B). Overexpression of TfR was also observed in Jurkat cells (Figure 7 C). These results suggest the possibility to target primary ATCs or Jurkat cells, as a surrogate T cell line, via TfR targeting strategy.

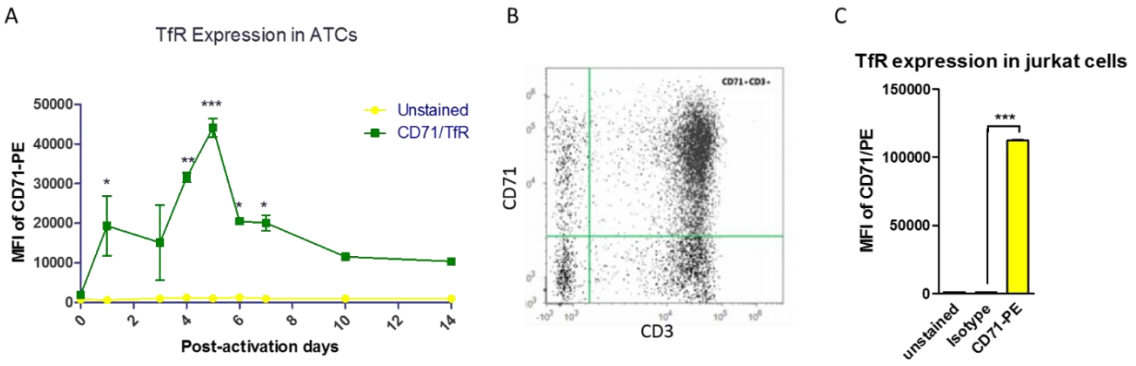

Figure 7 TfR expression in ATCs and Jurkat cells. (A) Human peripheral blood mononuclear cells (PBMCs) were activated by anti-CD3 antibody (OKT3) and stained with anti-CD71 antibody to determine the expression of CD71, namely transferrin receptor (TfR), on different post activation days. The median fluorescence intensity (MFI) of CD71 of cells were quantified by flow cytometry. (Data points indicate mean +/- SD, n=1-3; Compared with D0, *, $p< 0.05$, **, $p < 0.01$, ***, $p<0.005$). (B) ATCs were counterstained by CD71-PE and CD3-PE-Cy7 antibodies on day 6 post-activation. (C) Jurkat cells were stained with anti-CD71 antibody (TfR) or isotype antibody. The MFIs of antibody-stained of cells were quantified by flow cytometry. (Data points indicate mean +/- SD, n=2; One-way ANOVA, ***, $p<0.005$).

3.3.6 In vitro cellular uptake of polyplexes

To determine the targeting efficiency of Tf-PEI, primary ATCs were transfected for 24 h and the cellular uptake was quantified by flow cytometry. Tf-PEI polyplexes were formulated with Alexa Fluor 488 labeled siRNA (AF488-siRNA) at different N/P ratios (5, 7.5, 10, 15, 20). Unmodified PEI polyplexes and lipofectamine 2000 (LF) served as positive controls, and treatment with free siRNA and an untreated group were also included as negative controls. Initially, cellular uptake was determined at low N/P ratios (N/P= 5 & 7.5, Figure 8 A) at which 100% siRNA condensation was achieved by unmodified PEI but 80% and 100% condensation was achieved by Tf-PEI conjugates. Tf-PEI polyplexes can target ATCs, and significantly higher cellular uptake was observed compared with unmodified PEI at both N/P ratios, although only 80% siRNA were encapsulated inside Tf-PEI polyplexes at N/P 5 (Figure 5). These results were in line with our previously published results [91]. Moreover, ATC-selective delivery of Tf-PEI polyplexes was confirmed at higher N/P ratios (N/P 10, 15, 20) (Figure 8 B). Increased cellular uptake of both PEI and Tf-PEI was observed with increasing N/P ratios from 10 to 20. Tf-PEI polyplexes achieved 3.2 fold, 4.5 fold and 4.1 fold higher cellular uptake compared to PEI polyplexes at N/P 10, 15, 20, respectively. Most importantly, Tf-PEI achieved 1.8 fold more efficient cellular uptake at N/P 20 than LF mediated siRNA delivery. PEI polyplexes can non-

specifically associate on the cell surface due to electrical interaction between their positive surface charge and negative charge of cellular membranes and induce adsorptive endocytosis. This mechanism contributes to non-targeted cellular uptake. However, PEI polyplexes are not efficiently taken up by primary ATCs. These results agree with a previous report from our group which focused on the observation that Tf-PEI can selectively deliver siRNA to ATCs overexpressing TfR but not resting T cells which are TfR negative [91]. To estimate the percentage of extracellular fluorescence resulting from polyplexes that are bound but not internalized, 0.4% trypan blue quenching treatment was performed on ATCs treated by Tf-PEI (N/P 20), PEI (N/P 20), LF and free siRNA. As shown in Figure 8 C, the MFI slightly decreased in all trypan blue treated groups except the LF group. This result suggests that only a limited amount of extracellular fluorescence is associated with the surface of the cells but most of the fluorescent polyplexes were taken up intracellularly. The slightly increased MFI of the LF treated group (Figure 8 C) could be explained by the fact that apoptotic cells with a damaged cell membrane are stained completely by trypan blue and therefore no longer are detected by flow cytometry. As it is known that LF has a strong cytotoxic effect, especially on primary cells, it is possible that the MFI was skewed to only viable cells which seem to have a slightly higher MFI. To validate our results in a cell culture model, transfection experiments were also performed in Jurkat cells, which

are often used as a T cell model cell line. Jurkat cells are an immortalized lymphoma cell line, however, and not as hard-to-transfect as primary T cells. In agreement with the results obtained in ATCs, cellular uptake of Tf-PEI polyplexes in TfR-overexpressing Jurkat cells (Figure 7 C) was also significantly higher than that of PEI polyplexes (Figure 8 D). It needs to be noted, however, that the transfection efficiency of LF in Jurkat cells is higher than that of Tf-PEI polyplexes. The cellular endocytosis profile and molecular membrane composition of this immortalized cell line is expected to differ significantly from primary ATCs. Additionally, their viability under transfection is expected to be higher than that of ATCs which do not withstand the cytotoxic effects of commercially available transfection reagents. These characteristics may contribute to efficient transfection of Jurkat cell with LF, while primary ATCs are especially difficult to transfect cells [98a] and benefit from active targeting.

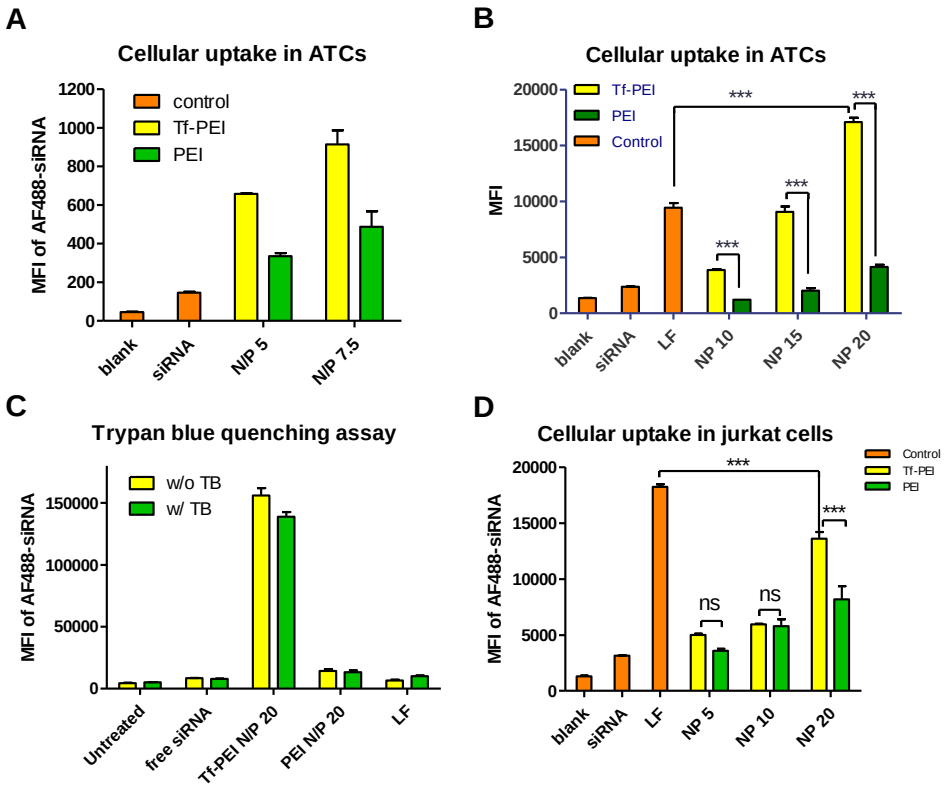

Figure 8 Cellular uptake of Tf-PEI and PEI in ATCs and Jurkat cells. MFI was determined by flow cytometry to evaluate the cellular uptake in primary human activated T cells (ATCs) of Tf-PEI, PEI and lipofectamine 2000 (LF) polyplexes/lipoplexes prepared with 50 pmol Alexa Fluor 488 labeled siRNA (AF488 siRNA) at low N/P ratios (5 and 7.5). (B) Cellular uptake of Tf-PEI, PEI and LF in ATC at high N/P ratio (10, 15 and 20). (C) Cellular uptake in ATCs of Tf-PEI, PEI and LF polyplexes at N/P 20 with or without trypan blue (TB) quench. (D) Cellular uptake in Jurkat cells of Tf-PEI, PEI and LF at different N/P ratios (5, 10 and 20). (Data points indicate mean +/- SD, n >2; One-way ANOVA, **, $p < 0.01$, ***, $p<0.005$).

For the competition assay, Jurkat cells were transfected with Tf-PEI and PEI polyplexes in the presence of different concentrations of free Tf. As shown in Figure 9, the cellular uptake of Tf-PEI polyplexes in Jurkat cells can be inhibited by the presence of free Tf and this inhibition depended on the concentration of free

Tf. The higher concentration of free Tf (2 mg/ml) can achieve significantly stronger inhibition compared to the lower concentration (0.1 mg/ml). However, free Tf has no effect on the uptake of PEI polyplexes. This result suggests that the selective delivery of Tf-PEI polyplexes to Jurkat cells was mediated by the targeting ligand. In primary cells, this effect is even stronger, as published in 2013, where almost no uptake is mediated by PEI or Tf-PEI in cells that do not express the receptor [60].

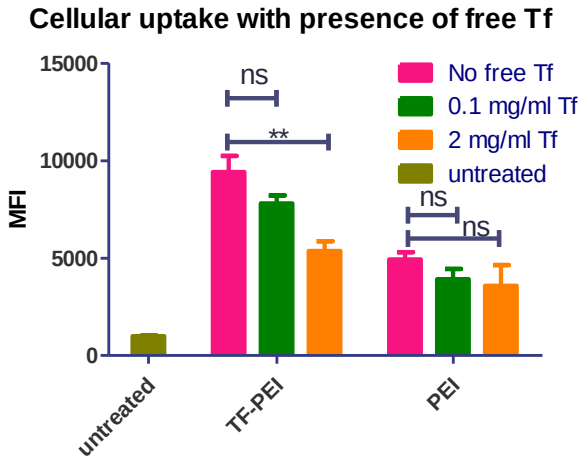

Figure 9 Free Tf competition assay. The cellular uptake in Jurkat cells of Tf-PEI or PEI polyplexes at N/P ratio 15 in presence of free Tf (0.1 and 2 mg/ml) was determined by flow cytometry (Data points indicate mean +/- SD, n= 2; One-way ANOVA, **, $p < 0.01$).

3.3.7 Confocal Laser Scanning Microscopy (CLSM)

To determine the cellular distribution of polyplexes, Jurkat cells were transfected with Tf-PEI, PEI and LF carrying siRNA-AF488 at N/P ratio of 15 for

24 h and a control, only treated with the according amount of free siRNA, was included. The cellular distribution of siRNA was observed by CLSM (Figure 10). As shown in Figure 10 A, negligible amounts of green dots (siRNA-AF488) can be observed suggesting that free siRNA cannot be efficiently delivered into the cells without carrier. The receptor-mediated cellular uptake of Tf-PEI/siRNA resulted in an even distribution of siRNA within the cytoplasm of the cells (Figure 10 D), while delivery with PEI or LF resulted in punctuated distribution (Figure 10 B and C). The point-shaped distribution of siRNA in the transfected cells could be a sign of endosomal entrapment of the LMW-PEI complexes.

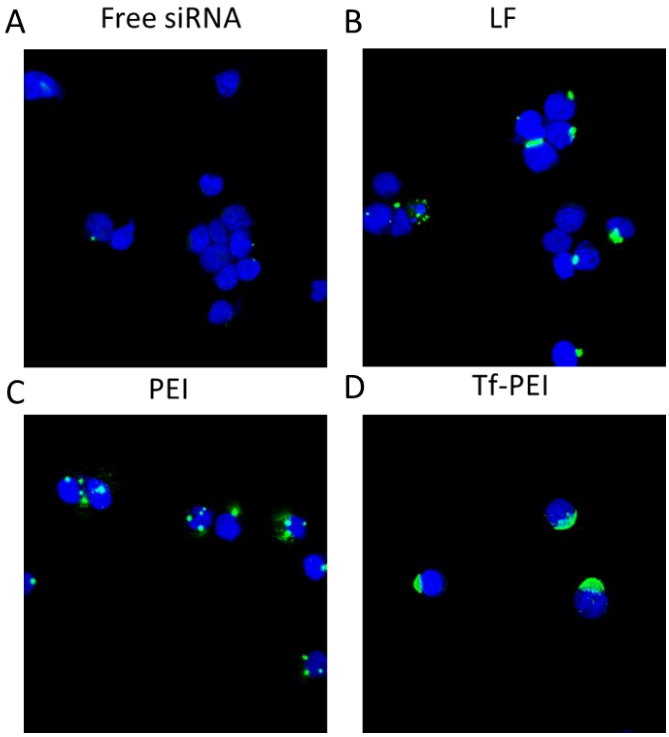

Figure 10 CLSM images of Jurkat cells. CLSM images of Jurkat cells transfected by Tf-PEI, PEI, LF and free siRNA-AF488 at N/P 15. The nuclei were stained with 5 µM of DRAQ5. (green: siRNA-AF488; blue: nucleus).

3.3.8 In vitro transfection efficacy

Next, we investigated whether the significantly higher internalization of Tf-PEI polyplexes could induce a corresponding fdownregulation of a targeted gene. Therefore, ATCs or Jurkat cells were transfected by Tf-PEI and PEI polyplexes prepared with siRNA against GAPDH or scrambled siRNA at N/P 15, and LF was included as additional positive control. GAPDH gene expression was normalized by β-actin gene expression and quantified via real time PCR (RT-PCR). As shown in Figure 11 A, GAPDH expression in ATCs treated with Tf-PEI/ siGAPDH polyplexes was 2 fold less than after transfection with PEI/siGAPDH. Moreover, significant downregulation of GAPDH expression was observed in Tf-PEI/siGAPDH group compared with Tf-PEI/scrambled siRNA group and untreated control. In contrast, there was no significant difference of GAPDH expression among PEI/siGAPDH, PEI/scramble siRNA treated cells and the untreated group. Unmodified PEI polyplexes can undergo endocytosis mediated by electrostatic interaction between their positive surface charge and the negative charge of the cellular membrane as demonstrated in cellular uptake study. However, this limited internalization was not sufficient to induce significant sequence-specific gene silencing compared with receptor mediated endocytosis. LF was too toxic for primary ATCs, and it was impossible to isolate sufficiently intact RNA after transfection. Therefore, no viable results were obtained in ATCs

and experiments were repeated in Jurkat cells. A similar outcome of GAPDH knock down was observed in Jurkat cells (Figure 11 B). CLSM images of Jurkat cells transfected with Tf-PEI and PEI polyplexes and LF lipoplexes (Figure 10) revealed the possibility that Tf-PEI could mediate more efficient endosomal escape and release siRNA into cytoplasm. This observation, taken together with the less efficient uptake of non-targeted polyplexes (Figure 8) could be one reason for the lack of gene knockdown. According to the efficient uptake results, LF mediated the most efficient gene knock down in Jurkat cells, which, however, is not representative for the transfection of primary ATCs.

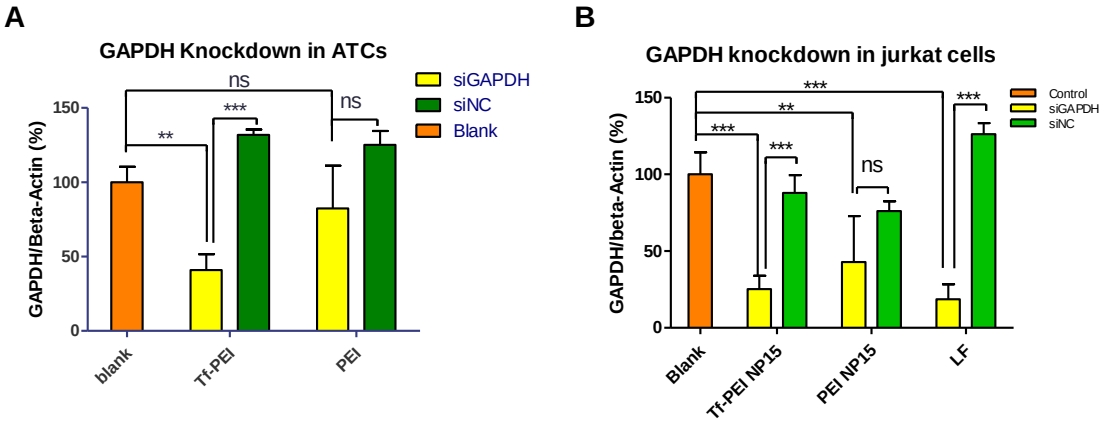

Figure 11 GAPDH Knockdown in ATCs and Jurkat cells. (A) GAPDH gene knockdown efficiency of Tf-PEI and PEI polyplexes at N/P 15 was validated in ATCs. (B) GAPDH gene knockdown efficiency of Tf-PEI, PEI or lipofectamine 2000 (LF) was measured in Jurkat cells. Tf-PEI or PEI were formulated with siRNA against GAPDH (siGAPDH) or scrambled siRNA (siNC). GAPDH expression was normalized with beta-actin expression and quantified by real time PCR. (Data points indicate mean + / - SD, n =3; One-way ANOVA, **, $p < 0.01$, ***, $p<0.005$).

3.3.9 Cytotoxicity assay

Biocompatibility of polyplexes is one of the most important considerations before the in vivo application. The potential toxicity of PEI may induce membrane damage and cells apoptosis. Therefore, an assay to determine the cellular membrane integrity would be idea to determine the potential toxicity of Tf-PEI polyplexes. Tf-PEI polyplexes are proposed to be administrated pulmonarily, therefore, A549 cells, a lung epithelial cell line, was used in this study. A549 cells were treated with Tf-PEI, 5k PEI and 25k PEI polyplexes containing scrambled siRNA (N/P ratio: 1, 3, 5, 7.5, 10, 15, 20, 25, 30 ,40). And the LDH release from cells with damaged membranes was determined. As shown in Figure 12, high molecular weight PEI (25k Da), which served as a positive control can cause cytotoxicity, started to cause LDH release from N/P 7.5. As the N/P ratio of 25k PEI increased, increasing LDH release was observed until N/P 30. At N/P 40 of 25k PEI, less LDH release compared to N/P 30 was measured which may be due to cell killing by high doses of 25k PEI polyplexes at early time points resulting in less cells available for the measurement of LDH release at the end point. On the other hand, Tf-PEI and low molecular weight PEI (5k) polyplexes treatment didn't induce any increase of LDH release at all tested N/P ratios compared to the untreated control. This result indicated the high biocompatibility of both 5k PEI and Tf-PEI polyplexes. The toxicity of PEI strongly depends on the molecular weight. Low molecular weight PEI (< 10k Da), which is used in this study,

demonstrates a better safety profile compared to higher molecular weight PEI (i.e. 25k Da). The positive charge of PEI also contributes to toxicity. As shown in Figure 5 B, Tf-PEI polyplexes have slightly negative surface charge which may also contribute to the low cytotoxicity of Tf-PEI polyplexes.

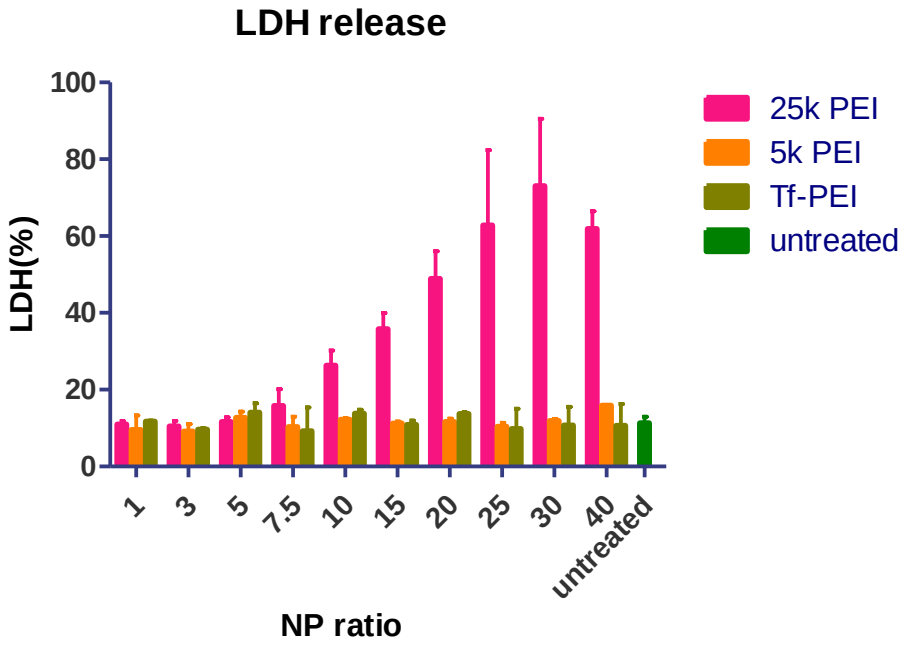

Figure 12 LDH release from A549 treated with polyplexes. LDH release from Tf-PEI, 5k PEI and 25k PEI polyplexes treated A549 cells was determined by CytoTox- ONE. The "no cells" control represents 0% LDH release, and cells treated with lysis buffer represent 100% LDH. (n = 3)

3.3.10 In vivo delivery of polyplexes

To further validate the possibility of pulmonary delivery of siRNA to ATCs via Tf-PEI, a murine model of allergen-induced asthma-like inflammatory reaction was established as shown in Figure 13 A. Animals were i.t administrated on 4 consecutive days with Tf-PEI or PEI polyplexes prepared with Alexa Fluor 647

labeled siRNA (siRNA-AF647), and administration of free siRNA-AF647 was included as negative control on day 35-38 (Figure 15 A). On day 39, lung function of animals was determined by PenH assay. Overall, the airway hyperresponsiveness (AHR) of asthmatic groups of animals was slightly higher than in corresponding saline-exposed, healthy groups of animals (Figure 15 B). Additionally, according to the AUC of airway responsiveness against methacholine concentration curve, mice within the asthmatic group treated with PEI/siRNA polyplexes showed the highest AHR which was significantly higher than within the corresponding healthy control. On the other hand, there is no significant difference between asthmatic mice treated with Tf-PEI/siRNA polyplexes and their corresponding healthy control group (Figure 13 C). This data may suggest that the treatment with positively charged PEI/siRNA polyplexes could have intensified the pre-existing lung inflammation in the asthmatic animals but not the treatment with Tf-PEI/siRNA polyplexes, which are shielded by the negatively charged glycoprotein.

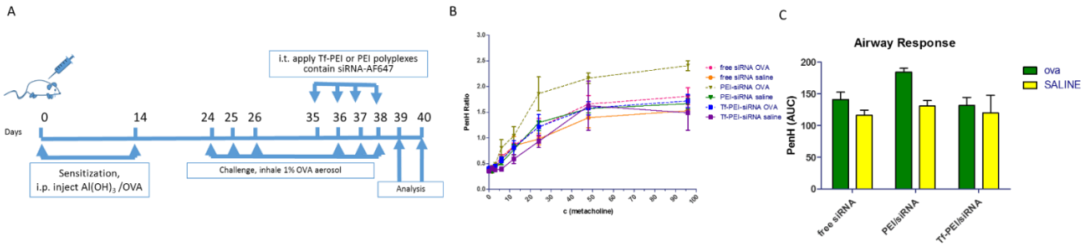

Figure 13 Murine asthma model. (A) Establishment of a murine asthma model. Balb/c mice were sensitized by i.p injection of $Al(OH)_3$ and ovalbumin (OVA) twice and challenged twice by inhalation of 1% OVA aerosol for 1 h daily for 3 consecutive days to induce airway inflammation. Animals treated by inhalation of saline served as healthy control. Polyplexes with 750 pmol Alexa Fluor 647 labeled siRNA (siRNA-AF647) were prepared with Tf-PEI or PEI at N/P 7.5 and applied intratracheally (i.t.), and free AF647 siRNA served as negative control. Lung function was determined on day 39. Bronchoalveolar lavage fluid (BALF), BALF cells and lung cells suspension were analyzed on day 40. (B) Airway hyperresponsiveness of methacholine-challenged mice after 4 consecutive days of treatment with free siRNA, PEI or Tf-PEI polyplexes. (C) Airway responses of animals were represented by AUC of airway responsiveness against methacholine concentration curve. (Data indicated as mean +/- SEM, n> 3)

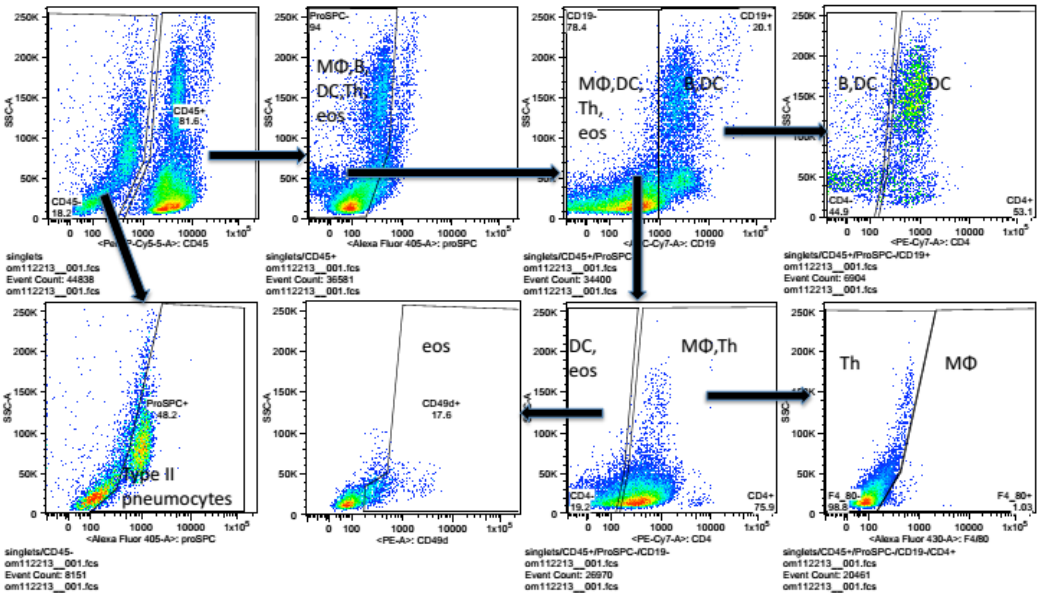

Figure 14 Differentiation of BALF. Strategy to differentiate cellular populations in BALF cells by flow cytometry.

On day 40, BALF, BAL cells and lung cells were collected and processed for determining concentration of IL-5 and IL-13, or for immunostaining, respectively. BAL cell populations were differentiated following the immunostaining strategy shown in Figure 14 and Table 2. As shown in Figure 15 A, Tf-PEI polyplexes uptake in T cells was significantly higher than that in B cells and eosinophils. More importantly, cellular uptake of Tf-PEI polyplexes in T cells was 1.3 and 1.5 fold higher than that in macrophages and type II pneumocytes, one type of alveolar cells, respectively. It has to be taken into account that lung resident macrophages serve as first line of cellular defense in the deep lung [138] by actively phagocytosing foreign particles, which may result in a significant amount of polyplexes being cleared. Additionally, the large interaction surface of type II pneumocytes with aerosolized particles also increases their possibility to associate with polyplexes. Considering that activated macrophages have elevated levels of TfR [139] also and epithelial cells express TfR as well [140], Tf-PEI polyplexes demonstrated very efficient T cell-targeted delivery. In lung suspension cells, uptake of Tf-PEI polyplexes in T cells was 1.7 fold higher than PEI polyplexes in asthmatic animals (OVA group). Furthermore, cellular uptake of Tf-PEI polyplexes in T cells from asthmatic animals was significantly higher than in healthy animals (saline), which demonstrated minimal cellular uptake similar to free siRNA treatment group (Figure 15 B). Tf-PEI and 5k PEI polyplexes didn’t

show toxicity toward A549 cells at N/P ratios ranging from 1 to 40 as assessed by LDH release assay (Figure 12). However, as suggested above, intratracheal administration, especially of positively charged polyplexes could induce additional inflammation. To evaluate the potential pro-inflammatory effects of polyplexes, IL-5 and IL-13 were determined by a mouse cytokine 20-plex panel. As shown in Figure 15 C, overall, IL-5 levels were higher in all asthmatic groups, which can be explained by the allergic inflammation induced by the OVA-sensitization and challenge. However, asthmatic animals treated with PEI polyplexes demonstrated significantly higher secretion of IL-5. On the other hand, no significant difference of secretion of IL-5 in Tf-PEI polyplexes and free siRNA treated OVA-sensitized animals was observed compared with healthy animals. Additionally, the levels of cytokines in OVA-sensitized animals treated with targeted polyplexes was not significantly different from untreated OVA-sensitized animals (data not shown). The same secretion profile was observed in IL-13 (Figure 15 D). These results agree with the airway hyperresponsiveness results (Figure 3.11 B and C) and suggest that the Tf-shielding of Tf-PEI polyplexes efficiently reduces the pro-inflammatory effect of PEI polyplexes in asthmatic animals. It is worth noting that the repeated treatment with low molecular weight PEI was tolerated very well in healthy animals (Figure 15 C and D). These results are in line with previous reports [51, 120].

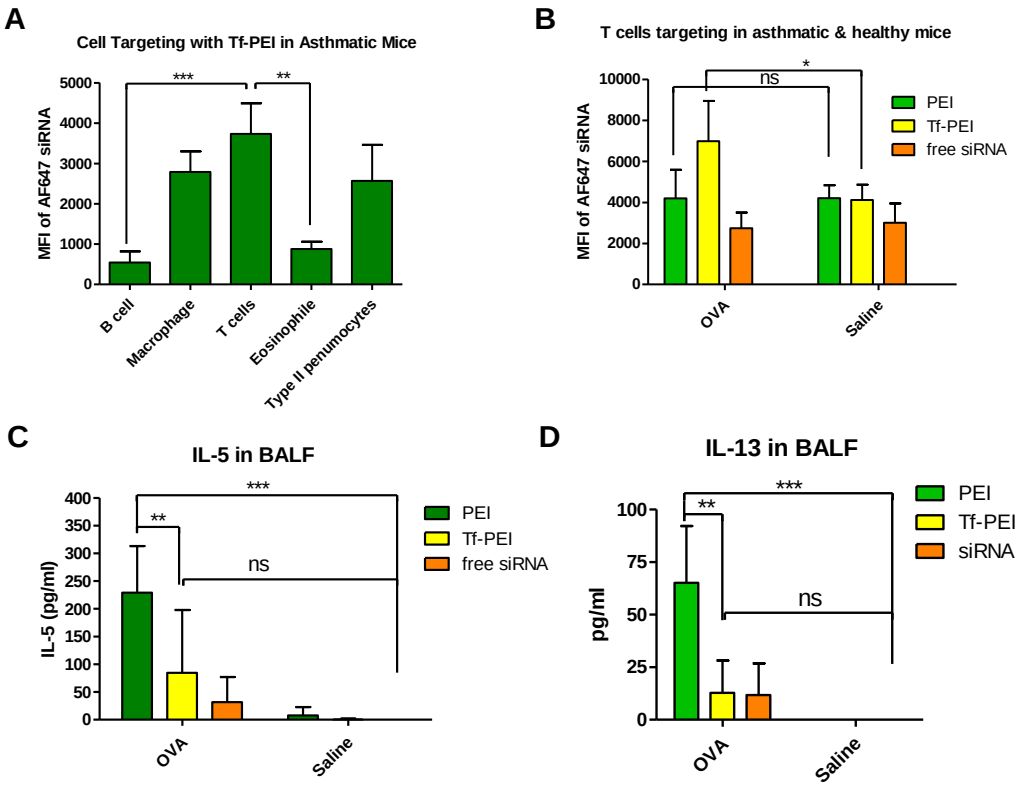

Figure 15 Biodistribution and biocompatibility of Tf-PEI and PEI. (A) Cellular uptake of Tf-PEI polyplexes in different BALF cell populations from OVA sensitized-animals and (B) Cellular uptake of Tf-PEI polyplexes, PEI polyplexes and free AF647 siRNA in the T cell population of the lung cell suspensions from asthmatic and healthy mice was quantified by flow cytometry. (C) IL-5 levels in BALF and (D) IL-13 levels in BALF were determined by the mouse cytokine 20-plex panel. (n>3, *, p< 0.05, **, p < 0.01, ***, p<0.005)

3.4 Conclusion

This study is the first attempt to deliver siRNA selectively to activated T cells for asthma therapy. Tf-PEI polyplexes exhibited desired physicochemical properties and achieved selective delivery of siRNA to ATCs followed by successful induction of gene knockdown. Such selectivity was also confirmed in a

murine asthma model. Our present work demonstrates the possibility to specifically deliver siRNA to ATCs via targeting TfR. Although repeated administration of a Tf conjugate of low molecular weight PEI was well tolerated in healthy animals and no toxicity was observed in our study, clinical application of PEI or its conjugates is still limited by concern of any possible toxicity. Therefore, after having established an efficient targeting strategy for primary T cells in the present paper, our next studies will be devoted to developing a more biocompatible polymer to replace PEI. Subsequently, therapeutic effects of downregulating clinically relevant genes such as the Th_2 transcription factor GATA-3 will be determined.

CHAPTER 4 POST-TRANSCRIPTIONAL REGULATION OF THE GASC1 ONCOGENE WITH ACTIVE TUMOR-TARGETED SIRNA-NANOPARTICLES

Please note that part of the content of this chapter is from a research article, "Post-transcriptional regulation of the GASC1 oncogene with active tumor-targeted siRNA-nanoparticles", was published in Molecular Pharmaceutics (S. Movassaghian, **Y. Xie**, et al., 2016). The authors of this article include Sara Movassaghian, Claudia Hildebrandt, Rayna Rosati, Ying Li, Na Hyung Kim, Denise Conti, Sandro RP da Rocha, Zeng-Quan Yang, Olivia M Merkel and me. Sara Movassaghian and me are joint first authors of this research paper.

4.1 Introduction

Basal-like breast cancer (BLBC) accounts for the most aggressive types of breast cancer and currently cannot be treated specifically. Therefore, investigation of new targets and treatment strategies is more than necessary. One possible new group of targets are 'epigenetic enzymes' (e.g. a histone modifying and DNA methylating enzymes) as the causative links between genetics and epigenetics in cancer development are well documented [141]. There is also an increasing appreciation that epigenetic aberrations that are often directly caused by genetic defects resulting in loss- or gain-of-function of epigenetic-regulators contribute significantly to cancer onset, severity and progression [142]. Specifically, a genetic alteration in the gene encoding an 'epigenetic enzyme' can lead to changes within

the histone code [143], which is involved in both tumorigenesis and cancer stem cell-generated hierarchies in multiple tumor types [143].

The possibility of reversing epigenetic codes may provide new targets for therapeutic intervention. In the present work, we focused on therapeutically down regulating a recently discovered gene which was first identified and cloned as a novel cancer gene by Yang et al. [144]. The gene amplified in squamous cell carcinoma 1 (GASC1- also referred to as JMJD2C/KDM4C) encodes a nuclear protein that catalyzes lysine demethylation of histones [144] and is involved in several cancers, including breast cancer [145]. Thus, down regulation of GASC1 expression represents an excellent therapeutic approach but is currently not possible in a cell specific manner. Moreover, recent findings clearly established that the GASC1 gene is amplified in approximately 15% of breast cancers [146], and its overexpression is more prevalent in basal-like breast cancers (BLBC) [111]. Besides, GASC1 overexpression is correlated with a poor prognosis and induces transformed phenotypes [146b]. Previous studies have demonstrated that therapeutic interference with GASC1 using an shRNA-based approach inhibits proliferation of breast cancer cells in vitro and in vivo [146b 108]. However, in these studies, viral vectors were used to express shRNA for GASC1 knock down. Besides the immunologic challenges and safety issues viral vectors bear, viruses do not

transduce cells in a specific manner. However, targeting can be achieved with chemically engineered artificial viruses [147].

Human breast carcinomas represent a heterogeneous group of tumors that are diverse in their behavior, outcome, and response to therapy. Breast cancer is generally classified in four main groups based on their expression of estrogen receptor (ER), progesterone receptor (PR), and Her2/neu receptor (HER2): two of the main groups are ER^+ and include luminal A (ER^+, PR^+, and $HER2^-$) and luminal B (ER^+, PR^+ and $HER2^+$) subtypes, and two groups are ER^-, HER2 overexpressing ($ER2^-$, PR^-, HER^+) and basal-like ($ER^{-/low}$, $PR^{-/low}$, $HER2^{-/low}$) [148].

Among the different types of breast cancer, basal-like breast cancers (BLBC) are particularly aggressive and are associated with high histological grade, prevalence of younger patient age, poor prognoses, and often relapse rapidly [148]. The treatment for BLBC consists of standard chemotherapy regimens as no effective molecularly-targeted therapies have been developed [149].

Failure in the current conventional therapies for BLBC patients urges the development of novel strategies to achieve favorable outcomes.

Therefore, siRNA against GASC1, the newly identified oncogenic histone modifying enzyme holds promise as a potential therapy of BLBC. Nanoparticles offer an unprecedented opportunity in rational drug and gene delivery by enhancing therapeutic efficacy and reducing side effects through overcoming

major obstacles in cancer therapy such as nonspecific biodistribution with consequent dose-limiting toxicity and multidrug resistance (MDR) [150]. Up-regulation of TfR expression in a wide variety of cancers, its function and highly efficient recycling pathway, provides a gate for intracellular gene and drug delivery to BLBC in a tumor-specific manner [151]. Thus, Tf-PEI could potentially deliver siRNA in a targeted way to BLBC overexpressing TfR.

In this chapter, we evaluated two Tf-SPDP-PEI and Tf-SPDP-PEG-PEI conjugates, which were conjugated using two different linkers, SPDP and PEG_4-SPDP, in different breast cancer cell lines or immortalized breast cell line. We identified a new siRNA sequence that efficiently reduces GASC1 expression if delivered intracellularly. Efficiency of GASC1 silencing was determined in BLBC cells overexpressing GASC1, and the inhibition of proliferation was investigated. To the best of our knowledge, this is the first report of developing a BLBC-targeted delivery system with a newly identified siRNA for therapeutic GASC1 gene knock down. Therefore, our approach is promising for therapeutic targeting of hard-to-treat BLBC and could result in new receptor mediated therapy options for BLBC.

4.2 Materials & Methods:

4.2.1 Materials

Polyethylenimine (PEI, MW 5 kDa) was obtained from BASF (Lupasol G100, Ludwigshafen, Germany). N-succinimidyl-3-(2-pyridyldithio) propionate (SPDP), a PEGylated SPDP (PEG4-SPDP), Lipofectamine® 2000, trypsin, penicillin/streptomycin, 4(2(hydroxyethyl))-1-piperazine ethanesulfonic acid (HEPES), heparin sodium (140,000 U/g), were purchased from Thermo Fisher Scientific (Waltham, MA, USA). Anti-human CD71 (transferrin receptor) PE was acquired from (eBioscience, CA, USA). Dithiothreitol (DTT) was purchased from Alfa Aesar, MA, USA. SYBR Gold dye and CellTiter-Blue® were obtained from Life Technologies (Carlsbad, CA, USA). RPMI-1640 medium (1X) with 2.05 mM L-glutamine, Ham's F-12 Medium, trypan blue (0.4%, sterile filtered) was purchased from HyClone (GE Health Care, Pittsburgh, PA, USA). Human holo Transferrin (80 kDa) was obtained from Calbiochem (Billerica, MA, USA). Dulbecco's phosphate buffered saline (PBS), fetal bovine serum (FBS), D (+)-glucose, 2-mercaptoethanol, dimethyl sulfoxide (DMSO, ≥99.7%), sodium bicarbonate ($NaHCO_3$) were purchased from Sigma-Aldrich (St. Louis, MO, USA). DNase I reaction buffer and DNase/RNase-free water were purchased from Zymo Research (Irvine, CA, USA). Hs_GASC1 primer (forward and reverse) and sequences V4, V6, and V7 (self-designed siRNA against GASC1 using the

GENtle software by Magnus Manske) were ordered from Invitrogen (Life Technologies, Carlsbad, CA, USA). Commercially available GASC1 specific siRNA was purchased from Qiagen (Valencia, CA, USA) for sequences A, B, C and D. SMART pool and sequences E, F, G and H (Table 3) were purchased from Dharmacon (Thermo Fisher, Waltham, MA, USA).

Table 3 Sequence of siRNA

	Sequence name	Sequences
Negative Control	MISSION® siRNA Universal Negative Control #1	
hGAPDH	IDT	5'-GGUCGGAGUCAACGGAUUUGGUC[dG][dT] 3'-UmUmCCmAGmCCmUCmAGmUUmGCmCUmAAACCAGCA
hGASC1	V4	5'-ACCGAAGACAUGGACCUCU[dT][dT] 3'-[dT][dT]UGGCUUCUGUACCUGGAGA
hGASC1	V6	5'-CAGAAUUUAUCAGAUCAUA 3'-[dT][dT]GUCUUAAAUAGUCUAGUAU
hGASC1	V7	5'-GUGAAGAUUUCAAUGGAUA[dT][dT] 3'-[dT][dT]CACUUCUAAAGUUACCUAU
hGASC1- A	Hs_KDM4C1	5'-CGAAGCUUCCAGUGUGCUA[dT][dT] 3'-[dG][dG]GCUUCGAAGGUCACACGAU
hGASC1- B	Hs_JMJD2C3	5'-GAUAUUAAUGGGAGCAUAU[dT][dT] 3'-[dG][dT]CUAUAAUUACCCUCGUAUA
hGASC1- C	Hs_JMJD2C4	5'-CCAGAAGUUCGAUUCACUA[dT][dT] 3'-[dA][dG]GGUCUUCAAGCUAAGUGAU
hGASC1-D	Hs_JMJD2C5	5'-CAUCGGAGGGAAAGACUAA[dT][dT] 3'-[dA][dT]GUAGCCUCCCUUUCUGAUU
hGASC1- E	J-004293-12	5'-GAGAAGUCGUCCAAGUCAAUU 3'-UUCUCUUCAGCAGGUUCAGUU

hGASC1- F	J-004293-11	5’-GCAUAUAUGAUGAGGGUGUUU 3’-UUCGUAUAUACUACUCCCACA
hGASC1- G	J-004293-10	5’-ACGAAGAUUUGGAGCGCAAUU 3’-UUUGCUUCUAAACCUCGCGUU
hGASC1-H	J-004293-9	5’-AUUACAUGCUUUCGACAUAUU 3’-UUUAAUGUACGAAAGCUGUAU

***** Deoxyribonucleotides are presented in parentheses with the letter d, and 2’O-methylated ribonucleotides are denoted with the letter m. The letter p indicates an additional phosphate.

4.2.2 Cell lines characteristic and culture conditions

The non-tumorigenic human mammary epithelial cell line MCF10A and human breast cancer cell line HCC1954 were purchased from the American Type Culture Collection (Manassas, VA, USA). The COLO824 cell line was obtained from DSMZ (Germany), and the cell lines SUM102, SUM225, SUM52, SUM149 were a kind gift from Dr. Stephen P Ethier (Department of Pathology and Laboratory Medicine, Medical University of South Carolina). The COLO824 and HCC1954 cell lines were retained and grown in RPMI-1640 cell culture medium supplemented with 10% fetal bovine serum. MCF10A and SUMs cell lines were cultured in a special DMEM/F12 media, containing 1% EGF (10 ng/ml), 0.1% hydrocortisone (1µg/ml), and 0.5% insulin (5 µg/ml). The cell lines characteristics are shown in Table 4.

4.2.3 Transferrin receptor expression study

Selected breast cancer cell lines were used to evaluate transferrin receptor expression levels (CD71, TfR) by flow cytometry. Of each cell suspension,

200,000 cells were transferred into an Eppendorf tube and spun down (350g for 5 min). The cell pellet was washed with PBS containing 2 mM EDTA. Afterwards, PE-labeled CD71 antibody and its corresponding isotype control were each added to assigned cell samples and incubated for 30 min at 4°C before analysis by flow cytometry (Attune acoustic focusing cytometer Life Technologies, Carlsbad, CA). Blank cells were not stained with any antibody. The excitation wavelength of 488 nm and an emission filter at 585 nm/42 nm were used. Cell gating and data analysis in the Attune cytometric software were performed using cell morphology and mean fluorescence intensity (MFI), respectively. The mean values and standard deviation (SD) of experiments with n=3 are shown.

Table 4 Different breast cell line model and their specifications

Cell line	Cell Source	Subtype	PR	ER	Her2/neu	GASC1
HCC1954	Grade III invasive ductal carcinoma	Basal	-	-	+	+++
COLO824	Mammary gland carcinoma	Basal	-	-	-	+++
MCF10A	Mammary gland-immortalized		-	-	-	-
SUM102	Intraductal carcinoma/microinvasion	Basal	-	-	-	-
SUM225	Chest wall recurrence of ductal carcinoma	HER2+	-	-	+	-
SUM149	Invasive ductal carcinoma (inflammatory)	Basal	-	-	-	+
SUM52	Pleural effusion	Luminal	-	+	-	-

4.2.4 Specific binding of transferrin to the corresponding receptor

To analyze the specificity of transferrin binding to TfR, Tf was fluorescently labeled with FITC (Invitrogen™, life Technologies). Bovine serum albumin (BSA) was used as a control. Transferrin and BSA were dissolved in 0.1 M of $NaHCO_3$. A ten-fold molar excess of FITC (dissolved in DMSO) was incubated with transferrin and BSA overnight at 4°C. The protein-FITC conjugates were subsequently separated from unbound FITC by gel permeation method (Sephadex G25 M, GE Healthcare PD-10 columns) using 20 mM HEPES-150 mM NaCl buffer. The BCA protein assay (Thermo Scientific) was used to measure the final concentration of transferrin and albumin after purification. The presence of FITC was found to not impact the measurements at the applied concentrations. After purification and characterization of the labeled (glyco-) proteins, HCC1954 and MCF10A cell lines (60,000 cells in 24 well plates) were incubated with different amounts of FITC-transferrin or FITC-BSA (20, 200 and 400 pmol) for 4 h at 37°C and 5% CO_2. Flow cytometry was used as described above to measure the binding of Tf-FITC or albumin-FITC to the cells with the emission filter set to 530/30 nm bandpass.

4.2.5 Conjugation synthesis and characterization

Two different heterobifunctional crosslinking agents, namely (N-succinimidyl-3-(2- pyridyldithio) propionate (SPDP) and a PEGylated SPDP

(PEG4-SPDP) containing four ethylene glycol units were used to conjugate transferrin to a 5 kDa LMW PEI as described before [20]. PEI (1 mg/ml) was reacted with SPDP or PEG4-SPDP (20 mM) in DMSO stirring at room temperature overnight (1:10 molar ratio relative to amines present). The intermediate products were purified by ultrafiltration using Amicon® Ultra 4 ml filters (MWCO 3000) and Vivaspin centrifugal ultra-filters (10,000 MWCO) as described [61]. The conjugates were separated from uncoupled Tf-SPDP by ion exchange FPLC via ÄKTA prime plus (GE Healthcare Bio-Sciences, Pittsburgh, PA, USA) as reported [152]. The products (Tf-PEI and Tf-PEG-PEI) were preserved at 4ºC until use. The degree of SPDP coupling onto PEI was determined as previously reported by spectrophotometric detection of release of the pyridine-2-thione group [47]. The characterization of the final products was performed by spectrophotometric detection of transferrin at 280 nm compared to standard curve [152] and quantification of PEI amines in using a modified TNBS method [153] in presence of the respective amount of transferrin as described by Germershaus et al. [152].

4.2.6 Preparation of siRNA-polymer nanoparticles

For preparing nanoparticles based on electrostatic interaction resulting in the formation of polyelectrolyte complexes, or polyplexes, the PEI/siRNA charge ratios (defined as N/P ratios) were calculated based on PEI nitrogen (N) groups per siRNA phosphate (P) groups. [75b]. Polymer (1 mg/ml) and siRNA (100 μM)

stock solutions were diluted with a 5% glucose solution (pH 7.4, prepared with RNase free water). Equal volumes of PEI or modified PEI and siRNA solutions were mixed to result in the respective N/P ratio, vortexed for 30 s, and incubated for 20 min at room temperature before use.

4.2.7 Analysis of hydrodynamic diameters and zeta (ζ)-potentials

The hydrodynamic diameters and zeta potential of polyplexes prepared with 40 pmol siRNA and polymer at N/P 7 were measured in PBS using a Zeta sizer Nano ZS (Malvern Instruments Inc., Westborough, MA, USA) and the refractive index and viscosity settings for water. Dynamic light scattering (DLS) was detected at 25°C at an angel of 173°. Results from triplicate samples are shown as Z average in nanometers ± SD. Samples were then diluted with 700 μL of PBS buffer for ζ-potential measurements. Results of three independent measurements are given in millivolts ± SD.

4.2.8 Atomic force microscopy

Polyplex morphology was determined using atomic force microscopy (AFM). For image acquisition, a drop of polyplexes prepared at N/P 7 was incubated for 5 min on freshly cleaved mica surface. Excess solution was rinsed off with deionized water, and the mica was dried and imaged at room temperature using a Pico LE atomic force microscope (Molecular Imaging, Agilent

Technologies) with a Si3Ni4 V-shaped cantilever in contact mode as described before [75b].

4.2.9 SYBR Gold condensation assays

The capacity of the Tf-PEI and Tf-PEG-PEI to condense siRNA at different N/P ratios (0-20) was evaluated in SYBR Gold assays, and PEI (5 kDa) was used as control. Formulations with 50 pmol of siRNA per well were placed in 96-well plate, vortexed and incubated at room temperature for 20 min. Fluorescence (Ex/Em: 495/537 nm) was measured after 10 min of incubation with a 4x SYBR Gold solution using a Synergy 2 microplate reader (BioTek, Winooski, VT, USA).

4.2.10 Stability of siRNA/PEI complexes - heparin dissociation assays

Polyplex formulations with 50 pmol of siRNA per well prepared at N/P 7 were incubated with a fixed heparin concentration (0.2 IU) over varying periods of time (5-180 min). Fluorescence was measured with a Synergy 2 microplate reader (BioTek Instruments) after adding a 4x SYBR Gold solution (Ex/Em: 495/537 nm). The mean values of three fluorescence intensity measurements of SYBR Gold dye only (0) and of three samples of SYBR Gold intercalating with free siRNA (1) were used for normalization and calculation of the relative stability of the polyplexes. Results of triplicate samples are shown as mean values ± SD.

4.2.11 Quantification of cellular siRNA uptake by flow cytometry

Cells were seeded with 80,000 cells per well in 24-well plates 24 h before they were transfected with polyplexes prepared with 50 pmol of Alexa Fluor 488-labeled siRNA per well at N/P 7. Negative controls included untreated cells and cells treated with free Alexa Fluor 488-labeled siRNA. PEI (5 kDa) was used as a positive control for comparison. After 4 h of transfection with 100 µL of polyplexes, 1 ml of medium was added and cells were incubated at 37°C and 5% CO_2 for another 24 h. The cells were washed with PBS and trypsinized. Intracellular fluorescence from siRNA was detected using an Attune® Acoustic Focusing Flow Cytometer (Thermo Fisher Scientific, Carlsbad, CA) and corresponding software. For the distinction between internalized and surface-bound siRNA, trypan blue (0.4%) was used to quench surface-bound fluorescence. Data were analyzed after gating for 10,000 viable cells, and median fluorescence intensity (MFI) values are given for three independent studies.

4.2.12 Confocal laser scanning microscopy

HCC 1954 cells were seeded in 8 well chamber slides at a density of 25,000 cells per well (Permanox® Slide, Nunc, Thermo Fisher Scientific) and allowed to grow for 24 h at 37°C in 5% CO_2. Polyethylenimine (PEI), Lipofectamine (LF) or Tf-PEI polyplexes made with Tye563-labeled siRNA (Ex/Em: 543/563 nm) were used to transfect cells as described earlier. Subsequently, the cells were washed

with PBS and fixed using 3% paraformaldehyde (Affymetrix, Cleveland, OH, USA) for 30 min, followed by nuclei staining with DAPI (Ex/Em: 405/470 nm). Finally, the cells were embedded using Fluorsave reagent (Calbiochem, Merck, Darmstadt, Germany) and covered with a coverslip. The images were recorded with a Zeiss LSM 780 microscope (Zeiss, Oberkochen, Germany). Representative pictures are shown in Figure 24 (100X magnification).

4.2.13 Cytotoxicity of polyplexes

Cells (HCC1954, COLO824, SUM102 and MCF10A) were seeded at a density of 10,000 cells in a 96-well plate (Thermo Scientific) and incubated for 24 h at 37°C and 5% CO_2. Polyplexes containing 50 pmol of siRNA were added to the cells, and plates were incubated for 24 h at 37°C. Subsequently, CellTiter-Blue® reagent was added directly to each well, the plates were incubated at 37°C for 2 h to allow the cells to convert resazurin to resorufin. The obtained fluorescence was measured at Ex/Em 560/590 nm. The percentage of cell viability and proliferation was calculated as the ratio between the fluorescence of a sample and the untreated control cells as follows: ([A] test/ [A] control) ×100%. Results are shown as the mean value ± SD of triplicate samples.

4.2.14 Knockdown measured by qRT-PCR and western blot

HCC1954 cells were seeded with 500,000 cells per well in 6-well plates (Corning Incorporated) and were incubated for 24 h before transfection. at 37°C and 5% CO_2. PEI, Tf-PEI, and Tf-PEG-PEI polyplexes were prepared with 100 pmol of GASC1 siRNA at N/P 7 in a total volume of 100 μL and were added to 900 μL of cell culture medium per well. The cells were incubated with the polyplexes for 4 h before 2 ml of fresh medium were added to each well. The cells were then incubated for an additional 24 for PCR or 72 h for Western Blot analysis. Lipofectamine (LF) (0.5 μL/10 pmol of siRNA) was used as a positive transfection control. Cells were transfected with samples in fresh medium and subsequently cells were washed with PBS and lysed with lysis buffer (PureLink RNA mini, Ambion, Fisher Scientific, USA). Total RNA was then isolated from cells according to the manufacturer's protocol with supplementary DNase I digestion; mRNA was mixed with qScript™ cDNA SuperMix kit (Quanta Biosciences, Gaithersburg, MD, USA), then converted into cDNA through a reverse transcription reaction for real time PCR (eppendorf Mastercycler gradient, Hauppauge, NY, USA). Primers set for GASC1 genes were ordered from Invitrogen (Life Technologies). A PUM1 primer (Qiagen, Valencia, CA, USA) was used for normalization. Semi-quantitative RT-PCR was performed using the FastStart Universal SYBR Green Master (ROX) using a Bio-Rad iCycler Thermal

Cycler (IQ 5™ multicolor read thermal PCR). Results are given as the average of n =3 ± SD.

For measuring protein levels after transfection of the HCC1954 cell lines with modified PEI formulations, western blot analysis was performed after protein extraction of the transfected cells following a 7 day in vitro incubation based on previous protocol optimization. The cells were lysed in RIPA buffer containing protease inhibitor cocktail (Calbiochem, CA, USA). Samples were size-fractionated by 7.5% SDS-PAGE (XCell SureLock™ Mini-Cell) and the blot was transferred to Immunobilon-PVDF membranes (Millipore, Bedford, MA, USA). The blot was then incubated in blocking buffer (5% milk, 0.1% Tween in TBS buffer) at room temperature for 1 h and subsequently incubated with rabbit anti-JMJD2C antibody (Bethyl Laboratories, Inc. Montgomery, TX, USA) in precooled blocking buffer overnight at 4 °C. After washing in TBS/0.1% Tween, The blot was incubated with horseradish peroxidase (HRP)-labeled anti-rabbit secondary antibody at room temperature for 1 h. After washing with TBS/0.1% Tween, the blot was developed by enhanced chemiluminescence (Thermo Scientific SuperSignal™ West Pico, MA, USA), and visualized with a hyblot CL film (Denvilla, NJ, USA).

4.2.15 Therapeutic effects of GASC-1 gene knockdown on cell proliferation

Therapeutic effects on cell proliferation were measured in MTT assays after transfection with siRNA against GASC1 or a scrambled control. In 24-well plates (Corning Incorporated), HCC1954 cells were seeded at a density of 8,000 cells per well and incubated for 24 h at 37°C and 5% CO_2. Polyplexes were prepared with 50 pmol of GASC1 siRNA or a scrambled negative control siRNA, and the cells were transfected on days 1, 3, and 6 after seeding. MTT assays were performed as described above on days 2 and 10 after seeding. The results are shown as mean values ± SD of 3 independent measurements in comparison to proliferation of untreated cells.

4.2.16 Statistical analysis

Results from all experiments represent at least three independent measurements and are presented as mean value ± SD as analyzed by Graph Pad Prism 6.0 software (GraphPad Software, La Jolla, CA, USA). Statistical tests were either one or two way ANOVA with a Bonferroni post hoc analysis (significance level 0.05). Significantly different results are indicated with an asterisk (*) in figures. Corresponding significance values are: * $P < 0.05$, ** $P < 0.01$, *** $P < 0.001$ and **** $P < 0.0001$.

4.3 Results

4.3.1 Screening for TfR expression levels

Transferrin receptor expression levels were determined via flow cytometry in a series of breast cell lines which were characterized as GASC1 positive or negative breast cell line to select a valid cell line model and its controls for the targeted siRNA delivery [146b]. The receptor expression of TfR (CD71) was compared to the MCF10A cell line, an immortalized, non-transformed epithelial cell line, showing no GASC1 amplification [146b]. The expression was verified using a PE-labeled anti-CD71 antibody. Non-specific binding of the antibody was precluded based on experimental results using an isotype IgG (negative control) and non-treated cells (blank). PE-labeled CD71 antibody and its corresponding isotype control were each added to assigned cell samples. Figure 16 depicts that MCF-10A cells bear only basal levels of TfR whereas the expression level in HCC1954 cells was almost 9-fold higher than in MCF10A. Therefore, HCC1954 cells were selected as cell model to verify GASC1 knock down via targeting the internalizing transferrin receptor. Screening of TfR expression levels in other breast cancer model cell lines showed that GASC1-amplified COLO824 cells present higher TfR expression levels than SUM102, SUM52 ($p < 0.001$) and MCF10A ($p < 0.0001$) but TfR levels were not significantly different between COLO824, SUM149, and SUM225 cell lines ($P > 0.05$). Therefore, all three of

those cell lines could be used as another valid cell culture model for therapeutic GASC1 knockdown.

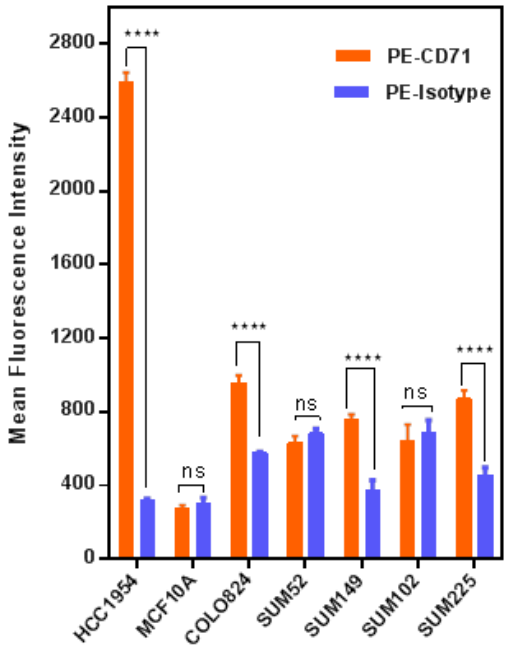

Figure 16 TfR expression in different breast cell lines. Screening of TfR expression levels in different cancer cell lines compared to MCF 10A cells. Using flow cytometry, TfR over-expression on the breast cancer cell line HCC1954 was verified, which also shows a comparably high GASC1 amplification. The transferrin receptor expression (CD71, TfR) was compared to the MCF-10A cell line, an immortalized, non-transformed epithelial cell line, showing no GASC1 amplification. The expression was verified by using a PE-labeled anti-CD71 antibody and non-specific binding of the antibody was precluded based on results with an isotype control. Data are expressed as the mean ± SD (n = 3), ns: non-significant, **** $p < 0.0001$.

4.3.2 Specific binding of Tf to transferrin receptor

To confirm the endocytosis activity of Tf receptors on cell lines determined to overexpress the receptor, HCC1954 and MCF10A cell lines were incubated

with FITC-labeled transferrin in comparison to FITC-labeled albumin. The same amount of transferrin (20 pmol) as used in the Tf-PEI uptake experiment was chosen, and results were compared to higher amounts of transferrin or albumin (200 and 400 pmol). Quenching of non-internalized Tf or albumin was achieved by trypan blue treatment. Figure 4. clearly shows that a 2.3-fold increase in Tf internalization is detectable in the HCC1954 cell line compared to albumin after incubation with 20 pmol FITC-labeled proteins. Meanwhile, FITC-transferrin showed an almost 3-fold higher internalization in HCC1954 cells compared to MCF10A for the same amount of transferrin. There was no significant difference in the uptake of FITC-Tf in the MCF10A cell line compared to FITC-albumin ($p > 0.05$). A notable increase in MFI of the HCC1954 cell line was detected with increasing the amount of FITC-transferrin from 20 to 200 and 400 pmol ($p < 0.0001$), however this was not the case for FITC-albumin ($p > 0.05$). The MFI in MCF10A cell lines with basal levels of TfR, however, did not change with increasing the amount of transferrin from 20 to 200 pmol or 200 to 400 pmol ($p > 0.05$).

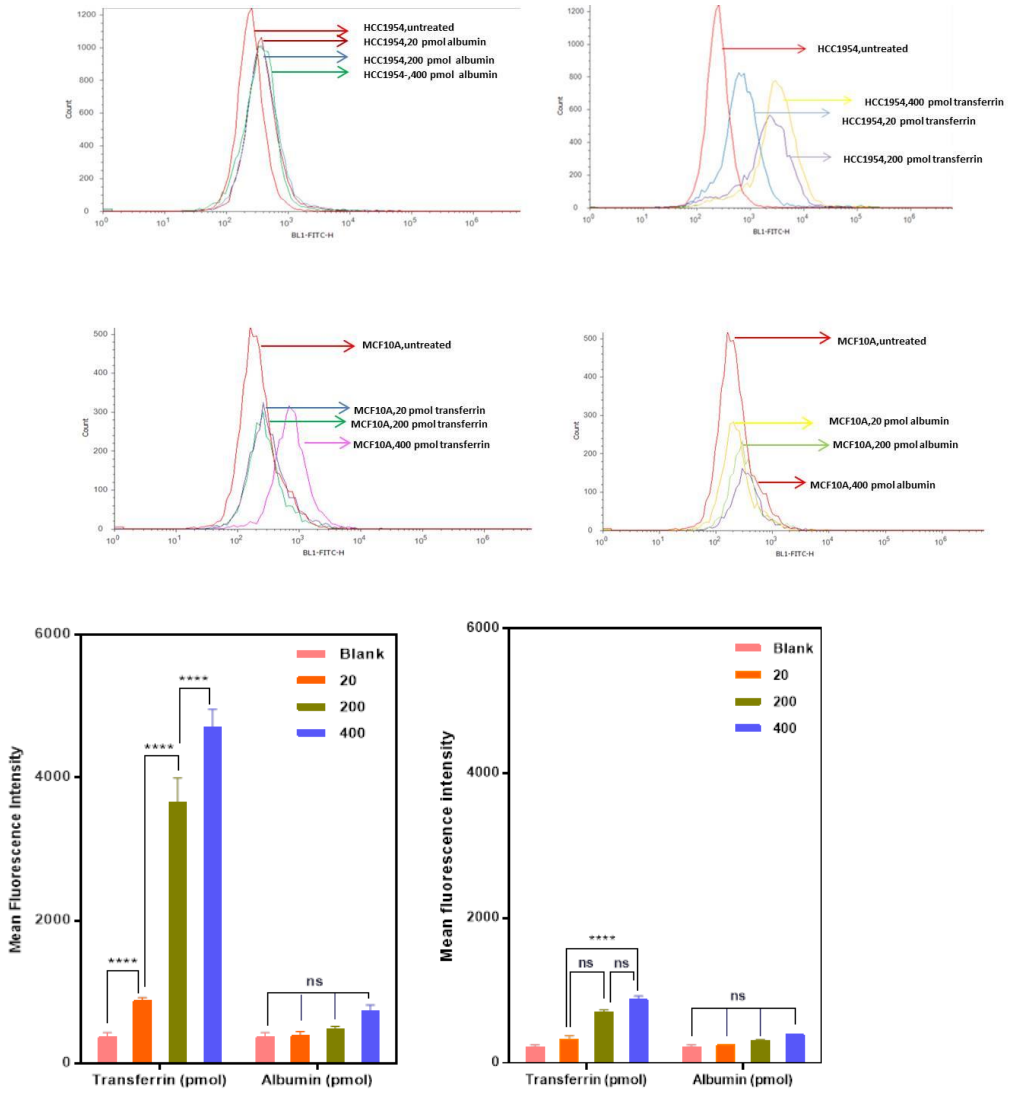

Figure 17 Cellular binding of Tf. Comparison of FITC-Transferrin or FITC-Albumin internalization in HCC1954 (lower left bar graph) and MCF10A (lower right bar graph) cell lines at different concentrations of transferrin and albumin via flow cytometry. Data are expressed as the mean ± SD (n = 3), ns: non-significant, **** $p < 0.0001$.

4.3.3 Development of transferrin-PEI conjugate

Coupling procedures for the synthesis of Tf-PEI conjugates are illustrated in Figure 18. SPDP and its PEGylated form (PEG4-SPDP) with a 25.7 Å ethylene glycol spacer are amine- and sulfhydryl- reactive heterobiofunctional cross linkers

that produce disulfide-containing linkages which are stable extracellularly but can be cleaved intracellularly [154]. This design was chosen to prevent premature release of the targeting ligand but will mediate release of the nanoparticle from Tf and the recycling TfR inside the cell.

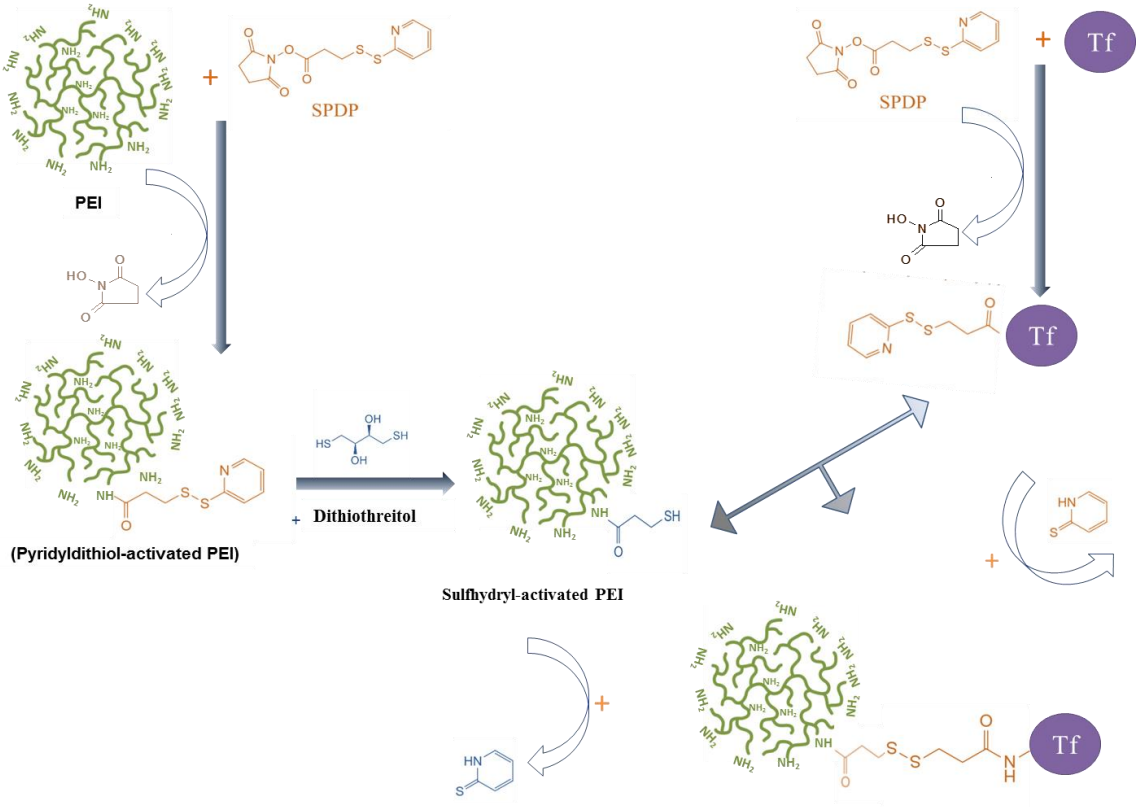

Figure 18 Schematic illustration of transferrin crosslinking with PEI by SPDP.

4.3.4 Physicochemical properties of the nanoparticles

Based on DLS and zeta potential measurements, both Tf-PEI and Tf-PEG-PEI more efficiently formed dense polyplexes with siRNA than non-modified 5 kDa PEI (Figure 19). Tf-PEI/siRNA and Tf-PEG-PEI/siRNA complexes at N/P 7 were compactly packed with 30 and 140 nm hydrodynamic diameters, respectively,

and narrow size distributions (PDI: 0.1). However, PEI/siRNA exhibited larger mean diameter of 700 nm with somehow broader distribution (PDI: 0.4). In addition, the zeta potentials of Tf-PEI (-0.6 ± 0.07 mV) and Tf-PEG-PEI (-0.01± 0.04 mV) complexes with siRNA were lower than those of PEI (39.9 ± 7 mV) complexes, implying that most of the positively charged portion of PEI in was shielded by Tf in the Tf-modified polyplexes. These results reveal that modified PEI produced significantly smaller and more compact structures with siRNA compared to PEI at the same N/P ratio.

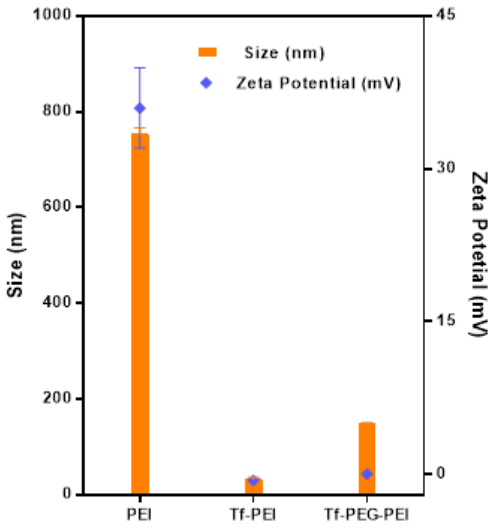

Figure 19 Size and zeta-potential of Tf-PEI, Tf-PEG-PEI and PEI polyplexes. Hydrodynamic diameter (nm) and zeta potential (mV) of siRNA polyplexes made with PEI, Tf-PEI, and Tf-PEG-PEI at N/P ratio of 7 at room temeprature. Data are expressed as the mean ± SD (n = 3).

The same trend was observed via AFM imaging which showed the tendency of PEI polyplexes to aggregate into particles of several hundred nanometers in size, whereas the morphology of the Tf-PEI complexes was more

homogenous, the size distribution was narrow, and the particles didn't show any aggregation tendency (Figure 20). In additional experiments, the capacity of PEI and the modified PEI polymers to condense siRNA at different N/P ratios was evaluated by SYBR Gold condensation assays. In these experiments, free (unbound) siRNA is accessible to the intercalating dye SYBR Gold. The free siRNA is thus subsequently quantified on the basis of fluorescence emitted after SYBR Gold treatment. Results were compared to PEI (5 kDa) as a control (Figure 21). PEI and Tf-PEI showed better siRNA condensation at N/P ratios 1-5, but all formulations showed similar condensation efficiency at N/P ratio of ≥ 7.

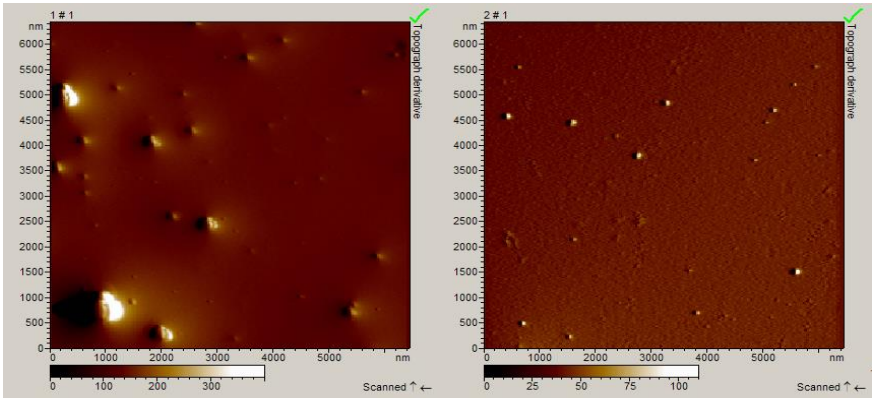

Figure 20 AFM images of Tf-PEI and PEI polyplexes. AFM topography of siRNA polyplexes made with PEI (left) and Tf-PEI (right) at N/P ratio of 7 and imaged after drying at room temeprature.

A heparin-induced decomplexation stability test was performed to determine the stability of the polyplexes. The release profiles of siRNA from all polyplexes reached a maximum siRNA release after 30 min of incubation and then leveled off over the remaining incubation time (Figure 21). After 30 min of

incubation with 0.2 IU heparin, PEI and Tf-PEG-PEI displayed around 50% and 85% of siRNA release, respectively, but Tf-PEI showed only 25% of siRNA release at that time point (Figure 22). The siRNA release from Tf-PEI polyplexes initially increased, then decreased gradually and remained unchanged (7%) until the end of the experiments (180 min) (Figure 22).

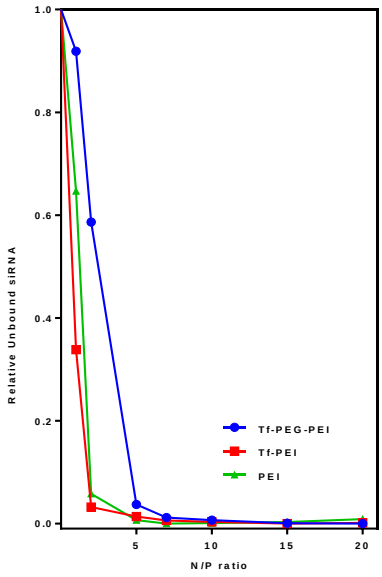

Figure 21 SYBR Gold assay of Tf-PEI, Tf-PEG-PEI and PEI. Condensation efficiency of Tf-PEI and Tf-PEG-PEI complexes with siRNA measured by SYBR Gold assay at different N/P ratios (1-20) compared to polyethylenimine (PEI 5 kDa). Results are given as the average of three measurements ± SD. (n = 3).

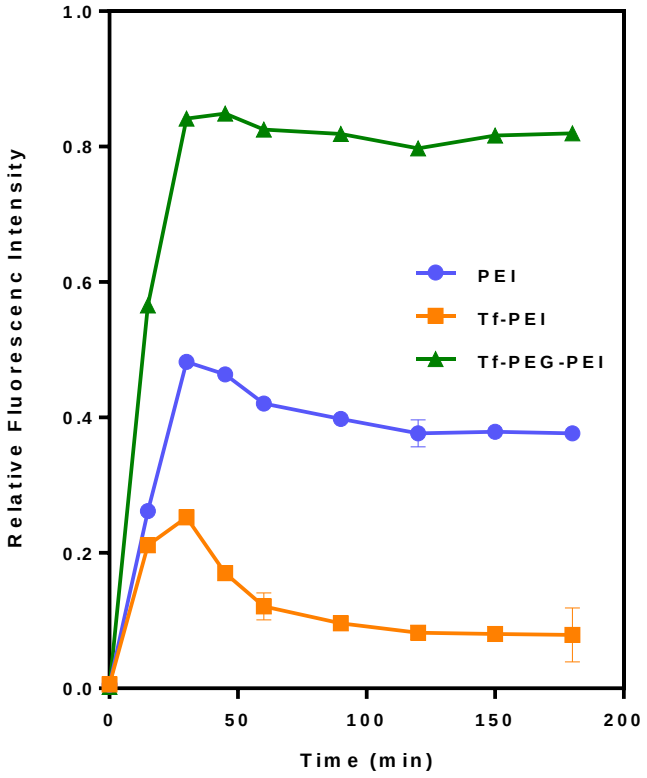

Figure 22 Heparin assay of Tf-PEI, Tf-PEG-PEI and PEI. Release profile of siRNA from transferrin modified polyplexes (N/P 7; 50 pmol siRNA/well) compared to polyethylenimine (PEI 5 kDa) as a function of time (0-185 min) with heparin concentration of 0.2 IU per well. Results are shown as relative mean fluorescence ± SD. (n = 3).

4.3.5Cellular uptake of the nanoparticles

Cellular uptake of polyplexes with 50 pmol of Alexa Fluor 488-labeled siRNA (N/P 7) was quantified in different cell lines (GASC1 positive and GASC1 negative) by flow cytometry. Trypan blue staining was employed on half of the samples to differentiate between surface bound and internalized siRNA. The results were compared to cells that were not treated with trypan blue, while cells treated with trypan blue are indicated with an asterisk in Figure 23. Overall, trypan

blue treated cells showed slightly lower mean fluorescence intensities compared to cells that did not undergo quenching of surface-bound siRNA, indicating that a small fraction of the siRNA polyplexes was attached to the cell membrane and was not taken up intracellularly. However, this difference was not significant in any of the samples ($p > 0.05$). As can be seen in Figure 23, there is a significant difference ($p < 0.0001$) in uptake of PEI/siRNA in GASC1 positive cell lines (HCC1954 and COLO824) and GASC1 negative cells (MCF10A and SUM102). Interestingly, PEI alone showed better uptake in MCF10A and SUM102 which could be caused by higher endocytic activity of these two cell lines [155]. However PEI conjugated transferrin (Tf-PEI and Tf-PEG-PEI) showed very high uptake in the HCC1954 cell line which was expected due to the higher level of TfR expression. The uptake efficiency of Tf-PEI polyplexes did not show any significant differences between HCC1954 and SUM102 cell lines ($p > 0.05$), although the TfR expression of HCC1954 cells is about 4 times higher than that of SUM102 cells (Figure 16). The mean fluoresce intensity in HCC1954 cells treated with Tf-PEI polyplexes was 2.5 and 10-fold higher than in MCF10A and COLO824 cells, respectively. As can be seen in Figure 23, Tf-PEG-PEI/siRNA polyplexes showed 2.6 times higher uptake in HCC1954 than in SUM102 cells. Uptake efficiency of the conjugates containing the PEG-spacer was 3.6 and 6 fold higher in HCC1954 than MCF10A and COLO824 cells, respectively (Figure 23).

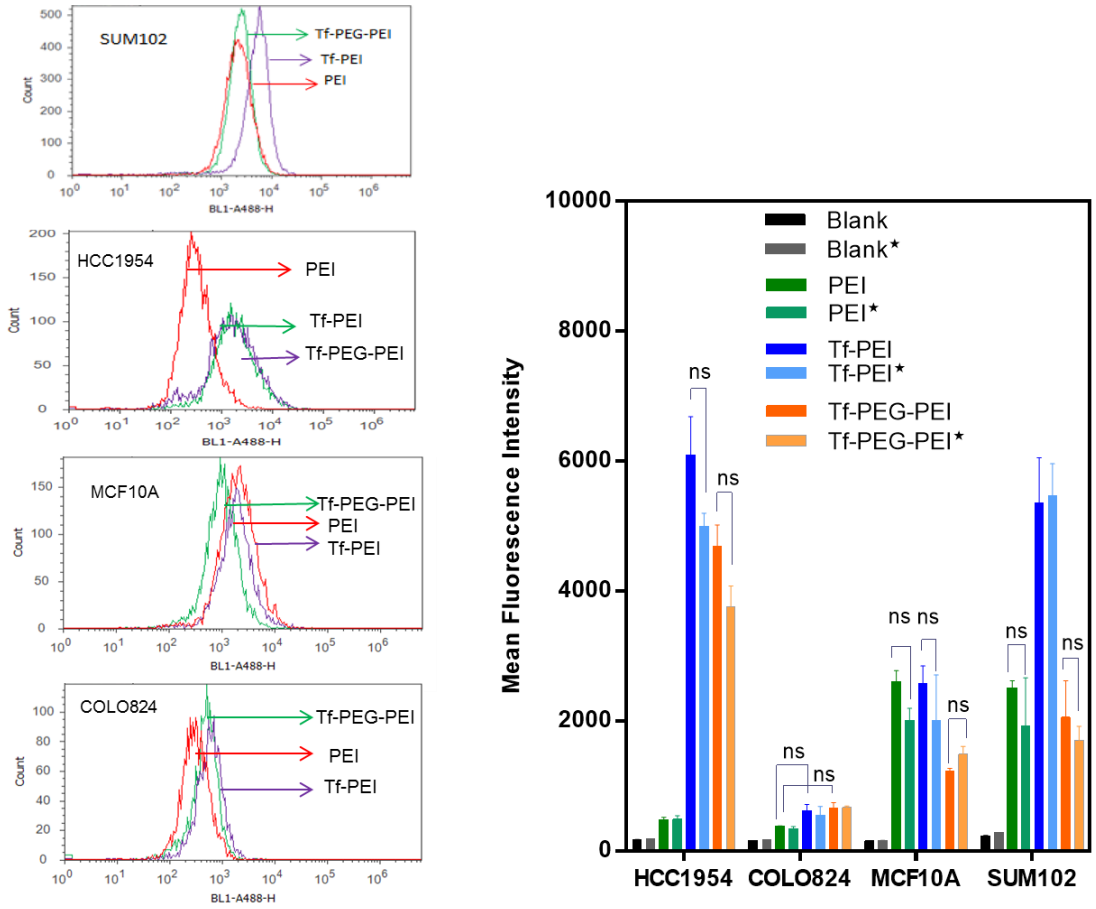

Figure 23 Cellular uptake of Tf-PEI, Tf-PEG-PEI and PEI. Comparison of siRNA uptake with different formulations (Blank (untreated cells), PEI (positive control), Tf-PEI, Tf-PEG-PEI) in GACS1 positive (HCC1954 and COLO824) and GASC1 negative (MCF10A and SUM102) cell line models after fluorescence quenching of membrane bound nanoparticles with trypan blue (asterisks indicate cell samples treated with trypan blue). Data are expressed as the mean ± SD (n = 3), ns: non-significant.

The intracellular uptake of the nanoparticles was then analyzed by confocal microscopy (Figure 24). The images obtained revealed the presence of concentrated fluorescence after 4 h of incubation with Tf-PEI conjugates. The internalization was detected using a Tye 563 labeled siRNA (Figure 24). Higher nanoparticle binding to the cell surface and cell entry of the Tf-PEI conjugate

compared to LF and polyethylenimine was visible. Interestingly, PEI delivered fluorescently labeled siRNA was not detected by microscopy which was consistent with the flow cytometry results showing very poor uptake of PEI polyplexes in HCC1954 cells.

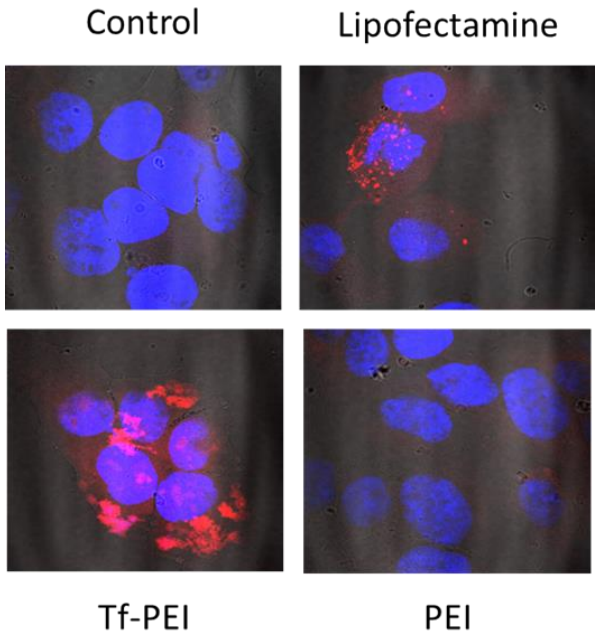

Figure 24 CLSM images of Tf-PEI and PEI. Confocal microscopy images of cellular interaction of different complexes with the HCC1954 cell line after 4 h incubation with siRNA polyplexes. HCC1954 cells were seeded with 25,000 cells per chamber and transfected with 25 pmol siRNA (Tye 563 labeled, indicated by red color) for 4 hours. Cells were fixed and the nuclei stained with DAPI (indicated by blue color). Representative pictures are shown (100X magnification). A) Blank; and siRNA polyplexes with B) Lipofectamine; C) Tf-PEI (N/P 7); and D) PEI (N/P 7).

4.3.6 Cytotoxicity

In order to test one aspect of biocompatibility of the nanoparticle systems investigated here, the cytotoxicity of PEI and Tf-shielded polyplexes was analyzed.

The rate of viability was assessed by CellTiter-Blue® assays which are based on the ability of active mitochondria to convert a redox dye (resazurin) into a fluorescent end product (resorufin). Neither the conjugate polyplexes (Tf-PEI/siRNA and Tf-PEG-PEI/siRNA) nor PEI/siRNA at N/P 7 appeared to have any apparent cytotoxicity, and cell survival rates greater than 85% were maintained for all treatments (Figure 4.25). There is a significant change in cell viability observed alone in PEI treated COLO824 cells compared to Tf-PEI ($p < 0.05$). No significant differences in cytotoxicity amongst the different cells lines were observed ($p > 0.05$).

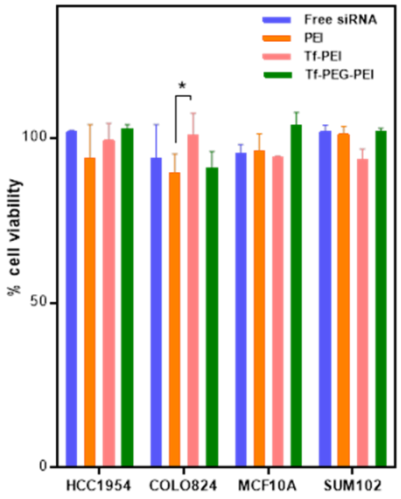

Figure 25 Cytotoxicity of PEI, Tf-PEI and Tf-PEG-PEI polyplexes. Cytotoxicity profile of siRNA polyplexes made with Tf-PEI or Tf-PEG-PEI measured by the Cell Titer-Blue method compared to PEI/siRNA polyplexes. HCC1954, COLO824, SUM102 and MCF10A cell lines were treated with polyplexes for 4 h and the viability of cells was measured after 24 h. Cell toxicity is presented as impaired cell viability as a percentage relative to control cells. Data are expressed as the mean ± SD (n = 5). * $P < 0.05$.

4.3.7 GASC1 knockdown optimization

To identify the amount of GASC1 knock-down on the mRNA level, several transfection parameters were optimized and determined by RT-PCR. The primary studies were performed with 9 commercially available siRNA sequences [(A-D) and (E-H and mixed)] to screen their efficacy against GASC1 since no validated sequences are available. LF was used as standard transfection agent. Figure 26 shows the GASC1 knock down efficiency in HCC1954 cells with the above mentioned siRNA sequences. Among the different sequences, the strongest relative reduction in GASC1 RNA was achieved with sequence “A”. However, there was no significant difference between A and sequences C, D and E ($p > 0.05$). Based on this result, sequence “A” was applied for further optimization experiments.

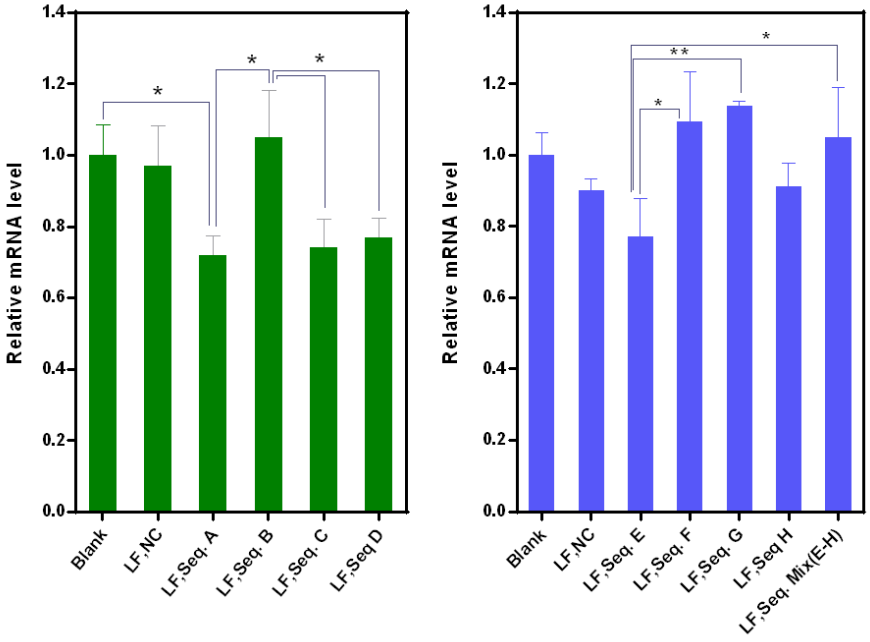

Figure 26 optimization of GASC1 siRNA sequence. GASC1 gene knock down optimization with different siRNA sequences [(A-D sequences from Qiagen) and siRNA sequences E-H and pooled siRNA from Dharmacon]. Per well, 500,000 HCC1954 cells were transfected with lipofectamine2000 (LF) for 24 hours with 100 pmol of different siRNA sequences against GASC1. RT-PCR was performed with specific GASC1 primers, normalization was carried out against the housekeeping gene PUM1. (NC=scrambled siRNA; error bars reflect SD, n=3). * $P < 0.05$ and ** $P < 0.01$.

Gene silencing efficiencies were investigated after 6, 17, 24, 48 h post transfection (Figure 27). Clearly, the GASC1 mRNA level was reduced significantly after 24 h but was not significantly further reduced 48 h post transfection ($p > 0.05$). However, there was no measurable gene knock down compared with the negative/non treated control at the 6h and 17 h time points. Additionally, the GASC1 mRNA levels measured at 6 h and 17 h were not significantly different as well as the levels measured at 17 h and 48 h post

transfections with sequence “A” (Figure 27). The optimum transfection time point of 24 h was then used to probe the effect of different siRNA doses (100, 150, 200, 250 pmol). However, the most efficient gene knockdown was already achieved at 100 pmol, so that further optimization was not successful.

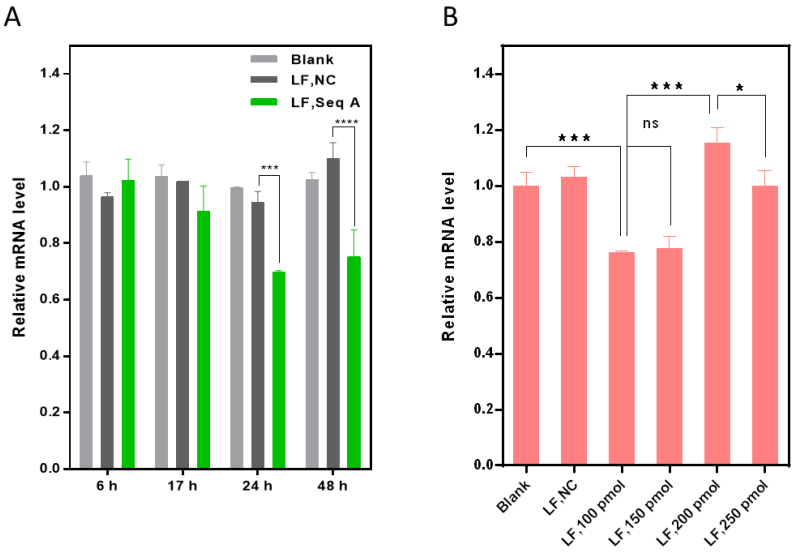

Figure 27 GASC1 gene knock down optimization. GASC1 gene knock down optimization with siRNA sequence A in HCC1954 cells at different time points (A), or different siRNA concentrations 24 h post transfection (B). Lipofectamine2000 (LF) was used as transfection agent and RT-PCR was performed with specific GASC1 primers, normalization was carried out against the housekeeping gene PUM1. (NC=scrambled siRNA; error bars reflect SD, n=3), ns: non-significant,* $P < 0.05$, *** $P < 0.001$ and **** $p < 0.0001$.

As these sequences did not reach an acceptable and therapeutically relevant level of knock down, we designed three new sequences of GASC1 siRNA (named V_4, V_6 and V_7) using GENtle software. Figure 28 A presents the results of mRNA knock down with the newly-designed GASC1 siRNA duplexes. GASC1 siRNA (V_4, V_6 and V_7, 100 pmol) were used to transfect HCC1954 cells with LF, PEI and

the different Tf-modified nanobioconjugates. hGAPDH siRNA was used as a positive control. Among the different siRNA sequences, V_7 showed the most efficient mRNA reduction with LF which was comparable with the positive control. Additionally, the Tf conjugate (Tf-PEI) also showed promising knock down with sequence V_7. There was no significant difference between the mRNA knock down achieved with V_7 when delivered with PEI or Tf-PEG-PEI. To verify the result of the RT-PCR assay, we performed western blot analysis to quantify the target protein levels. The analysis indicated that cells treated with the optimized Tf-PEI polyplexes with GASC1 siRNA (N/P 7) expressed less GASC1 protein compared to lysates of cells that were treated with scrambled control or non-targeted PEI/GASC1 siRNA complexes as was predicted based on the RT-PCR results (Figure 28 B).

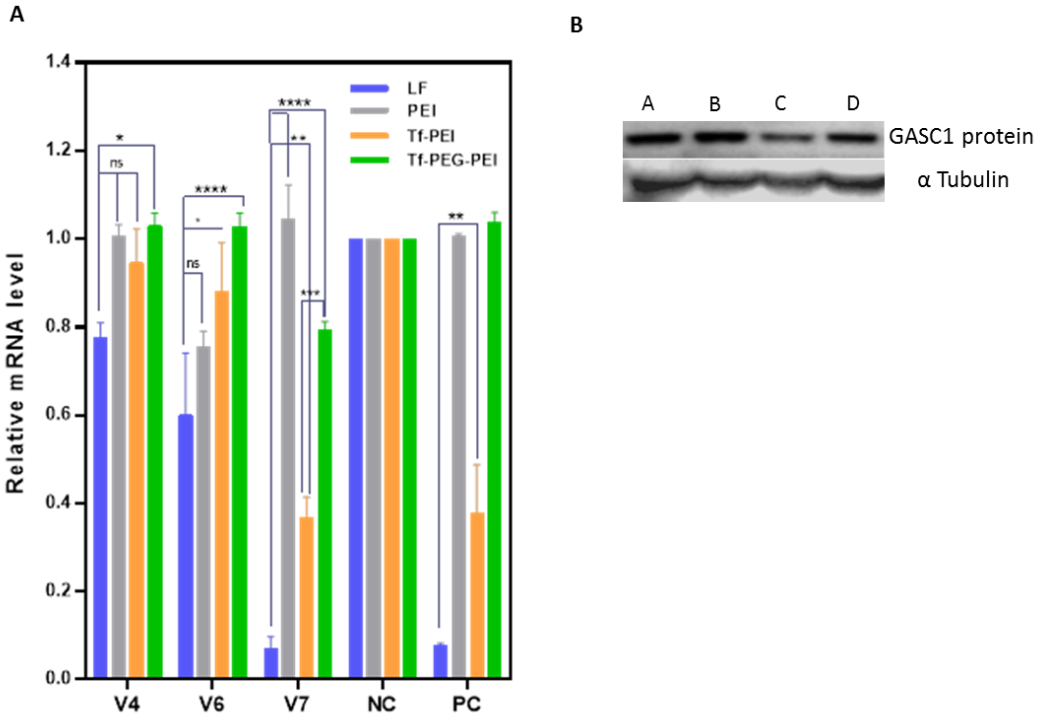

Figure 28 RT-PCR and western blot of GASC1 knock down. (A) GASC1 knockdown of Tf-PEI with siRNA sequence V7 shows that the conjugate was able to knock down mRNA levels of GASC1 more efficient than the commercially available siRNA sequences in HCC1954 cells. (V_4, V_6 and V_7 are self-designed GASC1 siRNA sequences. NC=scrambled siRNA; PC=positive control siRNA (hGAPDH), error bars reflect SD, n=3), ns: non-significant,* $P < 0.05$, ** $P < 0.01$, *** $P < 0.001$ and **** $p < 0.0001$. (B) GASC1 protein knockdown in HCC1954 cells with Tf-PEI compared to PEI alone was confirmed by western blot. Alpha-tubulin was used as the loading control. Top row shows (A: PEI/ V_7GASC1 siRNA, B: PEI/NC siRNA, C: Tf-PEI/V_7GASC1, D: Tf-PEI/NC siRNA.

4.3.8 Therapeutic effects

To determine if this gene knockdown on RNA and protein level would translate into a therapeutic effect, which would be reflected by a sequence-dependent inhibition of cell growth, MTT assays were performed after either one or multiple transfections. Even though a small effect on cell proliferation was

observed 24 h after a single transfection (2 days after seeding the cells), a more pronounced and clearly sequence-specific effect was observed after 3 transfections on day 10 after seeding the cells (Figure 29). While the proliferation after 3 transfections with the negative control siRNA seemed to be slightly inhibited, the proliferation of those cells was not significantly different from the untreated control cells.

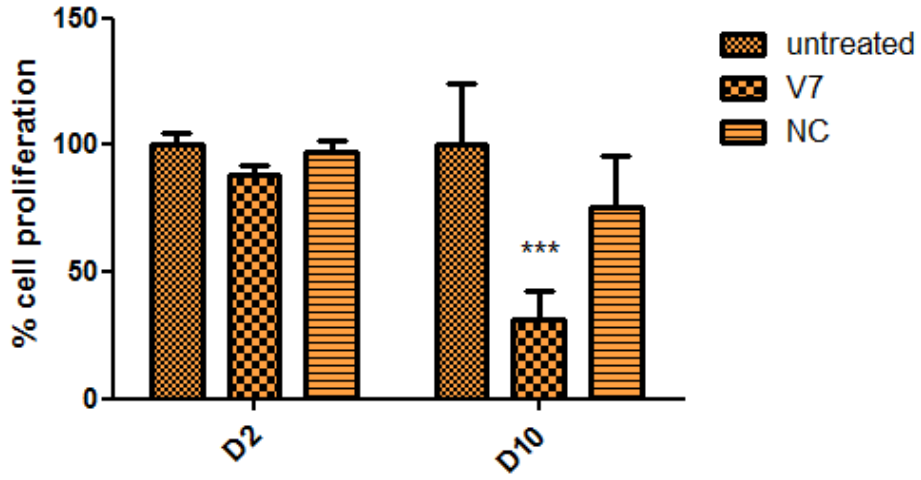

Figure 29 Inhibition of cell proliferation via GASC1 knockdown. Therapeutic effects of GASC1 knockdown with Tf-PEI polyplexes on days 2 (D2) and 10 (D10) after seeding measured as inhibition of proliferation of HCC1954 cells. V7 is a self-designed GASC1 siRNA sequence; NC=scrambled siRNA; error bars reflect SD, n=3).

4.4Discussion

Considering that epigenetics and genetics are accomplices in breast cancer tumor development, much attention has been paid to the investigation of molecular and biology insights which could lead to the design of more specifically tailored

therapies (e.g. gene therapy) [156]. siRNA mediated RNAi has become a powerful tool for its specificity and efficiency to knock down targets that cannot be readily down regulated by conventional chemotherapy [157]. However, siRNA clinical applications have been a very challenging task due to multiscale barriers, including rapid excretion of siRNA, low stability in blood serum, nonspecific accumulation in tissues, poor cellular uptake and inefficient intracellular release [157]. Several delivery strategies have been developed to address these issues [158]; Here, we aimed to design a specifically targeted nanoparticle delivery system with chemical modification and ligand decoration of the complexes to improve efficient delivery of siRNA for the down regulation of GASC1 overexpression in target cells. This strategy was chosen because GASC1 overexpression correlates with poor prognosis in BLBC patients [144].

Low molecular weight polyethylenimine (PEI) has been researched extensively as a safe and efficient nucleic acid delivery system based on its ability to electrostatically complex siRNA molecules into nanoscale polyplex and hence, to protect them from nuclease degradation [159]. However, PEI alone is not a suitable carrier for targeted gene delivery to specific cells [159b]. Meanwhile, TfR is cell membrane-associated glycoprotein serving as the main port of entry for iron through a clathrin/dynamin dependent endocytosis mechanism [160] and can be used as a gate for delivery of PEI when conjugated to a ligand such as transferrin that

selectively targets TfR on receptor expressing cells. Therefore, utilizing knowledge about the physiological function of the transferrin–transferrin receptor complex and the efficiency of its receptor mediated endocytosis provides the rationale to develop transferrin-targeted anticancer modalities. Moreover, studies have shown the elevated expression levels of TfR on cancer cells compared with normal cells; which correlates with tumor stage and poor prognosis (The Nottingham prognostic index (NPI)) [135, 161]. Among the different ligand targeting nanoparticles, there are four transferrin-conjugated nanoparticle delivery systems currently in early clinical evaluation studies [162]. Our TfR screening study confirmed distinct levels of TfR among breast cancer cell models (Figure 16), and the cell line HCC1954 (overexpressing GASC1) posses the highest TfR expression compared to the healthy breast cell line MCF10A (GASC1 negative control). The results of the binding capacity of transferrin to actively endocytosing TfR were in accordance with the transferrin receptor expression data and led to the assumption that the fluorescently labeled Tf remained its binding capacity after FITC labeling and was successfully internalized by the TfR in HCC1954 cells as a valid model for over expression of TfR (Figure 17).

Here, we used functionalized linkers (SPDP or PEG4-SPDP) to couple the targeting ligand transferrin to LMW-PEI (Figure 18). The effect of two different linker types and different molar stoichiometries (Tf:PEI) on nanoparticle

formation and efficacy were compared. The analysis of the prepared conjugates revealed that a Tf:PEI molar ratio between 1.3-2 results in better condensation of siRNA in the Tf-PEI polyplex which are considerably smaller than a ratio around 0.4 for Tf-PEG-PEI polyplex (Figure 19). The difference in transferrin coupling degrees observed in this study was a result of using different linkers, i.e. SPDP vs. PEG4-SPDP. However, it is also possible that the presence of PEG in the nanobioconjugate with the lower transferrin coupling degree interfered with dense condensation of siRNA based on electrostatics. The presence of PEG in the crosslinking agent may, however, benefit the ligand-receptor interaction of those conjugates as the spacer provides longer distance of the ligand from the polyplex and better solubility. Accordingly, this space may avoid steric hindrance of ligand-receptor binding by the bulky nanoparticle. However, it needs to be kept in mind that the coupling of substances to the primary amines of PEI may reduce its charge density and the proton sponge effect as well as the interaction with siRNA. Indeed, excessive grafting influences the complexation efficacy, complex stability, and complex architecture, and thus requires detailed analysis prior to application in vivo [159b].

The extent of siRNA condensation with transferrin conjugates was determined by measuring the change of the fluorescence intensity of SYBR Gold as nucleic acid intercalating agent at different N/P ratios. Increasing the N/P ratios

from 1 to 20 not only led to decreased amounts of free siRNA as shown in Figure 21, but also higher net positive charges of the polyplexes were obtained. This higher net charge increases the ability of polymer to electrostatically interact with negatively charged siRNA and to condense siRNA more efficiently. However, higher positive charges of the nanoparticles also correlate with non-specific toxicity and non-specific cell uptake. As shown by Plank et al., nanoparticles with a positive surface charge can bind nonspecifically to the cell surface and, in addition, activate the alternative complement system [163]. This interaction would also lead to rapid nanoparticle uptake by the reticuloendothelial system (RES) after in vivo administration, and as a consequence, rapid clearance of the nanoparticles is expected. However, modification of the polymer surface reduces this phenomenon [164]. In our experiments, the condensation efficiency for all three formulations (PEI, Tf-PEI and Tf-PEG-PEI) reached a plateau at N/P ratio of ≥ 7, indicating the ability of efficiently complexing with siRNA. The results in Figure 21 showed that the condensation ability of PEI was not compromised even after modification with transferrin. Therefore, polyplexes with N/P ratio of 7 were chosen as the optimal ratio for further experiments.

Particle size and zeta potential are key factors in the biological outcomes of a drug delivery system as they govern the biodistribution profile, their efficiency to accumulate in tumors through the enhanced permeability and retention (EPR)

effect and cellular uptake [165]. As a rough estimation, it is believed that the design of rigid and spherical nanoparticles ranging in size from 10 to 200 nm improves circulation half-life of nanoparticles and their uptake by tumors [166]. At the aforementioned N/P ratio, Tf-modified polyplexes displayed very promising small sizes with close to neutral zeta potentials (Figure 19). The latter property is of particular interest for potential in vivo use, since a neutral surface charge reduces nonspecific charge-based interactions and undesirable clearance by the RES such as liver and spleen macrophages, and improves the blood compatibility. Thus, small nanoparticles with close to neutral surface charge are expected to efficiently deliver anti-cancer drugs to tumor sites [167].

The stability of polyplexes is another critical component which determines the nanoparticles' efficiency. The presence of competing anions in the cell membrane or in serum is known to affect the stability of polyplexes which determines their in vivo fate [168]. Since conjugation of Tf to PEI might influence complex stability, this issue was addressed by incubating the complexes with the competing model polyanion heparin [169]. Results confirmed the ability of modified PEI (Tf-PEI) to protect the siRNA in the presence of polyanions even more efficiently than PEI alone, however, Tf-PEG-PEI showed lower stability compared to Tf-PEI and PEI alone (Figure 22). Our results reflect the enhanced stability of Tf-shielded polyplexes (Tf-PEI) which also has been reported by others [132]. Based

on the zeta potential results, we hypothesize that Tf is located on the surface of the nanoparticles and shields the PEI/siRNA from competing polyanions. The PEG-containing complexes, however, exhibited compromised stability which may be due to the less dense packaging of siRNA as hypothesized above. The peak of siRNA release that was especially prominent for the Tf-PEI and PEI formulation can be explained as an initial competition between bound siRNA and added heparin for binding with PEI. After longer incubation, however, a new equilibrium is reached, and possibly even ternary complexes of polymer, siRNA, and heparin are formed. A part of the initially released siRNA seems to be condensed again at 45 min or 60 min after incubation resulting in lower fluorescence intensities. In case of Tf-PEG-PEI, the siRNA was released almost quantitatively upon addition of heparin and further incubation did not lead to a re-complexation of siRNA. The weak condensation of siRNA by Tf-PEG-PEI therefore precludes any in vivo administration of this formulation.

The Tf-modified PEI formulations are also expected to avoid nonspecific cytotoxicity which is often caused by excess positive charges on PEI. This was confirmed by the CellTiter-Blue® assay (Figure 25). We propose that this modification of PEI could reduce the toxicity of the polymer backbone and also enhance the stability of Tf-PEI complexes as well as the circulation of polyplexes in vivo.

Superior internalization of the delivered siRNA with Tf modified PEI in GASC1 positive HCC1954 cell lines compared to PEI alone was confirmed by flow cytometry and confocal microscopy images (Figures 23 and 24). These interesting results implied that Tf-PEI/siRNA polyplexes undergo selective cellular uptake through transferrin receptor-mediated endocytosis, and therefore may exhibit increased therapeutic benefits through the ability to deliver high concentrations of relevant siRNA to the tumor site [161]. However, it must be taken into account that the final silencing effect depends also on the endo-lysosomal escape and the efficient incorporation of siRNA to the RNA-induced silencing machinery [170].

While the ligand choice depends on the receptor being targeted, an additional consideration for targeting is the type of cell entry pathway that will be induced after ligand-receptor binding. Therefore, the endocytic pathway which may be used by the vector depends on the targeting ligand, cell type and vector properties [171]. It was surprising that in COLO824 cells with relatively high levels of TfR (Figure 16), no significant transfection was detected with PEI alone or modified PEI (Figure 23). This could be related to the cell type which may have a very low endocytic activity, but an accurate answer requires further investigations.

It has been proposed that the majority of receptor-ligand complexes (e.g. Tf/TfR) enter cells by clathrin-mediated endocytosis [172]. Receptor binding

typically triggers the localized accumulation of clathrin structures on the cytoplasmic surface of the plasma membrane as it begins to invaginate, forming clathrin-coated pits [172]. TfR undergoes clathrin-mediated endocytosis and may enter two types of trafficking pathways [173]. In the first pathway, within 10 min after uptake, the receptor undergoes rapid recycling from early endosomes to the cell surface. In the second pathway, the receptor undergoes slow recycling to the cell surface from the recycling compartment, which is slightly acidic [173]. Importantly, studies showed that gene expression after delivery with nanoparticles which enter cells through clathrin-coated endocytosis is comparably less efficient than after delivery via other pathways, suggesting that this path is linked to endosomolytic degradation of the cargo. Therefore, vectors utilizing this pathway must incorporate a mechanism of release from either organelle [160]. Here, we used PEI for its important buffering feature with regard to the intracellular fate of the complexes. The so-called ‘proton sponge effect’ postulates a proton acceptor function of PEI, leading to the buffering of low pH values in the endosomal/lysosomal system and therefore reduced nuclease activity. The influx of chloride counter ions and the resulting osmotic influx of water then causes swelling and bursting of the endo-lysosomes, which eventually leads to release of the endo-lysosomal contents [174]. Therefore, as stated earlier, careful formulation of vector assembly should be taken into account not to compromise this property

through grafting with targeting moiety and reducing the accessible protonable amine groups.

As reported by a study for Tf-targeted nanoparticles (lipoplexes), it is likely that other yet unidentified cell surface components (nonreceptor endocytosis) also mediate complex binding and uptake. This might be the reason for the rather high transfection efficacies of Tf-PEI nanoparticles in SUM102 cells. The underlying molecular mechanisms have yet to be investigated.

It has been also demonstrated that conjugation/linker chemistry may have a significant effect on transfection efficiency and specificity in vitro [175]. In our study, we used two structurally different conjugates (Tf-PEI and Tf-PEG-PEI) which were comparable in physicochemical properties but different in transfection, binding, and uptake efficiencies. As a result, the efficiency of PEI conjugates strongly depends on the linker chemistry. The coupling of transferrin with SPDP to LMW-PEI was most efficient. In contrast, our second approach of using PEG chains in the form of PEG4-SPDP showed that a slightly longer spacer may hinder the proper presentation of transferrin, the condensation of siRNA, and/or have an effect on proton sponge features of PEI. Introducing a cyclic RGD peptide as a targeting moiety via direct coupling or PEG spacer linking to PEI studied by Kunath et al. showed that only direct coupling of the peptide to PEI via SPDP mediated efficient and specific DNA transfection, while an RGD-PEG-PEI

conjugate was inefficient. The authors concluded that the use of a PEG spacer seemed to impair targeting, possibly by not only shielding PEI, but also the RGD ligand [176]. In contrast, Moffatt et al. successfully utilized a PEG linker for coupling an anti-PSMA antibody to PEI/DNA polyplexes [177]. Polyethylene glycol (PEG) spacers are expected to preserve protein function by moving the targeting moiety away from the surface, by providing flexibility and reducing non-specific binding of environmental biomolecules [178]. In another study, antibody-PEI conjugates were prepared with three different linkers (SPDP, SMCC, and IBFB 110001) to prepare HER2 or CD90 targeted conjugates. Using these linkers, major differences in the degrees of conjugation and in target cell specificity of the resulting conjugates were found. Interestingly, none of the conjugates prepared with SPDP as a linker showed target cell specificity. Because of significant differences in the study design, direct comparison of these results proved to be difficult, however.

Optimization of GASC1 knockdown on the mRNA level was carried out by initially screening commercially available GASC1 siRNA sequences. The results revealed that three commercially available sequences (“A”, “C”, and “D” obtained from Qiagen) were able to reduce the GASC1 mRNA levels to about 75% after transfection with LF (Figure 26). While the general expression levels of GASC1 can not be compared to easy-to-knock down genes like the housekeeping gene GAPDH, the reduction to 75% residual expression even with LF was not

acceptable. Therefore, several parameters such as incubation time and siRNA concentration were attempted to be optimized (Figure 27). Since the gene knock down was not improved by this approach, new siRNA sequences (V_4, V_6 and V_7) were designed and transfected with LF, PEI and Tf-modified PEIs (Figure 28). The gene knock down efficacy was determined via RT-PCR. Among all sequences, V_7 showed very promising results after transfecting HCC1954 cells with LF and acceptable results after transfection with Tf-PEI/siRNA complexes (N/P 7, Figure 28A). This final formulation was therefore used to verify the protein knockdown level in HCC1954 cells after 7 days of incubation based on a previously optimized protocol. The western blot analysis confirmed the RT-PCR results (Figure 28B), indicating that the combination of Tf-PEI with V_7 siRNA is a promising formulation for GASC1 gene knock down in BLBC.

The question whether GASC1 gene knock down would result in efficient inhibition of cell proliferation was answered after optimizing the transfection approach. As shown in Figure 29, a single transfection did not yet lead to efficient inhibition of cell proliferation. This result is not surprising considering that previous approaches using shRNA[145a] or small molecule GASC1 inhibitors also required multiple treatments to inhibit cell proliferation.[179] The results also imply that GASC1 may have a long biologic half-life. Figure 29 shows that multiple treatments with negative control siRNA can have a small but not significant

impact on cell proliferation in comparison to untreated cells, whereas one single treatment does not affect the cells, which is in line with the cytotoxicity results shown in Figure 25.

4.5 Conclusions

The establishment of an efficient and cell type-specific gene delivery system is a most challenging objective, which in the context of cancer therapy ideally would allow for the specific introduction of a therapeutic transgene or knock out in malignant cells. Tf-PEI demonstrated enhanced gene transfer efficiency in BLBC cells overexpressing TfR compared to non-modified PEI. Through inhibiting the epigenetically and therapeutically relevant target gene GASC1 which is involved in multiple signaling pathways leading to tumorigenesis, Tf-PEI nanoparticles treatment has revealed promising results regarding gene silence efficiency and inhibition of breast cancer cell proliferation. However, it remains to be shown whether these properties can be exploited for targeted in vivo gene delivery after systemic administration.

CHAPTER 5 TARGETED DELIVERY OF SIRNA TO TRANSFERRIN RECEPTOR OVEREXPRESSING TUMOR CELLS VIA PEPTIDE MODIFIED POLYETHYLENIMINE

Please note that part of the content of this chapter is from a research article,"Targeted Delivery of siRNA to Transferrin Receptor Overexpressing Tumor Cells via Peptide Modified Polyethylenimine", was published in Molecules (Y. Xie, et al., 2016). The authors of this article include Bryan Killinger, Anna Moszczynska, Olivia M Merkel and me. I am the first author of this research paper. I performed the experiments and wrote the manuscripts.

5.1 Introduction

TfR is overexpressed in many kinds of cancers due to their increased consumption of iron but is expressed at a low level on most cells. Therefore, the upregulation of TfR in cancer cells makes it a promising target for the selective delivery of siRNA for cancer therapies [57b]. Several strategies have been explored to target TfR, including the use of holo-Tf or monoclonal antibodies raised against TfR [180] [181] which were coupled to polymers [44], and liposomes [182]. We have shown that Tf-PEI can efficiently deliver therapeutic siRNA to breast cancer cells overexpressing TfR in **Chapter 4**. However, high concentrations of endogenous Tf in blood plasma (25 μM) may competitively inhibit the uptake mediated by the holo-Tf or the anti-TfR antibody [183]. Furthermore, holo-Tf (molecular weight (MW) 80 kDa) and antibodies against TfR (e.g., the anti-human TfR antibody

5E9,

MW= 30 kDa [180]) are relatively large, and therefore, may introduce steric hindrance when the drug delivery system is synthesized. The stability of these proteins will also need to be taken into consideration in terms of synthesis conditions, storage, formulation, and expected shelf-life. A viable alternative to Tf and TfR specific antibodies is the use of TfR binding peptides. Two peptide sequences, HAIYPRH and THRPPMWSPVWP, discovered by phage display, were reported to be able to non-competitively bind to human TfR with high affinity and consequently trigger TfR internalization [184]. The chemico-physical properties of these peptides are more stable and their MWs are smaller than those of holo-Tf and antibodies.

The aim of this study was to develop a siRNA delivery system to target TfR overexpressing tumor cells. In this chapter, two TfR targeting peptides and bPEI were successfully coupled via two different crosslinkers, namely PEGylated succinimidyl 3-(2-pyridyldithio) propionate (PEG4- SPDP) and sulfosuccinimidyl 4-(N-maleimidomethyl) cyclohexane-1-carboxylate (sulfo-SMCC). The siRNA and bPEI or peptide-bPEI polyplexes were characterized regarding size, zeta-potential, and siRNA condensation efficiency. Selective delivery of siRNA using peptide-bPEI was investigated in the TfR overexpressing cell line H1299 and low TfR expressing cell lines A549 or H460. Gene knockdown efficiency of

siRNA/peptide-bPEI polyplexes was measured both at the mRNA and protein level in H1299 cells.

5.2 Materials and Methods

5.2.1 Materials

Branched 5k Da bPEI (Lupasol® G100) and 25k Da bPEI (Lupasol® HF) were obtained from BASF (Ludwigshafen, Germany). Succinimidyl 3-(2-pyridyldithio) propionate (SPDP), PEGylated succinimidyl 3-(2-pyridyldithio) propionate (PEG4- SPDP) and sulfosuccinimidyl 4-(N-maleimidomethyl) cyclohexane-1-carboxylate (sulfo-SMCC) were purchased from Thermo Fisher (Waltham, MA, USA). Dulbecco's phosphate buffered saline (PBS), 1,4-Dithio-DL-threitol (DTT), dimethyl sulfoxide (DMSO), HEPES, ethylenediaminetetraacetic acid disodium salt dehydrate (EDTA), picrylsulfonic acid solution (TNBS, 5% w/v), sodium pyruvate, sodium bicarbonate ($NaHCO_3$) and glucose were bought from Sigma-Aldrich (St. Louis, MO, USA). Human holo-transferrin was obtained from EMD Millipore (Billerica, MA, USA). Cysteine modified TfR binding peptide HAIYPRH (Cys-His-Ala-Ile-Tyr-Pro-Arg-His) was synthesized by BACHEM Americas (Torrance, CA, USA) and THRPPMWSPVWP (Thr-His-Arg-Pro-Pro-Met-Trp-Ser-Pro-Val-Trp-Pro-Cys) was synthesized by the American Peptide Company (Sunnyvale, CA, USA). Enhanced green fluorescent protein (eGFP) siRNA, amine modified eGFP siRNA,

siRNA fluorescently labeled with Ty563 (siRNA-Ty563), human glyceraldehyde-3- phosphate- dehydrogenase (GAPDH) siRNA and scrambled siRNA were purchased from Integrated DNA Technologies (Coralville, IA, USA).

Table 5 Sequence of siRNA.

Name	Sequence
eGFP siRNA	5´- pACCCUGAAGUUCAUCUGCACCACcg 3´-ACUGGGACUUCAAGUAGACGUGGUGGC
GAPDH siRNA	5´- pGGUCGGAGUCAACGGAUUUGGUCgt 3´UUCCAGCCUCAGUUGCCUAAACCAGCA
Scramble siRNA	5´-pCGUUAAUCGCGUAUAAUACGCGUat 3´CAGCAAUUAGCGCAUAUUAUGCGCAUAp

* Indication of modified nucleotides: “p” denotes a phosphate residue, lower case bold letters are 2´-deoxyribonucleotides, capital letters are ribonucleotides, and underlined capital letters are 2´-O-methylribonucleotides.

5.2.2 Synthesis of Peptide–bPEI Conjugate

The HAIYPRH peptide (HAI) was coupled to bPEI using two different crosslinkers, namely sulfo-SMCC and PEG4-SPDP. In the sulfo-SMCC crosslinking approach, as shown in Figure 30 B, 1 mg of 25k bPEI was dissolved in HEPES buffered saline (HBS) buffer (20 mM of HEPES and 150 mM of NaCl, pH=7.2) at 1 mg/mL, and 1 mg of sulfo-SMCC was dissolved in water at 10 mg/mL. bPEI solution and sulfo-SMCC were mixed together and allowed to stir for 4 h at room temperature (RT). bPEI-SMCC was purified using 10,000 molecular weight cut off (MWCO) centrifugal filters (Millipore) with HBS containing 2 mM of EDTA buffer. The bPEI-SMCC solution was mixed with 1

mg of HAI peptide dissolved in HBS containing 2mM of EDTA (5 mg/mL) and stirred overnight at RT. The next day, free HAI peptide was removed from HAI-bPEI using 10,000 MWCO centrifugal filters. In the PEG_4-SPDP crosslinking approach, as shown in Figure 30 A, 5 mg of 25k bPEI was dissolved in HBS buffer at 5 mg/mL, and 2 mg of PEG4-SPD was dissolved in DMSO at 20 mM. PEG4-SPDP was added drop-wise into the bPEI solution and stirred overnight at RT. Meanwhile, 2 mg of HAI peptide was dissolved in HBS containing 2 mM of EDTA buffer at 4 mg/mL and reduced by 10 molar excess DTT for 2 h. Reduced HAI peptide solution was transferred to a 500–1000 MWCO dialysis tube (Spectrum laboratories, Rancho Dominguez, CA, USA) and dialysis was performed against HBS containing 2 mM of EDTA buffer overnight at 4 °C. The next day, bPEI-SPDP was purified using 10,000 MWCO centrifugal filters with HBS containing 2 mM of EDTA buffer and then mixed with the reduced HAI peptide. The mixture was stirred for 24 h at RT followed by purification using 10,000 MWCO centrifugal filters with HBS. The concentration of HAI peptide in the conjugate was measured spectrophotometrically at 280 nm. The concentration of bPEI in the conjugate was determined by a TNBS assay [122]. Briefly, the according amount of HAI peptide was added into bPEI serial dilution to generate a standard curve in a clear 96-well plate (Corning, Corning, NY,USA). Then 30

µl of 3 mM of TNBS solution was added to 100 µl of bPEI/HAI solution and the absorbance at 405 nm was determined after 5 min.

5k bPEI (1 mg/mL) was dissolved in HBS buffer and mixed with 100 µl 20 mM of SPDP, stirred overnight, followed by purification via 3000 MWCO centrifugal filters. THRPPMWSPVWP peptide (THR peptide) was reduced by 10-fold excess TCEP HCl (Thermo Fisher) and purified using a PD10 column (GE healthcare). THR peptide was mixed with bPEI-SPDP overnight while stirring at RT. The concentrations of THR peptide and bPEI in conjugate were measured spectrophotometrically at 280 nm and by a TNBS assay, respectively.

5.2.3 Fluorescent Labeling of PEI, Transferrin, Peptide and siRNA

bPEI was fluorescently labeled with fluorescein-5-isothiocyanate (FITC) (Thermo Fisher). 15 mg of bPEI was dissolved in 0.1 M $NaHCO_3$ (pH= 9) at 2.5 mg/mL, and 2 mg of FITC was dissolved in 200 µl of DMSO. The FITC solution was added drop-wise to the bPEI solution and allowed to stir for 3 h at RT. Free FITC was removed using 10,000 MWCO centrifugal filters, and bPEI-FITC was stored in water. The bPEI concentration was determined by a TNBS assay as described above, and the presence of FITC showed no interference with the results, as reported before [47]. For the conjugates, 0.2 mg of FITC (1 mg/mL) in DMSO was added dropwise into 2 mg of HAI-bPEI synthesized via the sulfo-SMCC approach and allowed to react for 3 h with stirring. The concentration of

bPEI in the conjugate was determined by a TNBS assay with a bPEI-FITC standard curve. Holo human Transferrin was fluorescently labeled with Texas Red modified with succinimidyl ester (Thermo Fisher) following the manufacturer's protocol. Cysteine modified THR peptide was fluorescently labeled with a Alexa Fluor 488 modified with maleimide (Thermo Fisher) following the manufacture's protocol. Amine modified siRNA was fluorescently labeled with Alexa Fluor 488 modified with succinimidyl ester (Thermo Fisher) following the manufacturer's protocol, followed by purification using ethanol precipitation and silica spin column binding as reported before [123].

5.2.4 Preparation of Polyplexes

To prepare the siRNA and polymer polyplexes, polymer was diluted with 5% glucose to different concentrations. An equal volume of polymer solution was added to a predetermined amount of siRNA solution to yield different amine to phosphate ratios (N/P ratios) and allowed to incubate for 15 min at RT before measurement or transfection. The calculation to prepare polyplexes is based on the following equation: $m_{polymer}$ (pg) = n_{siRNA} (pmol) × $MW_{protonable}$ (g/mol) × N/P × $N_{nucleotide}$ ($MW_{protonable}$ of bPEI = 43.1 g/mol, $N_{nucleotide}$ of siRNA = 52).

5.2.5 . Measurement of Hydrodynamic Size and Zeta-Potential

Polyplexes were prepared with bPEI or HAI-SPDP-bPEI and 50 pmol of siRNA at N/P 5 in 100 µl 5% glucose buffer as described above and were

transferred to a disposable micro cuvette (Brand GMBH, Wertheim, Germany). Size measurement was performed in three runs using a Zetasizer Nano ZS (Malvern Instruments Inc., Westborough, MA,USA). Results were collected and analyzed with the Zetasizer Software (Malvern) with settings of 173° backscatter angle, 0.88 mPa*s for viscosity and 1.33 for refractive index. Subsequently, the same polyplex solutions were diluted to 1 mL with water and transferred to a folded capillary cell (Malvern). The zeta-potentials of polyplexes were determined in three runs using a Zetasizer Nano ZS (Malvern).

5.2.6 siRNA Condensation Measured by a SYBR Gold Assay

SYBR Gold is a fluorescent dye which is used to stain nucleic acids. It intercalates into siRNA and produces fluorescence. When siRNA is condensed by polymer and becomes inaccessible for SYBR Gold, the fluorescence will decrease. Polyplexes were prepared with bPEI or HAI-SPDP-bPEI and 50 pmol of siRNA at different N/P ratios (1, 2, 3, 5, 7, 10) in 100 µl per well in a FluoroNunc 96 well white plate (Thermo Fisher). Subsequently, 30 µl of 4 × SYBR Gold was added to each well and incubated for 10 min in the dark. The fluorescence of SYBR Gold was determined by a Synergy 2 multi-mode microplate reader (BioTek Instrument, Winooski, VT, USA) with an excitation filter 485/20 nm and an emission filter 520/20 nm. The fluorescence of free siRNA (N/P= 0) represented 100% free siRNA. The experiment was performed in triplicate.

5.2.7 Cell Culture

NCI-H1299 cells (human non-small cell lung carcinoma) and A549 cells (human non-small cell lung carcinoma) were purchased from ATCC (Manassas, VA, USA). NCI-H460 cells (human large cells lung carcinoma) were a kind gift from Dr. Larry H. Matherly (School of medicine, Wayne State University, USA). H1299/eGFP is a H1299 cell line stably expressing the reporter gene eGFP. H1299 and H460 cells were cultured in RPMI-1640 media (GE healthcare, Buckinghamshire, UK) supplemented with 10% heat inactivated fetal bovine serum (v/v) (Sigma), 1× penicillin/streptomycin (Corning), 1× GlutaMax (Thermo Fisher), 10 mM of HEPES, 1.5 g/L of $NaHCO_3$, 4.5 g/L of glucose and 1 mM of sodium pyruvate. A549 cells were cultured in DMEM media (Corning) supplemented with 10% fetal bovine serum (FBS) and 1× pen/strep. All cells were maintained in a humidified atmosphere and 5% CO_2 at 37 °C.

5.2.8 Immunofluorescent Staining

H1299, H460 and A549 cells were harvested from flasks and washed with PBS. Each sample contained 100,000 cells and was resuspended in 10 µl of a 50-fold diluted human Fc receptor binding inhibitor (eBioscience, San Diego, CA, USA) for 5 min on ice. Subsequently, 20 µl of a 20-fold diluted phycoerythrin (PE) labeled human CD71 antibody (OKT9, eBioscience) or 20 µl of a 20-fold diluted PE labeled mouse IgG1 isotype control antibody (P3.6.2.8.1, eBioscience) were

added to the samples and incubated for 30 min in the dark at 4 °C. Samples were washed with PBS/ 2 mM of EDTA three times and were resuspended in 400 µl of PBS/ 2 mM of EDTA. The median fluorescent intensity (MFI) of samples was quantified using an Attune® Cytometer (Life Technologies, Waltham, MA, USA) with an excitation laser 488 nm and emission filter 574/26 nm. Cell populations were gated according to the forward and side scattering channel, and 10,000 events were collected. Data analysis was performed using the Attune® cytometer software (Life Technologies). Experiments were conducted in duplicate.

5.2.9 Quantification of Cellular Uptake and Cellular Binding

For cellular uptake experiments, H1299, H460 and A549 cells were seeded at the density of 50,000 cells/well in 24-well plates (Corning). After 24 h of incubation, polyplexes were prepared with 50 pmol of siRNA-AF488 and bPEI, HAI-SMCC-bPEI, HAI-SPDP-bPEI or THR-PEI at N/P=5. The cells were transfected with polyplexes at the siRNA concentration of 125 nM for 4 h. To reduce the potential cytotoxicity induced by concentrated polyplexes, fresh media were added to dilute siRNA concentration to 50 nM followed by an additional 20 h of incubation. The cells were harvested and washed three times with PBS/2 mM of EDTA. All samples were resupended in 400 µl of PBS/2 mM of EDTA, and MFIs of samples were determined via an Attune® Cytometer (Life Technologies) with an excitation laser 488 nm and emission filter 530/30 nm. In each sample,

10,000 events were collected and data analysis was performed using the Attune® cytometer software (Life Technologies). Experiments were conducted in triplicate.

For the cellular binding experiment, H1299 and A549 cells were seeded as described above. After 24 h incubation, different concentrations (0, 0.1, 1, 2 µg/ml) of THR peptide fluorescently labeled with Alexa Fluor 488 (THR-AF488) were added into media and incubated for 1 h at 37 °C. The cells were harvested and the MFI was quantified via flow cytometry as described above. Experiments were conducted in duplicate.

5.2.10 Confocal Laser Scanning Microscopy

H1299 cells were seeded at the density of 50,000 cells/well in 24-well plates with a 12 mm circle cover glass (Fisherbrand, 12CIR. -1) in each well and were incubated for 24 h. To determine intracellular distribution of polyplexes, fluorescently labeled polymer bPEI-FITC and HAI-SMCC-bPEI-FITC were formulated with 50 pmol of siRNA-Ty563 at N/P= 5. Cells were transfected with polyplexes at a siRNA concentration of 125 nM for the first 4 h and 50 nM for an additional 44 h. Cells were washed with PBS and fixed with 4% paraformaldehyde (PFA) solution in PBS (Affymetrix, Thermo Fisher) for 20 min at RT at different transfection time points (1, 4, 24, 48 h). To investigate the co-localization of the HAI peptide binding part with TfR, cells were incubated with 2 µg/mL of Tf-Texas Red and polyplexes formulated with bPEI-FITC or HAI—SMCC-bPEI-

FITC and 50 pmol of siRNA at N/P= 5 for 1 h or 4 h. To determine the co-localization of THR peptide binding part with TfR, cells were incubated with 2 µg/ ml of THR-AF488 and Tf-Texas Red for 1 h. Slides were washed with PBS and fixed with 4% PFA. After fixation, the nuclei were stained with 5 µM of DRAQ5 (Invitrogen, Thermo Fisher) for 5 min and rinsed with PBS. Slides were mounted with a Fluoromount mounting medium (Southern Biotech, Birmingham, AL, USA). Slides were imaged by a Leica TCS SPE-II laser scanning confocal microscope (Leica, Wetzlar, Germany), and the images were exported from the Leica Image Analysis Suite (Leica).

5.2.11 In Vitro GAPDH Gene Knockdown

To determine mRNA level knockdown efficiency of polyplexes, silencing of housekeeping gene GAPDH in H1299 and H460 was determined by real time PCR (RT-PCR). Cells were seeded at the density of 50,000 cells/well in 24-well plates for 24 h. bPEI, HAI-bPEI or THR-PEI were formulated with 50 pmol of siRNA against GAPDH or scrambled siRNA at N/P= 5. Cells were transfected with polyplexes at a siRNA concentration of 125 nM for the first 4 h and 50 nM for an additional 20 h. Total mRNA was isolated from cells using the PureLink® RNA mini kit (Life techonologies) following the manufacturer's protocol in the addition of DNase I digestion (Sigma). The brilliant III ultra-fast SYBR® green QRT-PCR master mix kit (Agilent Technologies, Santa Clara, CA, USA) was used

to reverse transcribe 100 ng of mRNA to cDNA and perform RT-PCR. RT-PCR was conducted in a Stratagene Mx 3005p qPCR system (Agilent Technologies) and cycle threshold (Ct) values were exported from MxPro software (Agilent Technologies). Hs_GAPDH_2_SG primers for GAPDH and Hs_ACTB_2-SG primers for β-actin (Qiagen, Valencia, CA, USA) were used in this experiment. GAPDH gene expression was normalized to β-actin gene expression for quantification and comparison, and the untreated group represented 100% GAPDH expression. Experiments were conducted in triplicate.

5.2.12 In Vitro eGFP Knockdown

To determine the protein level knockdown efficiency of polyplexes, silencing of reporter gene eGFP was determined by flow cytometry. H1299/eGFP cells were seeded at the density of 50,000 cells/well in 24 well-plates for 24 h. On the day of transfection, old media were replaced with 350 µl of fresh media with or without 115 µM of chloroquine. Cells were transfected with 50 pmol of siRNA against eGFP formulated with bPEI or HAI-bPEI at N/P= 5, 10 in total volume of polyplexes of 50 µl. bPEI and HAI-bPEI polyplexes containing scrambled siRNA at N/P= 10 were included as the negative control. Cells were transfected with 50 µl of polyplexes and incubated for 4 h with or without 100 µM of chloroquine. To dilute the concentration of chloroquine and polyplexes, 600 µl of fresh media were added, and cells were incubated for an additional 44 h. Afterward, cells were

harvested and washed three times with PBS/2 mM of EDTA. Samples were resuspended in 400 µl of PBS/2 mM of EDTA, and the MFIs were determined by an Attune® Cytometer (Life Technologies) with an excitation laser 488 nm and emission filter 530/30 nm. In each sample, 10,000 events were collected, and data analysis was performed using Attune® cytometer software (Life Technologies). Experiments were conducted in triplicate.

5.2.13 Statistics

Results were represented as mean +/- standard deviation (SD). All statistical analysis used One-way ANOVA with Newman–Keuls multiple comparison post-test in GraphPad Prism software (Graph Pad Software, La Jolla, CA, USA).

5.3 Result

5.3.1 Synthesis of HAI-bPEI

HAI-bPEI conjugates were successfully synthesized using crosslinkers sulfo-SMCC or PEG_4-SPDP (Figure 30 A and B). To synthesize HAI-SMCC-bPEI, sulfo-SMCC was first reacted with primary amines in bPEI, then the maleimide group in bPEI-SMCC was reacted with sulfhydryl in the cysteine modified HAI peptide. To synthesize HAI-SPDP-bPEI, PEG_4-SPDP was first coupled with bPEI. After purification, bPEI-PEG_4-SPDP was coupled to DTT-reduced cysteine-modified HAI peptide. The molar ratios of HAI peptide to bPEI

were determined according to the absorbance at 280 nm and the 2,4,6-trinitrobenzene sulfonic acid (TNBS) assay. The molar ratio of HAI peptide to bPEI was 18.6 for HAI-SMCC-bPEI and 18.2 for HAI-SPDP-bPEI.

THR peptide was successfully conjugated to bPEI via crosslinker SPDP (Figure 30 C). bPEI first reacted with SPDP while THR peptide was activated with TCEP HCl. PEI-SPDP was coupled to reduced-THR peptide and yielded THR-PEI. The molar ratio of THR peptide to bPEI is 0.4.

(A)

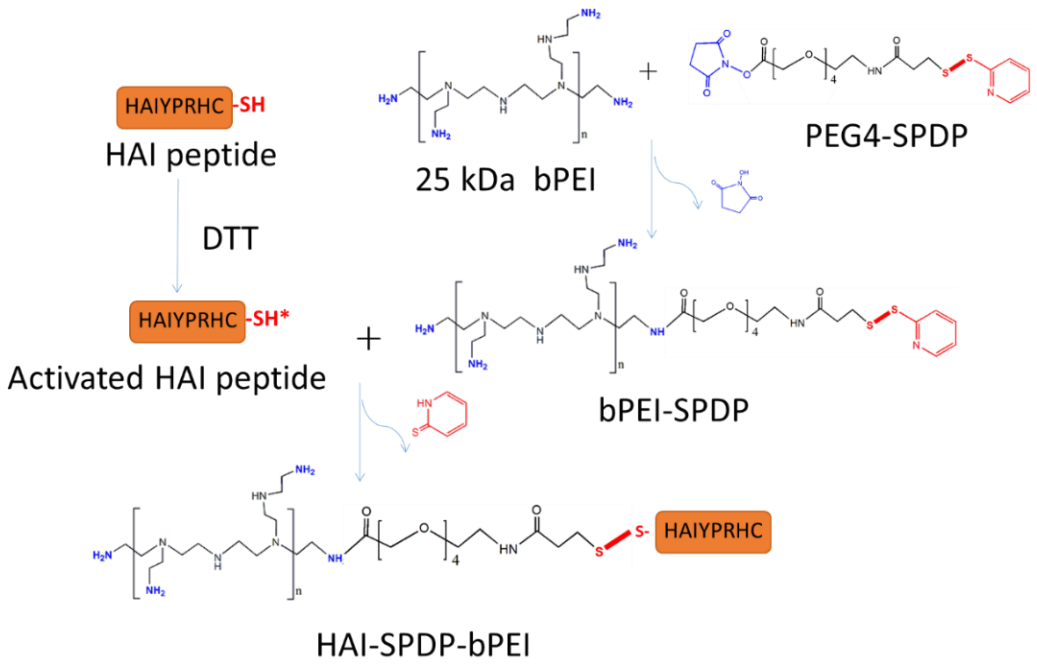

(B)

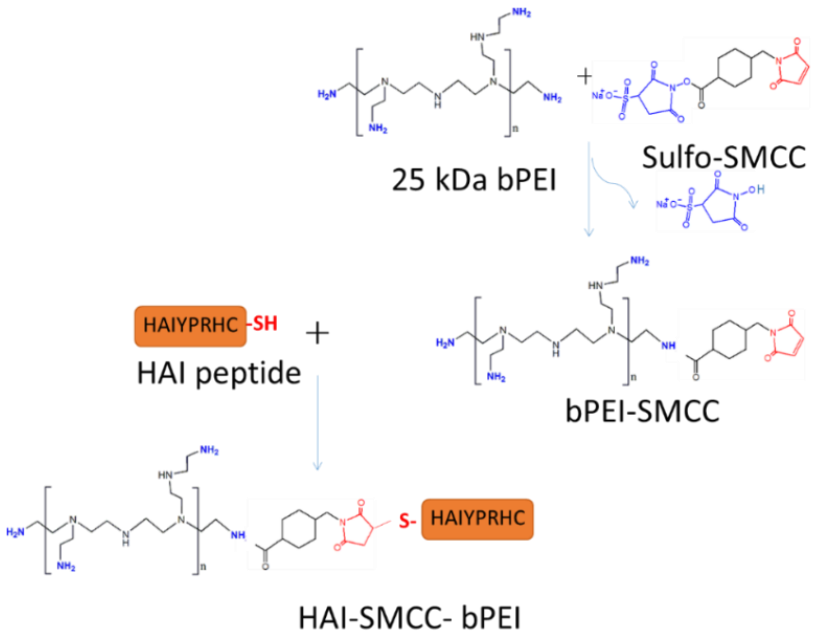

(C)

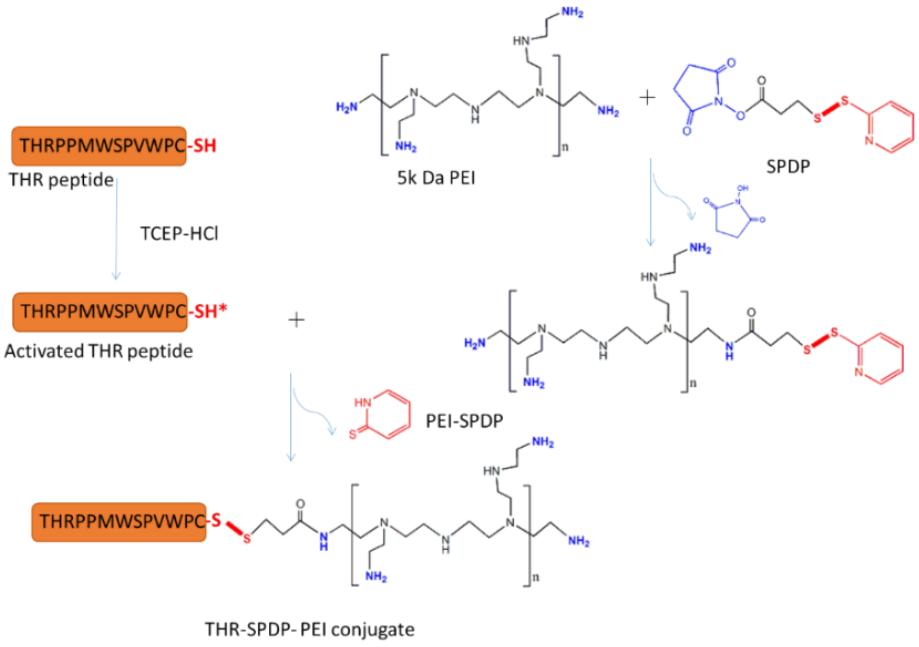

Figure 30 Synthesis scheme of HAI-SPDP-PEI, HAI-SMCC-PEI and THR-SPDP-PEI. (A) Synthesis approach of HAI-SPDP-bPEI.; (B) Synthesis approach of HAI-SMCC-bPEI. (C) Synthesis approach of THR-SPDP-bPEI. (bPEI: branched

polyethylenimine; PEG_4-SPDP: 2-Pyridyldithiol-tetraoxatetradecane-N-hydroxysuccinimide; sulfo-SMCC: sulfosuccinimidyl 4-[N-maleimidomethyl] cyclohexane-1-carboxylate; DTT: dithiolthreitol; SPDP: succinimidyl 3-(2-pyridyldithio) propionate; TCEP: Tris (2-carboxyethyl) phosphine hydrochloride)

5.3.2 siRNA Condensation Efficiency of bPEI and HAI-bPEI

Cationic polymers, such as bPEI, can condense siRNA via ionic interactions. The amount of uncondensed free siRNA can be quantified by SYBR® Gold, an intercalating fluorescent nucleic acid staining dye. Therefore, the condensation efficiency of bPEI and HAI-bPEI at different anime to phosphate (N/P) ratios (1, 2, 3, 5, 7, 10) was examined by a SYBR Gold assay. As shown in Figure 31, bPEI and HAI-SPDP-bPEI demonstrated similar condensation efficiency. Increasing the N/P ratio resulted in less free siRNA. Both bPEI and HAI-bPEI can achieve complete condensation of siRNA at an N/P ratio of 2 and all N/P ratios above 2, respectively.

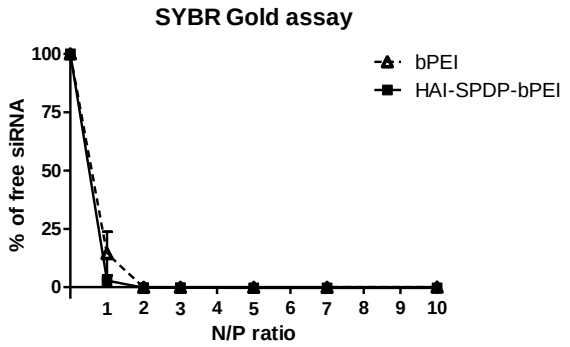

Figure 31 SYBR Gold assay of PEI and HAI-SPDP-PEI. The siRNA condensation efficiency of bPEI and HAI-SPDP-bPEI was determined by a SYBR® Gold assay at N/P ratio 1, 2, 3, 5, 7 and 10. At N/P= 0, the fluorescence represented 100% free siRNA. (Data points indicate mean +/- standard deviation (SD), n= 3.)

5.3.3 Hydrodynamic Size and Zeta-Potential of PEI and HAI-PEI Polyplexes

The particle size of HAI-SPDP-bPEI and bPEI polyplexes formulated with 50 pmol of siRNA at N/P=5 was measured by dynamic light scattering (Figure 32 A). HAI peptide modified bPEI polyplexes, as expected, had a slightly larger hydrodynamic diameter of around 144 nm with a polydispersity index (PDI) of around 0.3. Unmodified bPEI polyplexes exhibited a hydrodynamic diameter of around 117 nm with a PDI of around 0.2. The zeta-potential of HAI-SPDP-bPEI and bPEI polyplexes were also determined. As shown in Figure 32 B, the zeta-potentials of both polyplexes were slightly positive, and HAI-SPDP-bPEI polyplexes demonstrated a lower positive surface charge (13.3 +/- 1.7 mV) than bPEI polyplexes (17.2 +/- 9.2 mV).

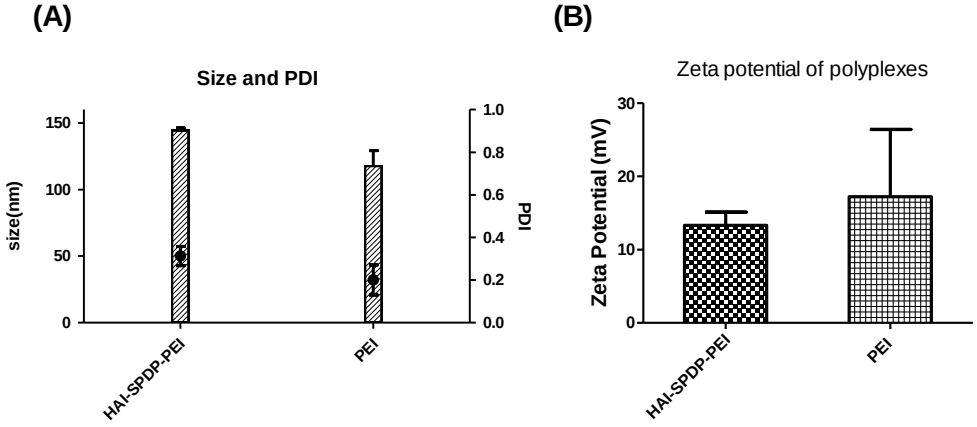

Figure 32 Size and zeta-potential of HAI-SPDP-PEI and PEI. (A) Hydrodynamic diameters (left y-axis) and polydispersity index (PDI, right y-axis) and (B) zeta-potential of bPEI and HAI-SPDP-bPEI polyplexes containing 50 pmol of siRNA at N/P= 5. (Data points indicate mean +/- SD, n= 3.)

5.3.4 TfR Expression

TfR expression levels in H1299, H460 and A549 cells were measured via flow cytometry. Cells were immunostained with a fluorescently labeled anti-CD71 antibody, namely the anti-TfR antibody, and with an isotype control antibody. As shown in Figure 33 A and B, median fluorescent intensity (MFI) across all three cell lines was unchanged when stained with the isotype antibody, indicating that little fluorescence was caused by non-specific binding of the antibody. On the other hand, H1299 cells demonstrated a significantly higher MFI after being stained with the anti-CD71 antibody compared with A549 and H460 cells. Therefore, H1299 cells were considered as a TfR overexpressing cell model while A549 and H460 cells were considered as TfR low expressing cell models for later studies.

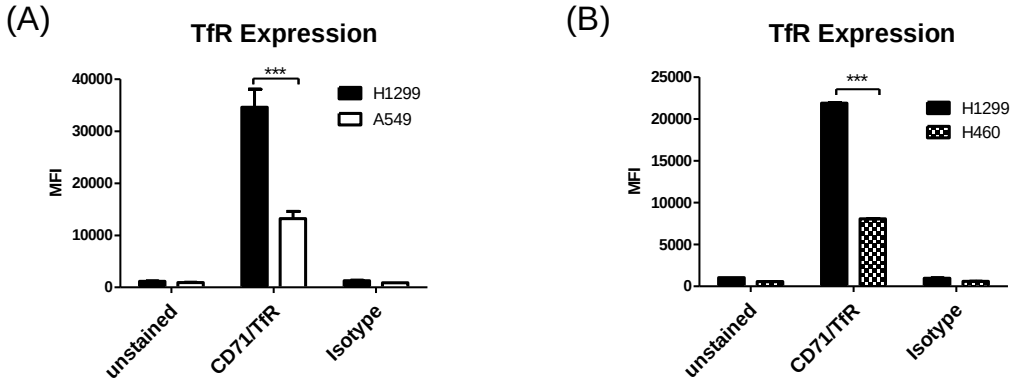

Figure 33. TfR expression in H1299 and A549. (A) H1299 and A549 cells were immunostained by the anti-CD71 antibody which binds to transferrin receptors (TfR) and by the isotype antibody which served as a control of non-specific binding. Median fluorescence intensity (MFIs) were quantified via flow cytometry. (B) H1299 and H460 cells were immunostained by the anti- CD71

antibody and by the isotype antibody (Data points indicate mean +/- SD, n= 2. *** $p < 0.001$).

5.3.5 Cellular Uptake of bPEI and HAI-bPEI Polyplexes

The bPEI modified by HAI peptide via two different crosslinkers—sulfo-SMCC or PEG_4-SPDP, HAI-SMCC-bPEI or HAI-SPDP-bPEI—were tested in this study. The cellular uptake of HAI-SMCC-bPEI or HAI-SPDP-bPEI polyplexes compared with bPEI polyplexes were determined in the TfR overexpressing cell line H1299, and in TfR low expressing cell lines H460 or A549 via flow cytometry. Cells were transfected by HAI-SMCC-bPEI, HAI-SPDP-bPEI or bPEI polyplexes containing siRNA labeled with Alexa Fluor 488 at N/P= 5 for 24 h. As shown in Figure 34 A, significantly stronger fluorescence was determined in H1299 cells treated with HAI-SMCC-bPEI polyplexes than in A549 cells. On the other hand, only a slightly stronger MFI was observed in H1299 cells treated with bPEI polyplexes than in A549 cells. In A549 cells, cellular uptake mediated by HAI-SMCC-bPEI polyplexes was only slightly higher than that mediated by bPEI polyplexes, however, the difference between cellular uptake mediated by HAI-SMCC-bPEI and bPEI polyplexes was more significant in H1299 cells. A comparison of the cellular uptake mediated by HAI-SPDP-bPEI and bPEI polyplexes was performed in H1299 and H460, as shown in Figure 34 B, and a similar cellular uptake profile was observed.

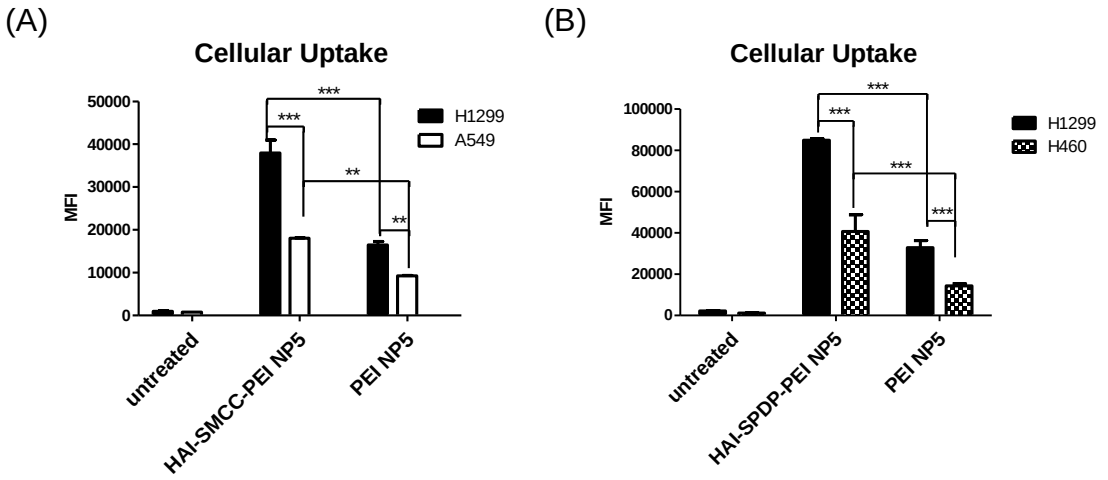

Figure 34 Cellular uptake of PEI and HAI-SPDP-PEI. (A) The cellular uptake of bPEI and HAI-SPDP-bPEI polyplexes was determined in TfR overexpressing cells H1299 and TfR low expressing cells A549. Polyplexes were prepared with 50 pmol of siRNA fluorescently labeled with Alexa Fluor 488 at N/P= 5 and transfected for 24 h. The MFIs were quantified by flow cytometry. (Data points indicate mean +/- SD, n= 2. **, p <0.01, *** p <0.001). (B) The cellular uptake of bPEI and HAI-SPDP-bPEI polyplexes was determined in TfR overexpressing cells H1299 and TfR low expressing cells H460. (Data points indicate mean +/- SD, n= 3. *** p <0.001)

5.3.6 Cellular Binding and Cellular Uptake of THR Peptide and THR-PEI

The cellular binding of THR-AF488 was determined in H1299 cells and A549 cells and quantified via flow cytometer. With increasing concentration of THR-AF488, the MFI of H1299 cells overexpressing TfR increased dramatically and was higher than the MFI of A549 cells expressing low level of TfR (5.6 a). The cellular uptake of THR-PEI or PEI polyplexes was also determined in H1299 and A549. Cells were transfected by THR-PEI or PEI polyplexes formulated with 50 pmol siRNA-AF488 at N/P=5 for 24 h. The MFIs of cells were quantified by flow cytometry. The cellular uptake mediated by THR-PEI polyplexes in H1299

and A549 was similar. Moreover, non-modified PEI mediated higher cellular uptake in both cell lines compared to THR-PEI (Figure 35 B).

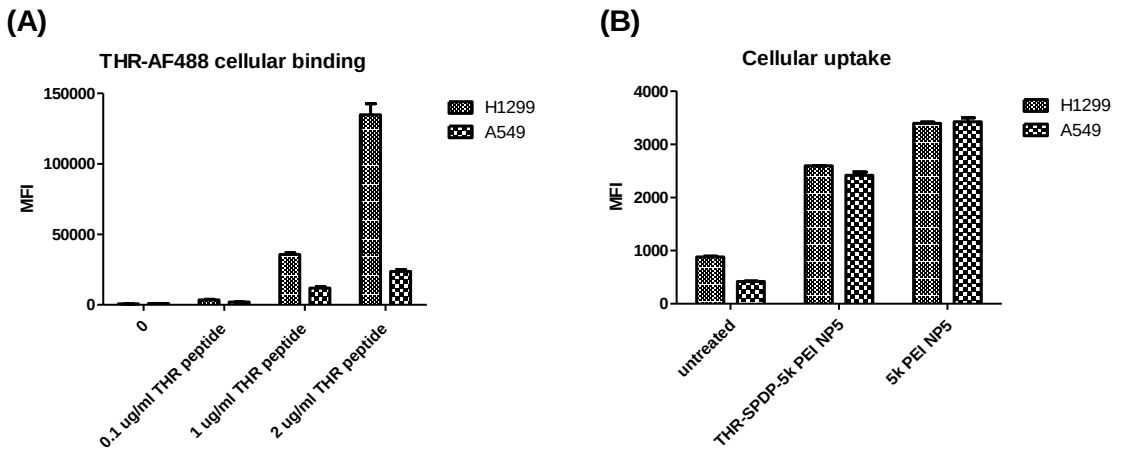

Figure 35 Cellular binding of THR peptide and cellular uptake of THR-PEI. (A) The cellular binding of THR-AF488 with H1299 and A549 were quantified by flow cytometry. (Data points indicate mean +/- SD, n= 3) (B) The cellular uptake of bPEI and THR-bPEI polyplexes was determined in H1299 and A549 cells and quantified by flow cytometry. (Data points indicate mean +/- SD, n= 2-3).

5.3.5 Imaging of Uptake by Confocal Laser Scanning Microscopy (CLSM)

To determine the sub-cellular distribution of polyplexes, H1299 cells were transfected by HAI-SMCC-bPEI fluorescently labeled by fluorescein isothiocyanate (HAI-SMCC-bPEI-FITC) and bPEI-FITC polyplexes containing siRNA fluorescently labeled with Ty563 at N/P= 5 for 48 h. The cellular distribution of polyplexes was observed at several time-points (1, 4, 24, and 48 h) by CLSM (Figure 36). H1299 cells treated with HAI-SMCC-bPEI polyplexes (Figure 36, lower panel) showed denser distribution of the red signal representing siRNA-Ty563 than cells treated with bPEI polyplexes (Figure 36, upper panel). At

24 and 48 h, bright yellow dots, representing co-localization of polymer-FITC (green) and siRNA-Ty563 (red), were observed in both cells treated with HAI-SMCC-bPEI and bPEI polyplexes. There were some red dots (siRNA-Ty563) evenly distributed in the cytoplasm of cells treated with HAI-SMCC-bPEI polyplexes, however, siRNA-Ty563 was exclusively co-localized with bPEI (yellow dots) and not present as free siRNA in cells transfected with bPEI polyplexes.

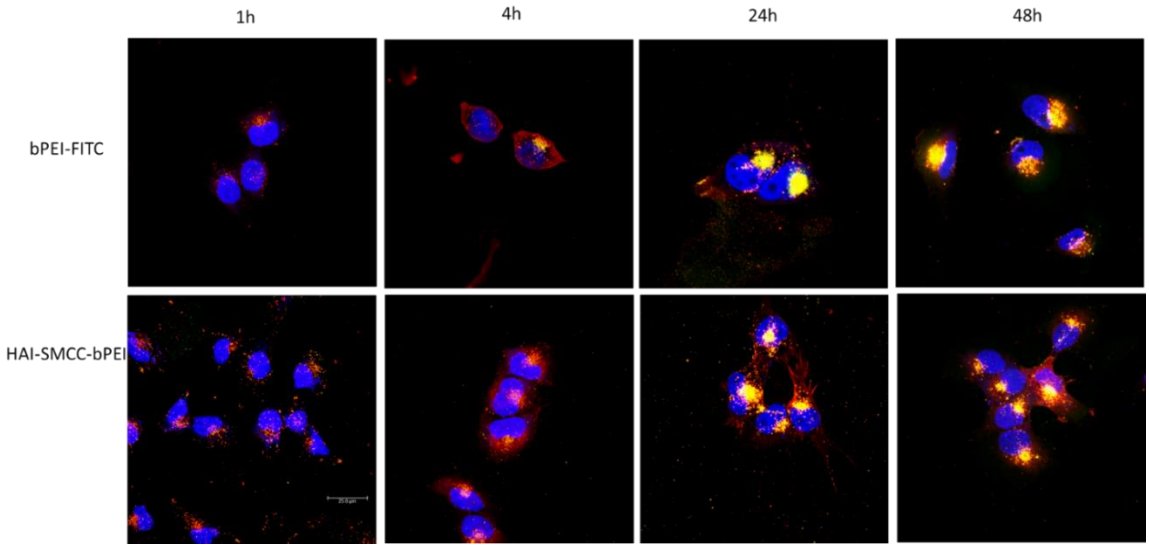

Figure 36 CLSM of subcellular distribution of PEI and HAI-SMCC-PEI polyplexes. Subcellular distribution of bPEI and HAI-SMCC-bPEI polyplexes in H1299 was imaged by confocal microscopy. H1299 cells were transfected with bPEI and HAI-SMCC-bPEI polyplexes prepared with 50 pmol of siRNA fluorescently labeled with Ty563 at N/P= 5 for 1, 4, 24 and 48 h. The polymers were fluorescently labeled with FITC and shown in green. siRNA-Ty563 was shown in red, and DRAQ5^{TM} stained nuclei were shown in blue.

To investigate the pathway of cellular internalization mediated by the HAI peptide, H1299 cells were incubated with 2 µg/mL of transferrin which was

fluorescently labeled with Texas Red (Tf-Texas Red) and HAI-SMCC-bPEI-FITC or bPEI-FITC polyplexes formulated with non-fluorescently labeled siRNA at N/P= 5 for 1 and 4 h. As shown in Figure 37, upper panel, after 1 h of incubation, more yellow dots representing co-localization of Tf-Texas Red (red) and polymer-FITC (green) were observed in cells treated with HAI-SMCC-bPEI polyplexes than in bPEI polyplexes transfected cells. At 4 h (Figure 37, lower panel), there was noticeably more co-localization between Tf and polymers in both bPEI and HAI-SMCC-bPEI transfected samples when compared with samples at 1 h (Figure 37, upper panel). The intensity of the co-localization was stronger in samples treated with HAI-SMCC-bPEI polyplexes than in bPEI polyplexes-transfected cells (Figure 37, lower panel).

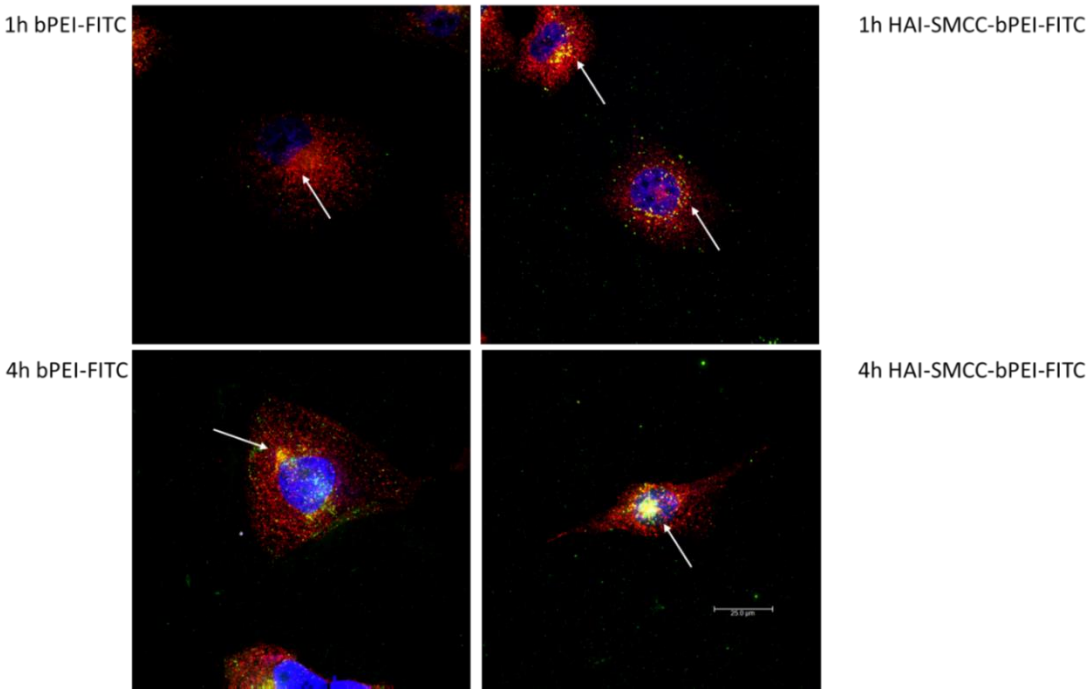

Figure 37 CLSM of co-localization of Tf and PEI or HAI-SMCC-PEI. Co-localization of transferrin (Tf) and bPEI or HAI-SMCC-bPEI polyplexes in H1299 was imaged by confocal microscopy. H1299 cells were incubated with Tf fluorescently labeled with Texas Red (Tf-Texas Red) and bPEI or HAI-SMCC-bPEI polyplexes prepared with 50 pmol of siRNA at N/P= 5 for 1 and 4 h. The polymers were fluorescently labeled with FITC and shown in green. Tf-Texas Red was shown in red, and DRAQ5 stained nuclei were shown in blue. The arrows pointing to the yellow dots represent co-localization spots of polyplexes and Tf.

To determine the co-localization of the cellular binding site of THR peptide with TfR, H1299 cells were incubated with 2 μg/mL of Tf-Texas Red and THR-AF488 for 1 h. As shown in Figure 38, red dots represented Tf-Texas Red evenly distributed in the cells, but green dots represented THR-AF488 and formed large aggregate on the cellular surface.

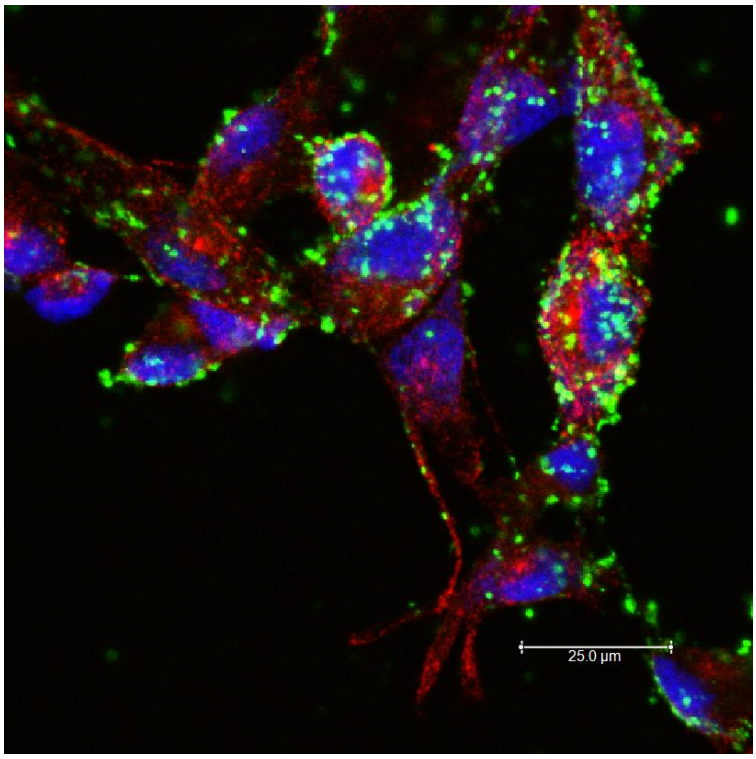

Figure 38 CLSM of co-localization of Tf and THR peptide. 2 µg/mL of THR-AF488 and Tf-Texas Red were incubated with H1299 for 1 h at 37 °C. The cellular distribution of THR-AF488 and Tf-Texas Red was observed under confocal laser scanning microscopy (CLSM).

5.3.6 In Vitro GAPDH Gene Knockdown

To investigate the selective delivery of siRNA with HAI-SPDP-bPEI or HAI-SMCC-PEI, we next measured the efficacy of HAI-SPDP-bPEI or HAI-SMCC-PEI/ siRNA polyplexes to silence GAPDH in H1299 cells. Cells were transfected with either HAI-SPDP-bPEI, HAI-SMCC-PEI or PEI polyplexes containing siRNA against GAPDH (siGAPDH), or scrambled siRNA at N/P= 5 for 24 h. GAPDH gene expression was normalized to β-actin gene expression. As shown in Figure 39 A, significantly higher GAPDH silencing was achieved by siGAPDH/HAI-SPDP-bPEI polyplexes compared with the group treated with

scrambled siRNA/HAI-SPDP-bPEI polyplexes, and with the untreated group. However, there was no significant difference among siGAPDH/bPEI, the scrambled siRNA/bPEI treated group, and the untreated group. On the other hand, HAI-SMCC-PEI failed to mediate significant GAPDH knockdown compared to its scramble siRNA control (Figure 39 B).

To further confirm the GAPDH gene silence mediated by HAI-SPDP-PEI, the GAPDH knockdown experiment was conducted in H460 cells which expressed low levels of TfR. As shown in Figure 39 C, there was no significant difference regarding GAPDH expression among the HAI-SPDP-PEI polyplexes treated group, PEI polyplexes treated group and untreated group.

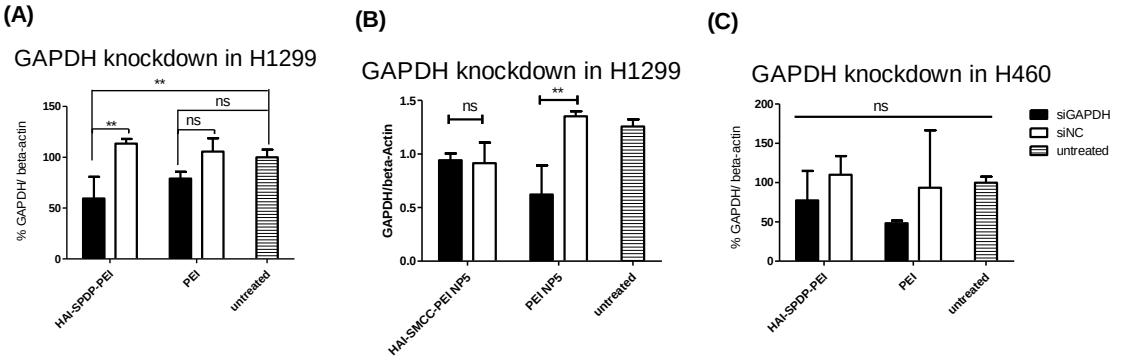

Figure 39 GAPDH knockdown in H1299 and H460. (A) H1299 were transfected with bPEI or HAI-SPDP-bPEI. (B) H1299 were transfected with bPEI or HAI-SMCC-bPEI polyplexes. (C) H460 cells were transfected with bPEI or HAI-SPDP-bPEI polyplexes. All polyplexes were formulated with 50 pmol of siRNA against GAPDH (siGAPDH) or scrambled siRNA at N/P= 5 and the cells were transfected for 24 h. The expression of GAPDH was determined by RT-PCR and normalized to the expression of β-actin. Untreated control represented 100% or 1 GAPDH/β-actin. (Data points indicate mean +/- SD, n= 3. ns, $p > 0.05$, **$p < 0.01$).

5.3.7 In Vitro eGFP Knockdown

To further determine the gene silencing efficiency of HAI-SPDP-bPEI polyplexes at the protein level, the in vitro knockdown efficiency of the reporter gene enhanced green fluorescent protein (eGFP) by HAI-SPDP-bPEI polyplexes was determined in a H1299 cell line stably expressing eGFP. Cells were transfected with HAI-SPDP-bPEI or bPEI polyplexes formulated with siRNA against eGFP (siGFP) or scrambled siRNA at N/P= 5 and 10 for 48 h with or without chloroquine treatment, a drug reported to increase the endosomal release of siRNA [185]. The MFIs of eGFP in cells were quantified by flow cytometry. As shown in Figure 40 A, there was no significant difference of MFI between cells transfected with bPEI and HAI-SPDP-bPEI polyplexes containing siGFP without chloroquine treatment at either N/P= 5 or 10. However, with additional chloroquine treatment (Figure 40 B), HAI-SPDP-bPEI polyplexes achieved significantly more eGFP knockdown compared with bPEI polyplexes at both N/P=5 and 10. Both HAI-SPDP-bPEI and bPEI polyplexes containing scrambled siRNA did not reduce the MFI of eGFP, indicating that the eGFP knockdown was not contributed to by the polymer, but by the siRNA against eGFP released in the cytoplasm.

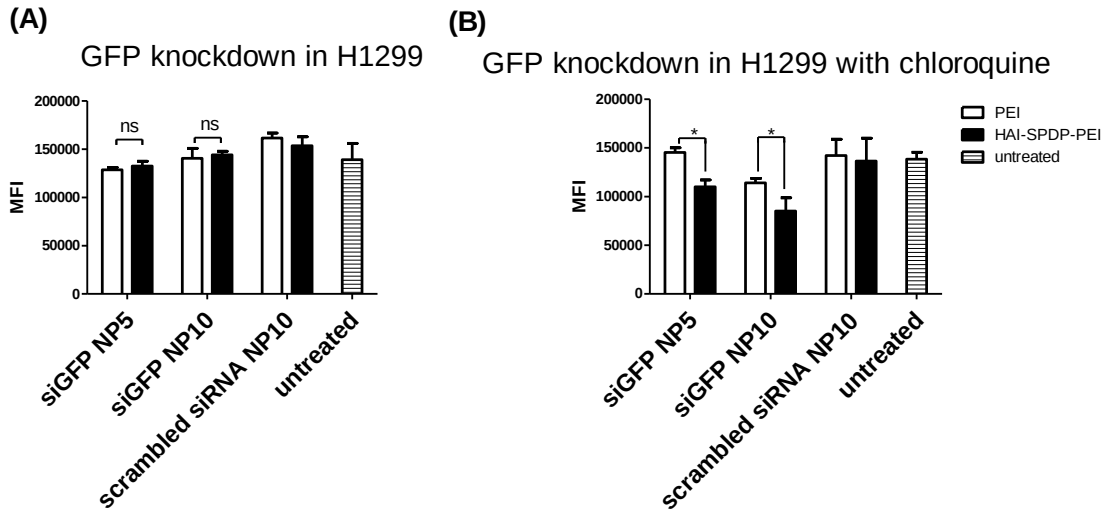

Figure 40 GFP knockdown in H1299. (A) H1299/eGFP cells were transfected with bPEI and HAI-SPDP-bPEI polyplexes for 48 h without chloroquine treatment. (B) H1299/eGFP cells, stably expressing eGFP, were transfected with bPEI or HAI-SPDP-bPEI polyplexes prepared with 50 pmol of siRNA against eGFP (siGFP) or scrambled siRNA at N/P= 5 and 10 for 48 h with chloroquine treatment. The MFIs of eGFP were quantified by flow cytometry. (Data points indicate mean +/- SD, n= 3. ns, $p > 0.05$, *$p < 0.05$)

5.4 Discussion

The selective and efficient delivery of siRNA to tumors is hindered by many biological barriers [95]. Numerous modifications of polymers have been discovered to target tumor cells including folic acid [19], transferrin [20], epidermal growth factor (EGF) [186] and the tripeptide arginine-glycine-aspartate RGD [47]. In this study, two human TfR binding peptides, HAIYPRH (HAI peptide) and THRPPMWSPVWP (THR peptide), were tested for gene delivery in TfR positive cells. Both peptides contain a distal cysteine to introduce an additional thiol group for further modification. The THR peptide was first evaluated since it

demonstrated a high affinity to TfR (1.5×10^{-8} M) compared to the affinity of native ligand Tf to TfR of 2.8×10^{-9} M; in contrast, the affinity constant of the HAI peptide was 4.4×10^{-4} M [184]. The THR peptide was successfully coupled to 5 kDa bPEI via linker SPDP as shown in Figure 30 C. Despite the fact that the THR peptide, which was fluorescently labeled with Alexa Fluor 488 (THR-AF488), did preferentially bind to TfR overexpressing H1299 cells compared to TfR low expressing A549 cells (Figure 35 A), the cellular uptake mediated by THR-bPEI polyplexes in H1299 cells was lower than that of bPEI polyplexes and showed no difference compared with A549 cells (Figure 35 B). It has been reported that the THR peptide conjugated with a chelator for radiolabeling demonstrated negligible uptake in a TfR positive cell line [187] and that THR modified gold nanoparticles did not efficiently cross the blood brain barrier without the addition of a hydrophobic peptide to facilitate membrane binding [188]. Therefore, it is possible that the binding cavity of the THR peptide to TfR is sterically very strict and only allows limited modification in the peptide. Consequently, THR modified with a small fluorescent probe, AF488 (MW= 720.66 Da), still demonstrated preferential binding to H1299 but THR conjugated to a large polymer, bPEI (MW= 5000 Da), cannot mediate significantly higher cellular uptake in H1299 cells compared with A549 cells. Another possible reason of low selective cellular uptake could be low receptor internalization efficiency. Confocal imaging revealed that THR-AF488 can bind to

the membrane of H1299 but little internalization was observed (Figure 38), and the co-localization of THR-AF488 and Tf was absent. Thus, THR may not be an optimal candidate for the TfR targeting of polyplexes.

The other peptide discovered in the same study, the HAI peptide, demonstrated different properties during evaluation for polyplex targeting. Firstly, the HAI peptide was successfully conjugated to 25k Da bPEI via two different linkers: sulfo-SMCC and PEG_4-SPDP. The coupling degrees were similar in both approaches and were around 18 HAI peptides per bPEI. It has been reported that protein/peptide modifications in polymer may result in less nucleic acid condensation efficiency compared to the non-modified polymer due to the introduction of steric hindrance [61, 189]. The siRNA condensation efficiency of bPEI and HAI-SPDP-bPEI was therefore determined by a SYBR Gold assay, and the results demonstrated that HAI-peptide modification did not have any negative impact on bPEI's condensation of siRNA (Figure 31). Chemico-physical properties of polyplexes are very important for successful and efficient siRNA delivery. Therefore, bPEI and HAI-SPDP-bPEI polyplexes (N/P=5) were fully characterized in terms of the hydrodynamic diameter, PDI and zeta-potential. As shown in Figure 32 A, HAI-SPDP-bPEI and bPEI polyplexes had narrow size ranges with PDIs of around 0.3, indicating that uniform polyplexes were formed with little aggregation. HAI-SPDP-bPEI polyplexes were slightly larger than bPEI

polyplexes which may be due to steric hindrance of the peptide during polyplexes formation. However, both polyplexes resulted in very small sizes (100–150 nm). These results suggested that both polyplexes may readily be taken up by cells [130], avoid rapid clearance from macrophages in the liver and spleen after systemic administration, and could potentially easily accumulate in a tumor through the EPR effect [24]. Both polyplexes demonstrated slightly positive surface charge (<30 mV) (Figure 32 B). Since HAI-SPDP-bPEI and bPEI can completely condense siRNA at N/P= 2 (Figure 31), it was expected that at N/P =5, an excess amount of cationic polymer formulated with siRNA would result in positive surface charges. HAI-SPDP-bPEI polyplexes exhibited a less positive charge than bPEI polyplexes which may be due to the assumption that the conjugated HAI peptide locates on the surface of the polyplexes and can shield some positive charge from bPEI. Another possible reason for the reduced surface charge of HAI-SPDP-PEI is that the SPDP coupling reaction consumed some of the primary amines in bPEI. A slightly positive surface charge could facilitate the binding between polyplexes and cellular membranes. Moreover, the HAI peptide located on the surface is expected to increase the possibility to interact with TfR, suggesting that efficient cellular uptake may be achieved by this formulation.

The TfR expression status of three different cell lines—H1299, A549 and H460—was determined by flow cytometry after immunostaining with the anti-

CD71 (TfR) antibody. Based on the results (Figure 33 A and B), H1299 cells served as a TfR overexpressing cell model, and A549 and H460 served as TfR low expressing cell models for later studies. The peptide mediated TfR selectivity was investigated by confocal microscopy. HAI-SMCC-bPEI and bPEI were fluorescently labeled with FITC (HAI-SMCC-bPEI-FITC, bPEI-FITC respectively), and polyplexes were formed with non-fluorescently labeled siRNA. H1299 cells were incubated with Tf-Texas Red and the aforementioned polyplexes. As shown in Figure 36, HAI-SMCC-bPEI polyplexes showed more binding (green dots) on the cell surface and more co-localization (yellow dots) with Tf-Texas Red (red dots) than bPEI polyplexes after 1 and 4 h of the co-incubation period, indicating that the HAI peptide can mediate selective binding to TfR overexpressing cells. Furthermore, HAI-SMCC-bPEI can achieve more co-localization with Tf, suggesting that HAI-SMCC-bPEI polyplexes may enter cells via a TfR mediated pathway in a non-competitive manner as reported before [184]. The subcellular distribution of both polyplexes over time was observed under the confocal microscope (Figure 36). H1299 cells were transfected with HAI-SMCC-bPEI-FITC or bPEI-FITC polyplexes (green dots) containing siRNA-Ty563 (red dots). HAI-SMCC-bPEI polyplexes clearly achieved more cellular binding on the membrane than bPEI polyplexes during the first 1 and 4 h, suggesting that HAI-SMCC-bPEI preferentially bound to TfR overexpressing cells compared with

bPEI polyplexes. At later time points (24 and 48 h), both bPEI and HAI-SMCC-bPEI polyplexes formed bright yellow dots in vesicle like structures, indicating that many of both types of polyplexes had accumulated and were trapped in endosomes or lysosomes. However, it is worth nothing that more siRNA distributed in the cytoplasm in the HAI-SMCC-bPEI treated group than in bPEI transfected cells. According to the cellular uptake results (Figure 34 A), it is possible that HAI-SMCC-bPEI polyplexes mediated higher cellular uptake in H1299 cells than bPEI polyplexes, consequently more siRNA escaped into the cytoplasm. The TfR specific cellular uptake mediated by the HAI peptide was also confirmed by flow cytometry (Figure 34 A and B). Both HAI-SMCC-bPEI and HAI-SPDP-bPEI polyplexes showed specific binding to the TfR overexpressing cell line (H1299 cells) compared with TfR low expressing cells (A549 and H460). Furthermore, both HAI peptide modified bPEI polyplexes mediated significantly higher cellular uptake in H1299 cells compared with non-modified bPEI, suggesting a specific interaction between the HAI peptide in the polymer and TfR on the cell membrane.

The gene knockdown efficiency of the HAI peptide, modified bPEI and non-modified bPEI was determined by RT-PCR, and the housekeeping gene GAPDH was targeted. Surprisingly, HAI-SMCC-bPEI polyplexes did not mediate efficient GAPDH gene knockdown, as shown in Figure 39 B, which did not agree

with the cellular uptake result (Figure 34 A) and the confocal microscopy result (Figures 35 and 36). It is possible that the HAI peptide modification reduced the number of primary amines in bPEI and consequently reduced the buffering capacity of bPEI. Furthermore, TfR rapidly recycles back to the cell surface after internalization [190], therefore, HAI-SMCC-bPEI polyplexes that are still bound to TfR are recycled back to the cell surface before siRNA can be released. To address this problem, HAI-SPDP-bPEI was synthesized using a linker PEG_4-SPDP. PEG_4-SPDP (25.7 Å) is longer than sulfo-SMCC (8.3 Å) which may make the HAI peptide more accessible to TfR and increase the binding efficiency. Moreover, it introduced a disulfide bond into the HAI-SPDP-bPEI conjugate which can be reduced in the endosomal compartment [191] and may facilitate the release of bPEI/siRNA complexes from the HAI peptide/TfR complexes before TfR recycles back to the cell surface. The GAPDH gene knockdown efficiency of HAI-SPDP-bPEI polyplexes was determined in H1299 and H460 cells. In line with previous cellular uptake results (Figure 34 B), HAI-SPDP-bPEI polyplexes can achieve more efficient GAPDH gene knockdown in H1299 cells (Figure 39 A) compared with bPEI polyplexes but not in H460 cells (Figure 39 C). These results revealed that the introduction of a long and reducible linker into target moiety-polymer conjugates may increase their transfection efficiency. Additionally, it was shown

that the transfection efficiency of HAI-SPDP-bPEI polyplexes is highly dependent on the TfR expression status of the targeted cells.

Next, the gene silencing efficiency of HAI-SPDP-bPEI polyplexes at the protein level was investigated in H1299/eGFP cells. H1299/eGFP cells were treated with HAI-SPDP-bPEI and bPEI polyplexes for 48 h, and the eGFP expression was determined by flow cytometry. However, as shown in Figure 40 A, there was no significant difference among the polyplexes treated groups and the untreated group. Based on the confocal images (Figure 36), it is possible that most polyplexes were trapped in the endosome and only a small amount of siRNA was released into the cytoplasm. Therefore, mRNA level silencing can be observed since mRNA is the direct target of siRNA. However, it is more difficult to achieve protein level silencing. A sufficient amount of siRNA needs to be released into the cytoplasm. Additionally, the silencing efficiency also depends on the half-life of the targeted protein, and wild type GFP has a relatively long half-life (around 26 h) [192]. To increase the release of siRNA from endosomes, H1299/eGFP cells were transfected with HAI-SPDP-bPEI and bPEI polyplexes in media containing chloroquine, which is a chemical that can dramatically increase the transfection efficiency by disrupting the endosomal membrane [185]. As shown in Figure 40 B, significantly higher eGFP knockdown can be achieved by siGFP/HAI-SPDP-bPEI polyplexes compared with siGFP/bPEI polyplexes in a dose dependent manner.

5.5 Conclusion

In conclusion, our optimized HAI-bPEI conjugate has desired chemico-physical properties as a siRNA delivery vector. It can achieve selective delivery of siRNA to TfR overexpressing tumor cells and efficient gene knockdown at the mRNA level. This study demonstrates the feasibility to target TfR using HAI peptide. However, results also indicate the need for further optimization of this conjugate to achieve better endosomal escape.

REFERENCES

1.El-Aneed, A., Current strategies in cancer gene therapy. *European journal of pharmacology* **2004,** *498* (1), 1-8.

2.Naldini, L., Gene therapy returns to centre stage. *Nature* **2015,** *526* (7573), 351-360.

3.Ginn, S. L.; Alexander, I. E.; Edelstein, M. L.; Abedi, M. R.; Wixon, J., Gene therapy clinical trials worldwide to 2012–an update. *The journal of gene medicine* **2013,** *15* (2), 65-77.

4.Nemunaitis, J.; Nemunaitis, J., Head and neck cancer: Response to p53-based therapeutics. *Head & neck* **2011,** *33* (1), 131-134.

5.Zarogoulidis, P.; Darwiche, K.; Sakkas, A.; Yarmus, L.; Huang, H.; Li, Q.; Freitag, L.; Zarogoulidis, K.; Malecki, M., Suicide gene therapy for cancer–current strategies. *Journal of genetic syndrome & gene therapy* **2013,** *4*.

6.Song, C.-Z., Gene Silencing Therapy Against Cancer. In *Gene Therapy for Cancer*, Springer: 2007; pp 185-196.

7.*Anti-Inflammatory Therapeutics Market by Indication (Arthritis, Respiratory diseases, Multiple sclerosis, Psoriasis, Inflammatory bowel disease) and Drug Class (Anti-inflammatory Biologics, Non-Steroidal Anti-inflammatory drugs (NSAIDs), Corticosteroids) - Global Opportunity Analysis and Industry Forecast, 2014 - 2020*; Allied Market Research: 2015.

8.Li, G.; Liu, Z.; Zhong, N.; Liao, B.; Xiong, Y., Therapeutic effects of DNA vaccine on allergen-induced allergic airway inflammation in mouse model. *Cell Mol Immunol* **2006,** *3* (5), 379-384.

9.Popescu, F.-D.; Popescu, F., A review of antisense therapeutic interventions for molecular biological targets in asthma. *Biologics* **2007,** *1* (3), 271-83.

10.Xie, Y.; Merkel, O. M., Pulmonary delivery of siRNA via polymeric vectors as therapies of asthma. *Archiv der Pharmazie* **2015,** *348* (10), 681-688.

11.Krug, N.; Hohlfeld, J. M.; Kirsten, A.-M.; Kornmann, O.; Beeh, K. M.; Kappeler, D.; Korn, S.; Ignatenko, S.; Timmer, W.; Rogon, C., Allergen-Induced Asthmatic Responses Modified by a GATA3-Specific DNAzyme. *New England Journal of Medicine* **2015**.

12.Cevher, E.; Sezer, A. D.; Çağlar, E. Ş., *Gene delivery systems: recent progress in viral and non-viral therapy*. INTECH Open Access Publisher: 2012.

13.Kohn, D. B.; Hershfield, M. S.; Carbonaro, D.; Shigeoka, A.; Brooks, J.; Smogorzewska, E. M.; Barsky, L. W.; Chan, R.; Burotto, F.; Annett, G., T lymphocytes with a normal ADA gene accumulate after transplantation of transduced autologous umbilical cord blood CD34+ cells in ADA-deficient SCID neonates. *Nature medicine* **1998,** *4* (7), 775.

14.Sibbald, B., Death but one unintended consequence of gene-therapy trial. *Canadian Medical Association Journal* **2001,** *164* (11), 1612-1612.

15.Kohn, D. B., Gene therapy for XSCID: the first success of gene therapy. *Pediatric research* **2000,** *48* (5), 578-578.

16.(a) Kohn, D. B.; Candotti, F., Gene therapy fulfilling its promise. *N Engl J Med* **2009,** *360* (5), 518-521; (b) Check, E., Gene therapy: a tragic setback. *Nature* **2002,** *420* (6912), 116-118.

17.Hill, A. B.; Chen, M.; Chen, C.-K.; Pfeifer, B. A.; Jones, C. H., Overcoming gene-delivery hurdles: Physiological considerations for nonviral vectors. *Trends in biotechnology* **2016,** *34* (2), 91-105.

18.Yin, H.; Kanasty, R. L.; Eltoukhy, A. A.; Vegas, A. J.; Dorkin, J. R.; Anderson, D. G., Non-viral vectors for gene-based therapy. *Nature Reviews Genetics* **2014,** *15* (8), 541-555.

19.(a) Jones, S. K.; Lizzio, V.; Merkel, O. M., Folate Receptor Targeted Delivery of siRNA and Paclitaxel to Ovarian Cancer Cells via Folate Conjugated Triblock Copolymer to Overcome TLR4 Driven Chemotherapy Resistance. *Biomacromolecules* **2015,** *17* (1), 76-87; (b) Liu, L.; Zheng, M.; Librizzi, D.; Renette, T.; Merkel, O. M.; Kissel, T., Efficient and Tumor Targeted siRNA Delivery by Polyethylenimine-graft-polycaprolactone-block-poly (ethylene glycol)-folate (PEI–PCL–PEG–Fol). *Molecular pharmaceutics* **2015,** *13* (1), 134-143; (c) Zwicke, G. L.; Mansoori, G. A.; Jeffery, C. J., Utilizing the folate receptor

for active targeting of cancer nanotherapeutics. *Nano Reviews & Experiments* **2012,** *3*.

20.Movassaghian, S.; Hildebrandt, C.; Xie, Y.; Rosati, R.; Li, Y.; Kim, N. H.; Conti, D.; da Rocha, S. R.; Yang, Z.-Q.; Merkel, O. M., Post-transcriptional regulation of the GASC1 oncogene with active tumor-targeted siRNA-nanoparticle. *Molecular pharmaceutics* **2016**.

21.Milla, P.; Dosio, F.; Cattel, L., PEGylation of proteins and liposomes: a powerful and flexible strategy to improve the drug delivery. *Current drug metabolism* **2012,** *13* (1), 105-119.

22.Merkel, O.; Beyerle, A.; Librizzi, D.; Pfestroff, A.; Behr, T.; Sproat, B.; Barth, P.; Kissel, T., Nonviral siRNA Delivery to the Lung: Investigation of PEG-PEI Polyplexes and Their In Vivo Performance. *Molecular Pharmaceutics* **2009,** *6* (4), 1246-1260.

23.Zhang, Y.; Satterlee, A.; Huang, L., In Vivo Gene Delivery by Nonviral Vectors: Overcoming Hurdles&quest. *Molecular Therapy* **2012,** *20* (7), 1298-1304.

24.Blanco, E.; Shen, H.; Ferrari, M., Principles of nanoparticle design for overcoming biological barriers to drug delivery. *Nature biotechnology* **2015,** *33* (9), 941-951.

25.Meyer, M.; Zintchenko, A.; Ogris, M.; Wagner, E., A dimethylmaleic acid–melittin-polylysine conjugate with reduced toxicity, pH-triggered endosomolytic

activity and enhanced gene transfer potential. *The journal of gene medicine* **2007,** *9* (9), 797-805.

26.(a) Breuzard, G.; Tertil, M.; Goncalves, C.; Cheradame, H.; Geguan, P.; Pichon, C.; Midoux, P., Nuclear delivery of NFκB-assisted DNA/polymer complexes: plasmid DNA quantitation by confocal laser scanning microscopy and evidence of nuclear polyplexes by FRET imaging. *Nucleic acids research* **2008,** *36* (12), e71-e71; (b) Hu, Q.; Wang, J.; Shen, J.; Liu, M.; Jin, X.; Tang, G.; Chu, P. K., Intracellular pathways and nuclear localization signal peptide-mediated gene transfection by cationic polymeric nanovectors. *Biomaterials* **2012,** *33* (4), 1135-1145.

27.(a) Kim, D.-H.; Behlke, M. A.; Rose, S. D.; Chang, M.-S.; Choi, S.; Rossi, J. J., Synthetic dsRNA Dicer substrates enhance RNAi potency and efficacy. *Nature biotechnology* **2005,** *23* (2), 222-226; (b) Lee, Y. S.; Nakahara, K.; Pham, J. W.; Kim, K.; He, Z.; Sontheimer, E. J.; Carthew, R. W., Distinct roles for Drosophila Dicer-1 and Dicer-2 in the siRNA/miRNA silencing pathways. *Cell* **2004,** *117* (1), 69-81.

28.Al-Dosari, M. S.; Gao, X., Nonviral gene delivery: principle, limitations, and recent progress. *The AAPS journal* **2009,** *11* (4), 671-681.

29.Wong, S. Y.; Pelet, J. M.; Putnam, D., Polymer systems for gene delivery—past, present, and future. *Progress in Polymer Science* **2007,** *32* (8), 799-837.

30.Cohen, H.; Levy, R.; Gao, J.; Fishbein, I.; Kousaev, V.; Sosnowski, S.; Slomkowski, S.; Golomb, G., Sustained delivery and expression of DNA encapsulated in polymeric nanoparticles. *Gene therapy* **2000,** *7* (22), 1896-1905.

31.Cun, D.; Jensen, D. K.; Maltesen, M. J.; Bunker, M.; Whiteside, P.; Scurr, D.; Foged, C.; Nielsen, H. M., High loading efficiency and sustained release of siRNA encapsulated in PLGA nanoparticles: quality by design optimization and characterization. *European Journal of Pharmaceutics and Biopharmaceutics* **2011,** *77* (1), 26-35.

32.Kasturi, S. P.; Sachaphibulkij, K.; Roy, K., Covalent conjugation of polyethyleneimine on biodegradable microparticles for delivery of plasmid DNA vaccines. *Biomaterials* **2005,** *26* (32), 6375-6385.

33.Nafee, N.; Taetz, S.; Schneider, M.; Schaefer, U. F.; Lehr, C.-M., Chitosan-coated PLGA nanoparticles for DNA/RNA delivery: effect of the formulation parameters on complexation and transfection of antisense oligonucleotides. *Nanomedicine: Nanotechnology, Biology and Medicine* **2007,** *3* (3), 173-183.

34.(a) Kundu, P. P.; Sharma, V., Synthetic polymeric vectors in gene therapy. *Current Opinion in Solid State and Materials Science* **2008,** *12* (5), 89-102; (b) Morille, M.; Passirani, C.; Vonarbourg, A.; Clavreul, A.; Benoit, J.-P., Progress in developing cationic vectors for non-viral systemic gene therapy against cancer. *Biomaterials* **2008,** *29* (24), 3477-3496.

35.Kim, S.; Choi, J. S.; Jang, H. S.; Suh, H.; Park, J., Hydrophobic modification of polyethyleneimine for gene transfectants. *BULLETIN-KOREAN CHEMICAL SOCIETY* **2001,** *22* (10), 1069-1075.

36.Navarro, G.; Essex, S.; Sawant, R. R.; Biswas, S.; Nagesha, D.; Sridhar, S.; de ILarduya, C. T.; Torchilin, V. P., Phospholipid-modified polyethylenimine-based nanopreparations for siRNA–mediated gene silencing: Implications for transfection and the role of lipid components. *Nanomedicine: Nanotechnology, Biology and Medicine* **2014,** *10* (2), 411-419.

37.Schroeder, A.; Dahlman, J. E.; Sahay, G.; Love, K. T.; Jiang, S.; Eltoukhy, A. A.; Levins, C. G.; Wang, Y.; Anderson, D. G., Alkane-modified short polyethyleneimine for siRNA delivery. *Journal of controlled release* **2012,** *160* (2), 172-176.

38.Aliabadi, H. M.; Landry, B.; Bahadur, R. K.; Neamnark, A.; Suwantong, O.; Uludağ, H., Impact of lipid substitution on assembly and delivery of siRNA by cationic polymers. *Macromolecular bioscience* **2011,** *11* (5), 662-672.

39.Fu, C.; Lin, L.; Shi, H.; Zheng, D.; Wang, W.; Gao, S.; Zhao, Y.; Tian, H.; Zhu, X.; Chen, X., Hydrophobic poly (amino acid) modified PEI mediated delivery of rev-casp-3 for cancer therapy. *Biomaterials* **2012,** *33* (18), 4589-4596.

40.Zheng, M.; Liu, Y.; Samsonova, O.; Endres, T.; Merkel, O.; Kissel, T., Amphiphilic and biodegradable hy-PEI-g-PCL-b-PEG copolymers efficiently

mediate transgene expression depending on their graft density. *International journal of pharmaceutics* **2012,** *427* (1), 80-87.

41.Boeckle, S.; Fahrmeir, J.; Roedl, W.; Ogris, M.; Wagner, E., Melittin analogs with high lytic activity at endosomal pH enhance transfection with purified targeted PEI polyplexes. *Journal of Controlled Release* **2006,** *112* (2), 240-248.

42.Kwon, E. J.; Liong, S.; Pun, S. H., A truncated HGP peptide sequence that retains endosomolytic activity and improves gene delivery efficiencies. *Molecular pharmaceutics* **2010,** *7* (4), 1260-1265.

43.Kleemann, E.; Neu, M.; Jekel, N.; Fink, L.; Schmehl, T.; Gessler, T.; Seeger, W.; Kissel, T., Nano-carriers for DNA delivery to the lung based upon a TAT-derived peptide covalently coupled to PEG–PEI. *Journal of Controlled Release* **2005,** *109* (1), 299-316.

44.Ogris, M.; Brunner, S.; Schüller, S.; Kircheis, R.; Wagner, E., PEGylated DNA/transferrin-PEI complexes: reduced interaction with blood components, extended circulation in blood and potential for systemic gene delivery. *Gene therapy* **1999,** *6* (4), 595-605.

45.Kunath, K.; Merdan, T.; Hegener, O.; Häberlein, H.; Kissel, T., Integrin targeting using RGD-PEI conjugates for in vitro gene transfer. *The journal of gene medicine* **2003,** *5* (7), 588-599.

46.Blessing, T.; Kursa, M.; Holzhauser, R.; Kircheis, R.; Wagner, E., Different strategies for formation of pegylated EGF-conjugated PEI/DNA complexes for targeted gene delivery. *Bioconjugate chemistry* **2001,** *12* (4), 529-537.

47.Merkel, O. M.; Germershaus, O.; Wada, C. K.; Tarcha, P. J.; Merdan, T.; Kissel, T., Integrin αvβ3 Targeted Gene Delivery Using RGD Peptidomimetic Conjugates with Copolymers of PEGylated Poly(ethylene imine). *Bioconjugate chemistry* **2009,** *20* (6), 1270-1280.

48.Luo, X.-h.; Huang, F.-w.; Qin, S.-y.; Wang, H.-f.; Feng, J.; Zhang, X.-z.; Zhuo, R.-x., A strategy to improve serum-tolerant transfection activity of polycation vectors by surface hydroxylation. *Biomaterials* **2011,** *32* (36), 9925-9939.

49.Taranejoo, S.; Liu, J.; Verma, P.; Hourigan, K., A review of the developments of characteristics of PEI derivatives for gene delivery applications. *Journal of Applied Polymer Science* **2015,** *132* (25).

50.Gosselin, M. A.; Guo, W.; Lee, R. J., Efficient gene transfer using reversibly cross-linked low molecular weight polyethylenimine. *Bioconjugate chemistry* **2001,** *12* (6), 989-994.

51.Peng, Q.; Zhong, Z.; Zhuo, R., Disulfide cross-linked polyethylenimines (PEI) prepared via thiolation of low molecular weight PEI as highly efficient gene vectors. *Bioconjugate chemistry* **2008,** *19* (2), 499-506.

52.Agrawal, N.; Dasaradhi, P.; Mohmmed, A.; Malhotra, P.; Bhatnagar, R. K.; Mukherjee, S. K., RNA interference: biology, mechanism, and applications. *Microbiology and molecular biology reviews* **2003,** *67* (4), 657-685.

53.Elbashir, S. M.; Harborth, J.; Lendeckel, W.; Yalcin, A.; Weber, K.; Tuschl, T., Duplexes of 21-nucleotide RNAs mediate RNA interference in cultured mammalian cells. *nature* **2001,** *411* (6836), 494-498.

54.(a) Bobbin, M. L.; Rossi, J. J., RNA interference (RNAi)-based therapeutics: delivering on the promise? *Annual review of pharmacology and toxicology* **2016,** *56*, 103-122; (b) Ozcan, G.; Ozpolat, B.; Coleman, R. L.; Sood, A. K.; Lopez-Berestein, G., Preclinical and clinical development of siRNA-based therapeutics. *Advanced drug delivery reviews* **2015,** *87*, 108-119.

55.Koldehoff, M.; Steckel, N.; Beelen, D.; Elmaagacli, A., Therapeutic application of small interfering RNA directed against bcr-abl transcripts to a patient with imatinib-resistant chronic myeloid leukaemia. *Clinical and experimental medicine* **2007,** *7* (2), 47-55.

56.Zuckerman, J. E.; Gritli, I.; Tolcher, A.; Heidel, J. D.; Lim, D.; Morgan, R.; Chmielowski, B.; Ribas, A.; Davis, M. E.; Yen, Y., Correlating animal and human phase Ia/Ib clinical data with CALAA-01, a targeted, polymer-based nanoparticle containing siRNA. *Proceedings of the National Academy of Sciences* **2014,** *111* (31), 11449-11454.

57.(a) Elliott, R.; Stjernholm, R.; Elliott, M., Preliminary evaluation of platinum transferrin (MPTC-63) as a potential nontoxic treatment for breast cancer. *Cancer detection and prevention* **1987,** *12* (1-6), 469-480; (b) Daniels, T. R.; Bernabeu, E.; Rodríguez, J. A.; Patel, S.; Kozman, M.; Chiappetta, D. A.; Holler, E.; Ljubimova, J. Y.; Helguera, G.; Penichet, M. L., The transferrin receptor and the targeted delivery of therapeutic agents against cancer. *Biochimica et Biophysica Acta (BBA)-General Subjects* **2012,** *1820* (3), 291-317.

58.Phan, A.; Takimoto, C.; Adinin, R.; Wood, L.; Xiong, H.; Matsuno, K.; Konno, S.; Fujisawa, T.; Beeram, M., Open label phase I study of MBP-426, a novel formulation of oxaliplatin, in patients with advanced or metastatic solid tumors. AACR: 2007.

59.Jones, A. R.; Shusta, E. V., Blood–brain barrier transport of therapeutics via receptor-mediation. *Pharmaceutical research* **2007,** *24* (9), 1759-1771.

60.Kim, N.; Nadithe, V.; Elsayed, M.; Merkel, O., Tracking and treating activated T cells. *Journal of drug delivery science and technology* **2013,** *23* (1), 17-21.

61.Xie, Y.; Kim, N. H.; Nadithe, V.; Schalk, D.; Thakur, A.; Kılıç, A.; Lum, L. G.; Bassett, D. J.; Merkel, O. M., Targeted delivery of siRNA to activated T cells via transferrin-polyethylenimine (Tf-PEI) as a potential therapy of asthma. *Journal of Controlled Release* **2016,** *229*, 120-129.

62.Organization, W. H. *The Global Asthma Report*; 2014.

63.orgnization, w. h. *Global surveillance, prevention and control of chronic respiratory diseases: a comprehensive approach*; 2007.

64.RnRMarketResearch.com *Global Markets for Asthma & COPD Drugs*; 2012.

65.Barnes, P. J., New drugs for asthma. *Nat Rev Drug Discov* **2004,** *3* (10), 831-844.

66.Barnes, P. J., New therapies for asthma: is there any progress? *Trends in pharmacological sciences* **2010,** *31* (7), 335-43.

67.Cockcroft, D. W., Clinical concerns with inhaled β2-agonists. *Clinic Rev Allerg Immunol* **2006,** *31* (2-3), 197-207.

68.Boulet, L. P., Influence of comorbid conditions on asthma. *The European respiratory journal* **2009,** *33* (4), 897-906.

69.Barnes, P. J., Pathophysiology of asthma. *Brit J Clin Pharmaco* **1996,** *42* (1), 3-10.

70.Pelaia, G.; Vatrella, A.; Maselli, R., The potential of biologics for the treatment of asthma. *Nat Rev Drug Discov* **2012,** *11* (12), 958-72.

71.Gould, H. J.; Sutton, B. J., IgE in allergy and asthma today. *Nature reviews. Immunology* **2008,** *8* (3), 205-17.

72.(a) Lloyd, C. M.; Hessel, E. M., Functions of T cells in asthma: more than just T(H)2 cells. *Nature reviews. Immunology* **2010,** *10* (12), 838-48; (b) Corrigan, C.

J.; Kay, A. B., T cells and eosinophils in the pathogenesis of asthma. *Immunology Today* **1992,** *13* (12), 501-507.

73.M Humbert, A. B. K., Chronic inflammation in asthma. *European Respiratory Society Journals* **2003,** (23), 126-137.

74.(a) Rettig, G. R.; Behlke, M. A., Progress toward in vivo use of siRNAs-II. *Molecular therapy : the journal of the American Society of Gene Therapy* **2012,** *20* (3), 483-512; (b) Deng, Y.; Wang, C. C.; Choy, K. W.; Du, Q.; Chen, J.; Wang, Q.; Li, L.; Chung, T. K.; Tang, T., Therapeutic potentials of gene silencing by RNA interference: principles, challenges, and new strategies. *Gene* **2014,** *538* (2), 217-27.

75.(a) Beck-Broichsitter, M.; Merkel, O. M.; Kissel, T., Controlled pulmonary drug and gene delivery using polymeric nano-carriers. *Journal of Controlled Release* **2012,** *161* (2), 214-224; (b) Elsayed, M.; Corrand, V.; Kolhatkar, V.; Xie, Y.; Kim, N. H.; Kolhatkar, R.; Merkel, O. M., Influence of oligospermines architecture on their suitability for siRNA delivery. *Biomacromolecules* **2014,** *15* (4), 1299-1310.

76.Rehman, R.; Bhat, Y. A.; Panda, L.; Mabalirajan, U., TRPV1 inhibition attenuates IL-13 mediated asthma features in mice by reducing airway epithelial injury. *International Immunopharmacology* **2013,** *15* (3), 597-605.

77.Liu, S.; Nugroho, A. E.; Shudou, M.; Maeyama, K., Regulation of mucosal mast cell activation by short interfering RNAs targeting syntaxin4. *Immunology and cell biology* **2012,** *90* (3), 337-45.

78.Zafra, M. P.; Mazzeo, C.; Gamez, C.; Rodriguez Marco, A.; de Zulueta, A.; Sanz, V.; Bilbao, I.; Ruiz-Cabello, J.; Zubeldia, J. M.; del Pozo, V., Gene silencing of SOCS3 by siRNA intranasal delivery inhibits asthma phenotype in mice. *PloS one* **2014,** *9* (3), e91996.

79.Khaitov, M. R.; Shilovskiy, I. P.; Nikonova, A. A.; Shershakova, N. N.; Kamyshnikov, O. Y.; Babakhin, A. A.; Zverev, V. V.; Johnston, S. L.; Khaitov, R. M., Small interfering RNAs targeted to interleukin-4 and respiratory syncytial virus reduce airway inflammation in a mouse model of virus-induced asthma exacerbation. *Human gene therapy* **2014,** *25* (7), 642-50.

80.Huang, H.; Lee, C.; Chiang, B., Small interfering RNA against interleukin-5 decreases airway eosinophilia and hyper-responsiveness. *Gene therapy* **2008,** *15* (9), 660-667.

81.Goh, F. Y.; Cook, K. L.; Upton, N.; Tao, L.; Lah, L. C.; Leung, B. P.; Wong, W. S., Receptor-interacting protein 2 gene silencing attenuates allergic airway inflammation. *Journal of immunology (Baltimore, Md. : 1950)* **2013,** *191* (5), 2691-9.

82.(a) Zhu, J.; Yamane, H.; Cote-Sierra, J.; Guo, L.; Paul, W. E., GATA-3 promotes Th2 responses through three different mechanisms: induction of Th2 cytokine production, selective growth of Th2 cells and inhibition of Th1 cell-specific factors. *Cell research* **2006,** *16* (1), 3-10; (b) Yagi, R.; Zhu, J.; Paul, W. E., An updated view on transcription factor GATA3-mediated regulation of Th1 and Th2 cell differentiation. *International immunology* **2011,** *23* (7), 415-20; (c) Zheng, W.; Flavell, R. A., The transcription factor GATA-3 is necessary and sufficient for Th2 cytokine gene expression in CD4 T cells. *Cell* **1997,** *89* (4), 587-96.

83.Finotto, S.; De Sanctis, G. T.; Lehr, H. A.; Herz, U.; Buerke, M.; Schipp, M.; Bartsch, B.; Atreya, R.; Schmitt, E.; Galle, P. R.; Renz, H.; Neurath, M. F., Treatment of allergic airway inflammation and hyperresponsiveness by antisense-induced local blockade of GATA-3 expression. *The Journal of experimental medicine* **2001,** *193* (11), 1247-60.

84.Lee, C. C.; Huang, H. Y.; Chiang, B. L., Lentiviral-mediated GATA-3 RNAi decreases allergic airway inflammation and hyperresponsiveness. *Molecular therapy : the journal of the American Society of Gene Therapy* **2008,** *16* (1), 60-5.

85.Sel, S.; Wegmann, M.; Dicke, T.; Sel, S.; Henke, W.; Yildirim, A. O.; Renz, H.; Garn, H., Effective prevention and therapy of experimental allergic asthma using a GATA-3-specific DNAzyme. *The Journal of allergy and clinical immunology* **2008,** *121* (4), 910-916.e5.

86.Pernis, A. B.; Rothman, P. B., JAK-STAT signaling in asthma. *The Journal of Clinical Investigation* **2002,** *109* (10), 1279-1283.

87.Darcan-Nicolaisen, Y.; Meinicke, H.; Fels, G.; Hegend, O.; Haberland, A.; Kühl, A.; Loddenkemper, C.; Witzenrath, M.; Kube, S.; Henke, W.; Hamelmann, E., Small Interfering RNA against Transcription Factor STAT6 Inhibits Allergic Airway Inflammation and Hyperreactivity in Mice. *The Journal of Immunology* **2009,** *182* (12), 7501-7508.

88.Edwards, M. R.; Bartlett, N. W.; Clarke, D.; Birrell, M.; Belvisi, M.; Johnston, S. L., Targeting the NF-kappaB pathway in asthma and chronic obstructive pulmonary disease. *Pharmacology & therapeutics* **2009,** *121* (1), 1-13.

89.Riccaboni, M.; Bianchi, I.; Petrillo, P., Spleen tyrosine kinases: biology, therapeutic targets and drugs. *Drug discovery today* **2010,** *15* (13-14), 517-30.

90.Stenton, G. R.; Ulanova, M.; Déry, R. E.; Merani, S.; Kim, M.-K.; Gilchrist, M.; Puttagunta, L.; Musat-Marcu, S.; James, D.; Schreiber, A. D.; Befus, A. D., Inhibition of Allergic Inflammation in the Airways Using Aerosolized Antisense to Syk Kinase. *The Journal of Immunology* **2002,** *169* (2), 1028-1036.

91.Huang, Z. Y.; Kim, M. K.; Kim-Han, T. H.; Indik, Z. K.; Schreiber, A. D., Effect of locally administered Syk siRNA on allergen-induced arthritis and asthma. *Molecular immunology* **2013,** *53* (1-2), 52-9.

92.Wu, W.; Chen, H.; Li, Y. M.; Wang, S. Y.; Diao, X.; Liu, K. G., Intranasal sirna targeting c-kit reduces airway inflammation in experimental allergic asthma. *International journal of clinical and experimental pathology* **2014,** *7* (9), 5505-14.

93.Suzuki, M.; Zheng, X.; Zhang, X.; Ichim, T. E.; Sun, H.; Kubo, N.; Beduhn, M.; Shunnar, A.; Garcia, B.; Min, W. P., Inhibition of allergic responses by CD40 gene silencing. *Allergy* **2009,** *64* (3), 387-97.

94.Asai-Tajiri, Y.; Matsumoto, K.; Fukuyama, S.; Kan-o, K.; Nakano, T.; Tonai, K.; Ohno, T.; Azuma, M.; Inoue, H.; Nakanishi, Y., Small interfering RNA against CD86 during allergen challenge blocks experimental allergic asthma. *Respiratory Research* **2014,** *15* (1), 132.

95.Whitehead, K. A.; Langer, R.; Anderson, D. G., Knocking down barriers: advances in siRNA delivery. *Nat Rev Drug Discov* **2009,** *8* (2), 129-138.

96.Merkel, O. M.; Rubinstein, I.; Kissel, T., siRNA Delivery to the lung: What's new? *Advanced Drug Delivery Reviews* **2014,** *75* (0), 112-128.

97.(a) Thomas, C. E.; Ehrhardt, A.; Kay, M. A., Progress and problems with the use of viral vectors for gene therapy. *Nat Rev Genet* **2003,** *4* (5), 346-358; (b) Pack, D. W.; Hoffman, A. S.; Pun, S.; Stayton, P. S., Design and development of polymers for gene delivery. *Nat Rev Drug Discov* **2005,** *4* (7), 581-93.

98.(a) Christopher, W.; Jamie, S.; Masayuki, S.; William, W., Transfection of primary mouse T cells for stimulation-dependent cytokine enhancer assays.

Protocol Exchange **2007,** *doi:10.1038/nprot.2007.236*; (b) Zhao, Y.; Zheng, Z.; Cohen, C. J.; Gattinoni, L.; Palmer, D. C.; Restifo, N. P.; Rosenberg, S. A.; Morgan, R. A., High-Efficiency Transfection of Primary Human and Mouse T Lymphocytes Using RNA Electroporation. *Molecular therapy : the journal of the American Society of Gene Therapy* **2006,** *13* (1), 151-159.

99.Kumar, P.; Wu, H.; McBride, J. L.; Jung, K.-E.; Hee Kim, M.; Davidson, B. L.; Kyung Lee, S.; Shankar, P.; Manjunath, N., Transvascular delivery of small interfering RNA to the central nervous system. *Nature* **2007,** *448* (7149), 39-43.

100.Kumar, P.; Ban, H. S.; Kim, S. S.; Wu, H.; Pearson, T.; Greiner, D. L.; Laouar, A.; Yao, J.; Haridas, V.; Habiro, K.; Yang, Y. G.; Jeong, J. H.; Lee, K. Y.; Kim, Y. H.; Kim, S. W.; Peipp, M.; Fey, G. H.; Manjunath, N.; Shultz, L. D.; Lee, S. K.; Shankar, P., T cell-specific siRNA delivery suppresses HIV-1 infection in humanized mice. *Cell* **2008,** *134* (4), 577-86.

101.Lee, J.; Yun, K. S.; Choi, C. S.; Shin, S. H.; Ban, H. S.; Rhim, T.; Lee, S. K.; Lee, K. Y., T cell-specific siRNA delivery using antibody-conjugated chitosan nanoparticles. *Bioconjugate chemistry* **2012,** *23* (6), 1174-80.

102.Balhara, J.; Gounni, A. S., The alveolar macrophages in asthma: a double-edged sword. *Mucosal Immunol* **2012,** *5* (6), 605-609.

103.Kim, S.-S.; Ye, C.; Kumar, P.; Chiu, I.; Subramanya, S.; Wu, H.; Shankar, P.; Manjunath, N., Targeted Delivery of siRNA to Macrophages for Anti-

inflammatory Treatment. *Molecular therapy : the journal of the American Society of Gene Therapy* **2010,** *18* (5), 993-1001.

104.Paulos, C. M.; Turk, M. J.; Breur, G. J.; Low, P. S., Folate receptor-mediated targeting of therapeutic and imaging agents to activated macrophages in rheumatoid arthritis. *Advanced Drug Delivery Reviews* **2004,** *56* (8), 1205-1217.

105.Yang, C.; Gao, S.; Kjems, J., Folic acid conjugated chitosan for targeted delivery of siRNA to activated macrophages in vitro and in vivo. *Journal of Materials Chemistry B* **2014,** *2* (48), 8608-8615.

106.Zheng, X.; Vladau, C.; Zhang, X.; Suzuki, M.; Ichim, T. E.; Zhang, Z. X.; Li, M.; Carrier, E.; Garcia, B.; Jevnikar, A. M.; Min, W. P., A novel in vivo siRNA delivery system specifically targeting dendritic cells and silencing CD40 genes for immunomodulation. *Blood* **2009,** *113* (12), 2646-54.

107.Zhang, Q.; Hossain, D. M. S.; Nechaev, S.; Kozlowska, A.; Zhang, W.; Liu, Y.; Kowolik, C. M.; Swiderski, P.; Rossi, J. J.; Forman, S.; Pal, S.; Bhatia, R.; Raubitschek, A.; Yu, H.; Kortylewski, M., *TLR9-mediated siRNA delivery for targeting of normal and malignant human hematopoietic cells in vivo*. 2013; Vol. 121, p 1304-1315.

108.Luo, W.; Chang, R.; Zhong, J.; Pandey, A.; Semenza, G. L., Histone demethylase JMJD2C is a coactivator for hypoxia-inducible factor 1 that is

required for breast cancer progression. *Proc. Natl. Acad. Sci. U. S. A.* **2012,** *109* (49), E3367–E3376.

109.Barnes, P. J., Immunology of asthma and chronic obstructive pulmonary disease. *Nature reviews. Immunology* **2008,** *8* (3), 183-92.

110.Ortega, H. G.; Liu, M. C.; Pavord, I. D.; Brusselle, G. G.; FitzGerald, J. M.; Chetta, A.; Humbert, M.; Katz, L. E.; Keene, O. N.; Yancey, S. W., Mepolizumab treatment in patients with severe eosinophilic asthma. *New England Journal of Medicine* **2014,** *371* (13), 1198-1207.

111.Han, W.; Jung, E. M.; Cho, J.; Lee, J. W.; Hwang, K. T.; Yang, S. J.; Kang, J. J.; Bae, J. Y.; Jeon, Y. K.; Park, I. A.; Nicolau, M.; Jeffrey, S. S.; Noh, D. Y., DNA copy number alterations and expression of relevant genes in triple-negative breast cancer. *Genes Chromosomes Cancer* **2008,** *47* (6), 490-9.

112.Kanasty, R.; Dorkin, J. R.; Vegas, A.; Anderson, D., Delivery materials for siRNA therapeutics. *Nature materials* **2013,** *12* (11), 967-977.

113.(a) Fra, A. M.; Williamson, E.; Simons, K.; Parton, R. G., Detergent-insoluble glycolipid microdomains in lymphocytes in the absence of caveolae. *Journal of Biological Chemistry* **1994,** *269* (49), 30745-30748; (b) Lamaze, C.; Dujeancourt, A.; Baba, T.; Lo, C. G.; Benmerah, A.; Dautry-Varsat, A., Interleukin 2 receptors and detergent-resistant membrane domains define a clathrin-independent endocytic pathway. *Molecular cell* **2001,** *7* (3), 661-671.

114.Costello, E.; Munoz, M.; Buetti, E.; Meylan, P.; Diggelmann, H.; Thali, M., Gene transfer into stimulated and unstimulated T lymphocytes by HIV-1-derived lentiviral vectors. *Gene therapy* **2000,** *7* (7), 596-604.

115.The delivery problem. *Nature Biotechnology* **2006**.

116.O'neill, M.; Kennedy, C.; Barton, R.; Tatake, R., Receptor-mediated gene delivery to human peripheral blood mononuclear cells using anti-CD3 antibody coupled to polyethylenimine. *Gene therapy* **2001,** *8* (5), 362-368.

117.Ding, Q.; Si, X.; Liu, D.; Peng, J.; Tang, H.; Sun, W.; Rui, M.; Chen, Q.; Wu, L.; Xu, Y., Targeting and liposomal drug delivery to CD40L expressing T cells for treatment of autoimmune diseases. *Journal of Controlled Release* **2015,** *207*, 86-92.

118.Pelosi, E.; Testa, U.; Louache, F.; Thomopoulos, P.; Salvo, G.; Samoggia, P.; Peschle, C., Expression of transferrin receptors in phytohemagglutinin-stimulated human T-lymphocytes. Evidence for a three-step model. *Journal of Biological Chemistry* **1986,** *261* (7), 3036-3042.

119.Lungwitz, U.; Breunig, M.; Blunk, T.; Göpferich, A., Polyethylenimine-based non-viral gene delivery systems. *European Journal of Pharmaceutics and Biopharmaceutics* **2005,** *60* (2), 247-266.

120.Werth, S.; Urban-Klein, B.; Dai, L.; Höbel, S.; Grzelinski, M.; Bakowsky, U.; Czubayko, F.; Aigner, A., A low molecular weight fraction of polyethylenimine

(PEI) displays increased transfection efficiency of DNA and siRNA in fresh or lyophilized complexes. *Journal of Controlled Release* **2006,** *112* (2), 257-270.

121.Kircheis, R.; Kichler, A.; Wallner, G.; Kursa, M.; Ogris, M.; Felzmann, T.; Buchberger, M.; Wagner, E., Coupling of cell-binding ligands to polyethylenimine for targeted gene delivery. *Gene therapy* **1997,** *4* (5), 409-18.

122.Snyder, S. L.; Sobocinski, P. Z., An improved 2, 4, 6-trinitrobenzenesulfonic acid method for the determination of amines. *Analytical biochemistry* **1975,** *64* (1), 284-288.

123.Merkel, O. M.; Librizzi, D.; Pfestroff, A.; Schurrat, T.; Béhé, M.; Kissel, T., In vivo SPECT and real-time gamma camera imaging of biodistribution and pharmacokinetics of siRNA delivery using an optimized radiolabeling and purification procedure. *Bioconjugate chemistry* **2008,** *20* (1), 174-182.

124.Wegmann, M.; Fehrenbach, H.; Fehrenbach, A.; Held, T.; Schramm, C.; Garn, H.; Renz, H., Involvement of distal airways in a chronic model of experimental asthma. *Clinical and experimental allergy : journal of the British Society for Allergy and Clinical Immunology* **2005,** *35* (10), 1263-71.

125.Neuhaus-Steinmetz, U.; Glaab, T.; Daser, A.; Braun, A.; Lommatzsch, M.; Herz, U.; Kips, J.; Alarie, Y.; Renz, H., Sequential development of airway hyperresponsiveness and acute airway obstruction in a mouse model of allergic

inflammation. *International archives of allergy and immunology* **2000,** *121* (1), 57-67.

126.Breunig, M.; Lungwitz, U.; Liebl, R.; Goepferich, A., Breaking up the correlation between efficacy and toxicity for nonviral gene delivery. *Proceedings of the National Academy of Sciences* **2007,** *104* (36), 14454-14459.

127.Camp, E.; Wang, C.; Little, E.; Watson, P.; Pirollo, K.; Rait, A.; Cole, D.; Chang, E.; Watson, D., Transferrin receptor targeting nanomedicine delivering wild-type p53 gene sensitizes pancreatic cancer to gemcitabine therapy. *Cancer gene therapy* **2013,** *20* (4), 222-228.

128.Ogris, M.; Steinlein, P.; Kursa, M.; Mechtler, K.; Kircheis, R.; Wagner, E., The size of DNA/transferrin-PEI complexes is an important factor for gene expression in cultured cells. *Gene therapy* **1998,** *5* (10), 1425-1433.

129.Cardoso, A.; Simoes, S.; De Almeida, L.; Pelisek, J.; Culmsee, C.; Wagner, E.; Pedroso de Lima, M., siRNA delivery by a transferrin-associated lipid-based vector: a non-viral strategy to mediate gene silencing. *The journal of gene medicine* **2007,** *9* (3), 170-183.

130.Cherng, J.-Y.; van de Wetering, P.; Talsma, H.; Crommelin, D. J.; Hennink, W. E., Effect of size and serum proteins on transfection efficiency of poly ((2-dimethylamino) ethyl methacrylate)-plasmid nanoparticles. *Pharmaceutical research* **1996,** *13* (7), 1038-1042.

131.Grayson, A. C. R.; Doody, A. M.; Putnam, D., Biophysical and structural characterization of polyethylenimine-mediated siRNA delivery in vitro. *Pharmaceutical research* **2006,** *23* (8), 1868-1876.

132.Kircheis, R.; Wightman, L.; Schreiber, A.; Robitza, B.; Rossler, V.; Kursa, M.; Wagner, E., Polyethylenimine/DNA complexes shielded by transferrin target gene expression to tumors after systemic application. *Gene therapy* **2001,** *8* (1), 28-40.

133.Harush-Frenkel, O.; Bivas-Benita, M.; Nassar, T.; Springer, C.; Sherman, Y.; Avital, A.; Altschuler, Y.; Borlak, J.; Benita, S., A safety and tolerability study of differently-charged nanoparticles for local pulmonary drug delivery. *Toxicology and applied pharmacology* **2010,** *246* (1), 83-90.

134.Goerke, J., Pulmonary surfactant: functions and molecular composition. *Biochimica et Biophysica Acta (BBA)-Molecular Basis of Disease* **1998,** *1408* (2), 79-89.

135.Habashy, H. O.; Powe, D. G.; Staka, C. M.; Rakha, E. A.; Ball, G.; Green, A. R.; Aleskandarany, M.; Paish, E. C.; Douglas Macmillan, R.; Nicholson, R. I.; Ellis, I. O.; Gee, J. M., Transferrin receptor (CD71) is a marker of poor prognosis in breast cancer and can predict response to tamoxifen. *Breast Cancer Res Treat* **2010,** *119* (2), 283-93.

136.Neckers, L. M.; Cossman, J., Transferrin receptor induction in mitogen-stimulated human T lymphocytes is required for DNA synthesis and cell division and is regulated by interleukin 2. *Proc Natl Acad Sci U S A* **1983,** *80* (11), 3494-8.

137.Neckers, L.; Yenokida, G.; James, S., The role of the transferrin receptor in human B lymphocyte activation. *The Journal of Immunology* **1984,** *133* (5), 2437-2441.

138.Kopf, M.; Schneider, C.; Nobs, S. P., The development and function of lung-resident macrophages and dendritic cells. *Nature immunology* **2015,** *16* (1), 36-44.

139.Testa, U.; Petrini, M.; Quaranta, M.; Pelosi-Testa, E.; Mastroberardino, G.; Camagna, A.; Boccoli, G.; Sargiacomo, M.; Isacchi, G.; Cozzi, A., Iron up-modulates the expression of transferrin receptors during monocyte-macrophage maturation. *Journal of Biological Chemistry* **1989,** *264* (22), 13181-13187.

140.Curiel, D. T.; Agarwal, S.; Romer, M.; Wagner, E.; Cotten, M.; Birnstiel, M. L.; Boucher, R. C., Gene transfer to respiratory epithelial cells via the receptor-mediated endocytosis pathway. *Am. J. Respir. Cell Mol. Biol* **1992,** *6*, 247-252.

141.(a) Waldmann, T.; Schneider, R., Targeting histone modifications--epigenetics in cancer. *Curr Opin Cell Biol* **2013,** *25* (2), 184-9; (b) Dawson, M. A.; Kouzarides, T., Cancer epigenetics: from mechanism to therapy. *Cell* **2012,** *150* (1), 12-27.

142.DeCarlo, D.; Hadden, M. K., Oncoepigenomics: Making histone lysine methylation count. *European Journal of Medicinal Chemistry* **2012,** *56* (0), 179-194.

143.Esteller, M., Cancer epigenomics: DNA methylomes and histone-modification maps. *Nat Rev Genet* **2007,** *8* (4), 286-298.

144.Yang, Z.-Q.; Imoto, I.; Fukuda, Y.; Pimkhaokham, A.; Shimada, Y.; Imamura, M.; Sugano, S.; Nakamura, Y.; Inazawa, J., Identification of a Novel Gene, GASC1, within an Amplicon at 9p23–24 Frequently Detected in Esophageal Cancer Cell Lines. *Cancer Research* **2000,** *60* (17), 4735-4739.

145.(a) Wu, J.; Liu, S.; Liu, G.; Dombkowski, A.; Abrams, J.; Martin-Trevino, R.; Wicha, M. S.; Ethier, S. P.; Yang, Z. Q., Identification and functional analysis of 9p24 amplified genes in human breast cancer. *Oncogene* **2012,** *31* (3), 333-341; (b) Holowatyj, A.; Yang, Z.-Q., The Role of Histone Demethylase GASC1 in Cancer and its Therapeutic Potential. *Current Cancer Therapy Reviews* **2013,** *9* (1), 78-85.

146.(a) Beroukhim, R.; Mermel, C. H.; Porter, D.; Wei, G.; Raychaudhuri, S.; Donovan, J.; Barretina, J.; Boehm, J. S.; Dobson, J.; Urashima, M.; Mc Henry, K. T.; Pinchback, R. M.; Ligon, A. H.; Cho, Y.-J.; Haery, L.; Greulich, H.; Reich, M.; Winckler, W.; Lawrence, M. S.; Weir, B. A.; Tanaka, K. E.; Chiang, D. Y.; Bass, A. J.; Loo, A.; Hoffman, C.; Prensner, J.; Liefeld, T.; Gao, Q.; Yecies, D.; Signoretti, S.; Maher, E.; Kaye, F. J.; Sasaki, H.; Tepper, J. E.; Fletcher, J. A.;

Tabernero, J.; Baselga, J.; Tsao, M.-S.; Demichelis, F.; Rubin, M. A.; Janne, P. A.; Daly, M. J.; Nucera, C.; Levine, R. L.; Ebert, B. L.; Gabriel, S.; Rustgi, A. K.; Antonescu, C. R.; Ladanyi, M.; Letai, A.; Garraway, L. A.; Loda, M.; Beer, D. G.; True, L. D.; Okamoto, A.; Pomeroy, S. L.; Singer, S.; Golub, T. R.; Lander, E. S.; Getz, G.; Sellers, W. R.; Meyerson, M., The landscape of somatic copy-number alteration across human cancers. *Nature* **2010,** *463* (7283), 899-905; (b) Liu, G.; Bollig-Fischer, A.; Kreike, B.; van de Vijver, M. J.; Abrams, J.; Ethier, S. P.; Yang, Z.-Q., Genomic amplification and oncogenic properties of the GASC1 histone demethylase gene in breast cancer. *Oncogene* **2009,** *28* (50), 4491-4500.

147.Crommelin, D. J. A.; Hennink, W. E.; Mastrobattista, E.; van der Aa, M. A. E. M., Artificial viruses: a nanotechnological approach to gene delivery. *Nat. Rev. Drug Discovery* **2006,** *5*, 115+.

148.Pazaiti, A.; Fentiman, I. S., Basal phenotype breast cancer: implications for treatment and prognosis. *Womens Health (Lond Engl)* **2011,** *7* (2), 181-202.

149.Shastry, M.; Yardley, D. A., Updates in the treatment of basal/triple-negative breast cancer. *Curr Opin Obstet Gynecol* **2013,** *25* (1), 40-8.

150.Essex, S.; Navarro, G.; Sabhachandani, P.; Chordia, A.; Trivedi, M.; Movassaghian, S.; Torchilin, V. P., Phospholipid-modified PEI-based nanocarriers for in vivo siRNA therapeutics against multidrug-resistant tumors. *Gene therapy* **2015,** *22* (3), 41-50.

151.Geninatti Crich, S.; Cadenazzi, M.; Lanzardo, S.; Conti, L.; Ruiu, R.; Alberti, D.; Cavallo, F.; Cutrin, J. C.; Aime, S., Targeting ferritin receptors for the selective delivery of imaging and therapeutic agents to breast cancer cells. *Nanoscale* **2015,** *7* (15), 6527-6533.

152.Germershaus, O.; Neu, M.; Behe, M.; Kissel, T., HER2 Targeted Polyplexes: The Effect of Polyplex Composition and Conjugation Chemistry on in Vitro and in Vivo Characteristics. *Bioconjugate chemistry* **2008,** *19* (1), 244-253.

153.Fischer, D.; Bieber, T.; Li, Y.; Elsasser, H. P.; Kissel, T., A novel non-viral vector for DNA delivery based on low molecular weight, branched polyethylenimine: effect of molecular weight on transfection efficiency and cytotoxicity. *Pharm Res* **1999,** *16* (8), 1273-9.

154.Martinez-Fong, D.; Navarro-Quiroga, I.; Ochoa, I.; Alvarez-Maya, I.; Meraz, M. A.; Luna, J.; Arias-Montaño, J.-A., Neurotensin-SPDP-poly-l-lysine conjugate: a nonviral vector for targeted gene delivery to neural cells. *Mol. Brain Res.* **1999,** *69* (2), 249-262.

155.Sartor, C. I.; Dziubinski, M. L.; Yu, C.-L.; Jove, R.; Ethier, S. P., Role of Epidermal Growth Factor Receptor and STAT-3 Activation in Autonomous Proliferation of SUM-102PT Human Breast Cancer Cells. *Cancer Research* **1997,** *57* (5), 978-987.

156.Deng, Z. J.; Morton, S. W.; Ben-Akiva, E.; Dreaden, E. C.; Shopsowitz, K. E.; Hammond, P. T., Layer-by-Layer Nanoparticles for Systemic Codelivery of an Anticancer Drug and siRNA for Potential Triple-Negative Breast Cancer Treatment. *ACS Nano* **2013,** *7* (11), 9571-9584.

157.Shim, M. S.; Kwon, Y. J., Efficient and targeted delivery of siRNA in vivo. *FEBS Journal* **2010,** *277* (23), 4814-4827.

158.Ardana, A.; Whittaker, A. K.; McMillan, N. A. J.; Thurecht, K. J., Polymeric siRNA delivery vectors: knocking down cancers with polymeric-based gene delivery systems. *Journal of Chemical Technology & Biotechnology* **2015,** *90* (7), 1196-1208.

159.(a) Taranejoo, S.; Liu, J.; Verma, P.; Hourigan, K., A review of the developments of characteristics of PEI derivatives for gene delivery applications. *J. Appl. Polym. Sci.* **2015,** *132* (25), n/a-n/a; (b) Hobel, S.; Aigner, A., Polyethylenimines for siRNA and miRNA delivery in vivo. *Wiley Interdiscip Rev Nanomed Nanobiotechnol* **2013,** *5* (5), 484-501.

160.Mayle, K. M.; Le, A. M.; Kamei, D. T., The intracellular trafficking pathway of transferrin. *Biochim. Biophys. Acta* **2012,** *1820* (3), 264-281.

161.Tortorella, S.; Karagiannis, T., Transferrin Receptor-Mediated Endocytosis: A Useful Target for Cancer Therapy. *J Membrane Biol* **2014,** *247* (4), 291-307.

162.van der Meel, R.; Vehmeijer, L. J.; Kok, R. J.; Storm, G.; van Gaal, E. V., Ligand-targeted particulate nanomedicines undergoing clinical evaluation: current status. *Adv Drug Deliv Rev* **2013,** *65* (10), 1284-98.

163.Plank, C.; Mechtler, K.; Szoka, F. C., Jr.; Wagner, E., Activation of the complement system by synthetic DNA complexes: a potential barrier for intravenous gene delivery. *Human gene therapy* **1996,** *7* (12), 1437-46.

164.Merkel, O. M.; Zheng, M.; Debus, H.; Kissel, T., Pulmonary gene delivery using polymeric nonviral vectors. *Bioconjugate chemistry* **2011,** *23* (1), 3-20.

165.Gemma Navarro; Movassaghian, S.; Torchilin, V. P., Current Trends in the Use of Cationic Polymer Assemblies for siRNA and Plasmid DNA Delivery. *Pharm. Nanotechnol.* **2013,** *1* (3), 165-183.

166.Movassaghian, S.; Torchilin, V. P., Chapter 18 - Long-Circulating Therapies for Cancer Treatment. In *Novel Approaches and Strategies for Biologics, Vaccines and Cancer Therapies*, Singh, M.; Salnikova, M., Eds. Academic Press: San Diego, 2015; pp 433-462.

167.Xiao, K.; Li, Y.; Luo, J.; Lee, J. S.; Xiao, W.; Gonik, A. M.; Agarwal, R. G.; Lam, K. S., The effect of surface charge on in vivo biodistribution of PEG-oligocholic acid based micellar nanoparticles. *Biomaterials* **2011,** *32* (13), 3435-3446.

168.Zuckerman, J. E.; Gale, A.; Wu, P.; Ma, R.; Davis, M. E., siRNA delivery to the glomerular mesangium using polycationic cyclodextrin nanoparticles containing siRNA. *Nucleic Acid Ther* **2015,** *25* (2), 53-64.

169.Merdan, T.; Callahan, J.; Petersen, H.; Kunath, K.; Bakowsky, U.; Kopeckova, P.; Kissel, T.; Kopecek, J., Pegylated polyethylenimine-Fab' antibody fragment conjugates for targeted gene delivery to human ovarian carcinoma cells. *Bioconjugate chemistry* **2003,** *14* (5), 989-96.

170.Li, Z.; Rana, T. M., Molecular Mechanisms of RNA-Triggered Gene Silencing Machineries. *Accounts of Chemical Research* **2012,** *45* (7), 1122-1131.

171.Medina-Kauwe, L. K.; Xie, J.; Hamm-Alvarez, S., Intracellular trafficking of nonviral vectors. *Gene therapy* **2005,** *12* (24), 1734-51.

172.Akhtar, M. J.; Ahamed, M.; Alhadlaq, H. A.; Alrokayan, S. A.; Kumar, S., Targeted anticancer therapy: overexpressed receptors and nanotechnology. *Clin Chim Acta* **2014,** *436*, 78-92.

173.Sheff, D. R.; Daro, E. A.; Hull, M.; Mellman, I., The receptor recycling pathway contains two distinct populations of early endosomes with different sorting functions. *J Cell Biol* **1999,** *145* (1), 123-39.

174.Behr, J.-P., The Proton Sponge: a Trick to Enter Cells the Viruses Did Not Exploit. *CHIMIA International Journal for Chemistry* **1997,** *51* (1-2), 34-36.

175.(a) Gopal, V.; Xavier, J.; Kamal, M. Z.; Govindarajan, S.; Takafuji, M.; Soga, S.; Ueno, T.; Ihara, H.; Rao, N. M., Synthesis and Transfection Efficiency of Cationic Oligopeptide Lipids: Role of Linker. *Bioconjugate chemistry* **2011,** *22* (11), 2244-2254; (b) Zhao, F.; Yin, H.; Zhang, Z.; Li, J., Folic Acid Modified Cationic γ-Cyclodextrin-oligoethylenimine Star Polymer with Bioreducible Disulfide Linker for Efficient Targeted Gene Delivery. *Biomacromolecules* **2013,** *14* (2), 476-484.

176.Kunath, K.; Merdan, T.; Hegener, O.; Haberlein, H.; Kissel, T., Integrin targeting using RGD-PEI conjugates for in vitro gene transfer. *J Gene Med* **2003,** *5* (7), 588-99.

177.Moffatt, S.; Papasakelariou, C.; Wiehle, S.; Cristiano, R., Successful in vivo tumor targeting of prostate-specific membrane antigen with a highly efficient J591//PEI//DNA molecular conjugate. *Gene therapy* **2006,** *13* (9), 761-772.

178.Otsuka, H.; Nagasaki, Y.; Kataoka, K., PEGylated nanoparticles for biological and pharmaceutical applications. *Adv. Drug Delivery Rev.* **2003,** *55* (3), 403-419.

179.Ye, Q.; Holowatyj, A.; Wu, J.; Liu, H.; Zhang, L.; Suzuki, T.; Yang, Z. Q., Genetic alterations of KDM4 subfamily and therapeutic effect of novel demethylase inhibitor in breast cancer. *Am J Cancer Res* **2015,** *5* (4), 1519-30.

180.Xu, L.; Huang, C.-C.; Huang, W.; Tang, W.-H.; Rait, A.; Yin, Y. Z.; Cruz, I.; Xiang, L.-M.; Pirollo, K. F.; Chang, E. H., Systemic Tumor-targeted Gene

Delivery by Anti-Transferrin Receptor scFv-Immunoliposomes 1 This work was supported in part by National Cancer Institute Grant R01 CA45158 (to EC), National Cancer Institute Small Business Technology Transfer Phase I Grant R41 CA80449 (to EC), and a grant from SynerGene Therapeutics, Inc. 1. *Molecular cancer therapeutics* **2002,** *1* (5), 337-346.

181.Suzuki, S.; Inoue, K.; Hongoh, A.; Hashimoto, Y.; Yamazoe, Y., Modulation of doxorubicin resistance in a doxorubicin-resistant human leukaemia cell by an immunoliposome targeting transferring receptor. *British journal of cancer* **1997,** *76* (1), 83.

182.Soni, V.; Kohli, D.; Jain, S., Transferrin-conjugated liposomal system for improved delivery of 5-fluorouracil to brain. *Journal of drug targeting* **2008,** *16* (1), 73-78.

183.Hillery, A. M.; Lloyd, A. W.; Swarbrick, J., *Drug delivery and targeting: for pharmacists and pharmaceutical scientists*. CRC Press: 2002.

184.Lee, J. H.; Engler, J. A.; Collawn, J. F.; Moore, B. A., Receptor mediated uptake of peptides that bind the human transferrin receptor. *European Journal of Biochemistry* **2001,** *268* (7), 2004-2012.

185.Erbacher, P.; Roche, A. C.; Monsigny, M.; Midoux, P., Putative role of chloroquine in gene transfer into a human hepatoma cell line by DNA/lactosylated polylysine complexes. *Experimental cell research* **1996,** *225* (1), 186-194.

186.(a) Tseng, C.-L.; Wu, S. Y.-H.; Wang, W.-H.; Peng, C.-L.; Lin, F.-H.; Lin, C.-C.; Young, T.-H.; Shieh, M.-J., Targeting efficiency and biodistribution of biotinylated-EGF-conjugated gelatin nanoparticles administered via aerosol delivery in nude mice with lung cancer. *Biomaterials* **2008,** *29* (20), 3014-3022; (b) Master, A. M.; Sen Gupta, A., EGF receptor-targeted nanocarriers for enhanced cancer treatment. *Nanomedicine* **2012,** *7* (12), 1895-1906.

187.Wängler, C.; Nada, D.; Höfner, G.; Maschauer, S.; Wängler, B.; Schneider, S.; Schirrmacher, E.; Wanner, K. T.; Schirrmacher, R.; Prante, O., In vitro and initial in vivo evaluation of 68Ga-labeled transferrin receptor (TfR) binding peptides as potential carriers for enhanced drug transport into TfR expressing cells. *Molecular Imaging and Biology* **2011,** *13* (2), 332-341.

188.Prades, R.; Guerrero, S.; Araya, E.; Molina, C.; Salas, E.; Zurita, E.; Selva, J.; Egea, G.; López-Iglesias, C.; Teixidó, M., Delivery of gold nanoparticles to the brain by conjugation with a peptide that recognizes the transferrin receptor. *Biomaterials* **2012,** *33* (29), 7194-7205.

189.Park, I. K.; Lasiene, J.; Chou, S. H.; Horner, P. J.; Pun, S. H., Neuron-specific delivery of nucleic acids mediated by Tet1-modified poly (ethylenimine). *The journal of gene medicine* **2007,** *9* (8), 691-702.

190.Ciechanover, A.; Schwartz, A.; Dautry-Varsat, A.; Lodish, H., Kinetics of internalization and recycling of transferrin and the transferrin receptor in a human

hepatoma cell line. Effect of lysosomotropic agents. *Journal of Biological Chemistry* **1983,** *258* (16), 9681-9689.

191.Yang, J.; Chen, H.; Vlahov, I. R.; Cheng, J.-X.; Low, P. S., Evaluation of disulfide reduction during receptor-mediated endocytosis by using FRET imaging. *Proceedings of the National Academy of Sciences* **2006,** *103* (37), 13872-13877.

192.Corish, P.; Tyler-Smith, C., Attenuation of green fluorescent protein half-life in mammalian cells. *Protein engineering* **1999,** *12* (12), 1035-1040.

ABSTRACT

TRANSFERRIN RECEPTOR TARGETED DELIVERY OF SIRNA FOR GENE THERAPY

by

YURAN XIE

May 2017

Advisor: Dr. Olivia Merkel

Major: Pharmaceutical Sciences

Degree: Doctor of Philosophy

Gene therapy is thought to be a solution for various difficult to treat diseases such as cancer. Small interfering RNA (siRNA) as a promising class of anti-sense molecules can specifically silence disease related genes and has been evaluated in different diseases. However, lack of safe and efficient siRNA delivery systems limits the application of siRNA therapy in the clinic. Transferrin receptor (TfR) is an essential transmembrane receptor involved in iron uptake. TfR is universally expressed in most cells/ tissues but is upregulated in certain cells, for example, many cancer cells and activated T cells (ATCs). To overcome the biological barriers and increase siRNA delivery efficiency, in this dissertation, various TfR targeted siRNA delivery systems have been developed. Holo-Tf was conjugated to PEI via reducible linker succinimidyl 3-(2-pyridyldithio) propionate

(SPDP) or PEG_4-SPDP to generate Tf-PEI. Tf-PEI was firstly evaluated for potential therapy of asthma. Tf-PEI demonstrated satisfactory physicochemical properties and can efficiently deliver siRNA to human primary ATCs e*x vivo.* Furthermore, pulmonary administration of Tf-PEI in a murine asthma model resulted in ATCs selective delivery of siRNA and minimum toxicity.

Gene amplified in squamous cell carcinoma 1 (GASC1) is an oncogene overexpressed in basal like breast cancer (BLBC), an aggressive type of breast cancer, and is an essential epigenetic factor involved in tumorigenesis. Tf-PEI polyplexes containing siRNA against GASC1 gene were exploited as a potential treatment of BLBC. Tf-PEI can selectively deliver siRNA to BLBC overexpressing TfR and achieve efficient silencing of GASC1 gene leading to inhibition of proliferation of BLBC.

Two TfR binding peptides, HAIYPRH (HAI) and THRPPMWSPVWP (THR), as alternative TfR targeting moieties were conjugated with PEI via reducible linker PEG_4-SPDP or non-reducible linker sulfosuccinimidyl 4-[N-maleimidomethyl] cyclohexane-1-carboxylate (SMCC). Both peptide-PEI conjugates were investigated in lung cancer cells expressing low or high level of TfR. HAI-PEI preferentially bound to cells overexpressing TfR while THR-PEI didn't demonstrate TfR selectivity. Reducible HAI-SPDP-PEI achieved better gene silencing *ex vivo* than non-reducible HAI-SMCC-PEI. In conclusion, the

present study described the feasibility to efficiently deliver siRNA to ATCs in asthma and cancer cells via targeting TfR. These results could help the development of siRNA therapies for asthma and cancer.

AUTOBIOGRAPHICAL STATEMENT

Yuran Xie

Education

2012- 2017 Ph.D. Pharmaceutical Sciences; Wayne State University, Detroit, MI
2008- 2012 B.Sc. Pharmacy; China Pharmaceutical University, Nanjing, China

Publications

1. D. Feldmann, **Y. Xie**, S. Jones, D. Yu, A. Moszczynska, O.M. Merkel. The impact of microfluidic mixing of triblock micelleplexes on in vitro / in vivo gene silencing and intracellular trafficking. Under reviewed. (**2017**)
2. **Y. Xie**, B. Killinger, A. Moszczynska, O.M. Merkel. Targeted delivery of siRNA to transferrin receptor overexpressing tumor cells via peptide modified polyethylenimine. *Molecules*. (**2016**)
3. **Y. Xie**, R. Kandil, OM. Merkel. Bridging the Gap between Bench and Clinic; Asthma, Nanomedicine for Inflammatory Diseases. Under reviewed. (**2016**)
4. S. Movassaghian, **Y. Xie**, C. Hildebrandt, R. Rosati, Z. Yang, O.M. Merkel. Post-transcriptional regulation of the GASC1 oncogene with active tumor-targeted siRNA-nanoparticle, *Molecular Pharmaceutics*. (**Joint first author**) (**2016**)
5. M. Mohammadi, DG. Abebe, Y. Li, **Y. Xie**, R. Kandil, T. Kraus, N. Gomez-Lopez, T. Fujiwara, O.M. Merkel. Folate receptor Targeted Three-Layered Micelles for gene delivery to activated macrophages. *Journal of Controlled Release*. (**2016**)
6. **Y. Xie**, N.H. Kim, V. Nadithe, D. Schalk, A. Thakur, A. Kılıç, L.G. Lum, D.J. Bassett, O.M. Merkel. Targeted delivery of siRNA to activated T Cells via transferrin-polyethylenimine (Tf-PEI) as a potential therapy of asthma, *Journal of Controlled Release*. (**2016**)
7. **Y. Xie**, O.M. Merkel. Pulmonary Delivery of siRNA via Polymeric Vectors as Therapies of Asthma, *Archiv der Pharmazie*. (**2015**)
8. M. Elsayed, V. Corrand, V. Kolhatkar, **Y. Xie**, N.H. Kim, R. Kolhatkar, O.M. Merkel. Influence of oligospermines architecture on their suitability for siRNA delivery, *Biomacromolecules*. (**2014**)

Scholarships and Awards

Frank O. Taylor Pharmacy Scholarship (2016)

Membership of Professional Societies

Member of American Association of Pharmaceutical Scientists (AAPS) (2013-2014, 2015-2016)
Vice chair of AAPS Wayne State University student chapter (2015-2016)